Uncovering novel regulation of pathogen-induced callose deposition through chemical inhibition and natural variation

By

Brian D. Keppler

A dissertation submitted in partial fulfillment of

the requirements for the degree of

Doctor of Philosophy

(Cellular and Molecular Biology)

at the

UNIVERSITY OF WISCONSIN-MADISON

2016

Date of final oral examination: 11/09/2016

The dissertation is approved by the following members of the Final Oral Committee:
Andrew F. Bent, Professor, Plant Pathology
Richard M. Amasino, Professor, Biochemistry
Jean-Michel Ané, Professor, Bacteriology
Sebastian Y. Bednarek, Professor, Biochemistry
Xuehua Zhong, Assistant Professor, Genetics

Abstract

Plant cell wall reinforcement is a ubiquitous plant innate immune response first observed by de Bary over 150 years ago. The β-1,3-glucan callose is the most abundant and commonly identified component in these pathogen-induced cell wall thickenings. 3-aminobenzamide (3AB) is an established inhibitor of poly(ADP-ribosyl)ation, and it blocks the callose deposition elicited by flg22 or elf18, two microbe-associated molecular patterns (MAMPs). Poly(ADP-ribosyl)ation is a post-translational modification in which chains of ADP-ribose are added to an acceptor protein by poly(ADP-ribose) polymerases (PARPs). Poly(ADP-ribosyl)ation functions in a variety of cellular processes including DNA damage repair and more recently has been shown to contribute to plant immune responses. Despite clear roles of poly(ADP-ribosy)ation in plant immunity, we show that the inhibition of callose by 3AB is largely independent of poly(ADP-ribosyl)ation. Specifically, we find that an *Arabidopsis thaliana parp1parp2parp3* triple mutant does not exhibit loss of MAMP-induced callose deposition. Additionally, more potent and specific PARP inhibitors do not block callose deposition. We further utilize 3AB as a chemical genetic tool to probe the unique pathways that regulate pathogenesis-related callose deposition. 3AB does not block wound-induced PMR4-dependent callose deposition. Intriguingly, 3AB increases PMR4 protein abundance in the presence of flg22, despite no callose being produced, suggesting novel mechanisms of PMR4 regulation. To further explore the regulation of pathogen-induced callose deposition, we identified naturally occurring genetic variation in the MAMP-induced callose response. We used Arabidopsis accessions Bay-0 and Sha to perform quantitative trait loci (QTL) analysis to identify candidate genes responsible for this variation. Together, these findings enhance our understanding of the poorly understood pathways from pathogen perception to cell wall reinforcement with callose.

Acknowledgments

First and foremost, I am grateful to Andrew Bent for giving me the opportunity to work in the lab. The project took a few twists and turns over the years, but Andrew was there with excellent advice and support throughout. I would also like to thank the other four members of my committee, Rick Amasino, Sebastian Bednarek, Jean-Michel Ané, and Xuehua Zhang for their help and valuable feedback. I also owe tremendous gratitude to Allan Showalter at Ohio University for that first opportunity to do plant molecular biology research as an undergraduate.

Everyone in the Bent lab, both past and present, have been wonderful whether seeking advice for an experiment or an interesting conversation. Each of them had an impact in their own way and deserves mention: Junqi Song, Laura Helft, David Cook, Teresa Koller, Yangrong Cao, Xiaoli Guo, Adam Bayless, Alice Teillet, Stephen Mosher, Katelyn Horgan, Patrick McMinn, Ryan Zapotocny, John Smith, Shaojie Han, and Derrick Grunwald. There is nothing like being in a small office with five other people to develop a sense of closeness and camaraderie. I must especially thank Junqi Song for all the technical expertise he provided throughout the project.

I'm thankful to the CMB program for the opportunity to come to UW-Madison and pursue my PhD. From the first week of orientation until now, I've been nothing but impressed with my fellow students, the faculty, and the administration of CMB. I was more than happy to volunteer as a weekend recruitment manager for three years to share the excellence of CMB with prospective graduate students. Plant pathology has been an outstanding home department. I cannot imagine a more warm and welcoming group of people or a department with a stronger sense of community.

Finally, I thank my family. It goes without saying that I would not be where I am today without the continued love, support, and encouragement of my parents and siblings.

Table of Contents

Chapter 1: Introduction

1.1 Cell wall reinforcement and PTI

Plant cell wall reinforcement in response to fungal invasion was first observed as early as 150 years ago (De Bary, 1863). These cell wall appositions, known as papillae, were subsequently identified throughout the plant kingdom and in response to a variety of pathogens, whether fungus, bacteria, oomycete, or nematode (Aist, 1976). Although not always successful in preventing pathogen entry, papillae are believed to provide a hard, impermeable physical barrier to slow pathogen ingress (Stone and Clarke, 1992). Callose is one of the most abundant and commonly identified components in papillae, yet its precise role in the papillae in still not clear (Voigt, 2014).

Callose deposition and cell wall reinforcement are components of the plant immune response known as pattern-triggered immunity (PTI). Plants encode pattern recognition receptors (PRRs) that recognize conserved characteristics of microbes known as microbe (or pathogen)-associated molecular patterns (MAMPs/PAMPs) to initiate the PTI response (Jones and Dangl, 2006; Boller and Felix, 2009). Two of the best characterized PRRs are FLS2 and EFR, which recognize bacterial flagellin (flg22) and elongation factor Tu (elf18), respectively (Gomez-Gomez and Boller, 2000; Zipfel et al., 2006). Similarly, fungal chitin fragments are recognized by CERK1, a LysM receptor kinase (Miya et al., 2007; Wan et al., 2008). PTI signaling is further introduced in Chapter 4 and has been reviewed extensively (Schwessinger and Zipfel, 2008; Boller and Felix, 2009; Macho and Zipfel, 2014; Li et al., 2016). While many MAMP responses occur within minutes, such as the production of reactive oxygen species (ROS), activation of MAP kinase pathways, and the induction of defense-related gene expression, callose deposition is generally considered a late PTI response, detectable by aniline

blue staining 16 to 24 hours following MAMP perception, although an earlier callose response has also been documented at approximately 60 to 90 minutes following flg22 treatment (Ellinger and Voigt, 2014).

1.2 Arabidopsis callose synthases

Arabidopsis callose synthases were initially identified based on sequence homology to *FKS1*, which encodes a yeast β-1,3-glucan synthase (Douglas et al., 1994; Hong et al., 2001). The Arabidopsis genome encodes 12 putative callose synthases, members of the GLUCAN SYNTHASE LIKE (GSL) family (Richmond and Somerville, 2000). A CALLOSE SYNATHASE (CALS) nomenclature was also proposed (Hong et al., 2001) but has not been as widely adopted. As the various nomenclatures can lead to confusion, an overview is provided in **Table I**.

GSL5 is the callose synthase involved in both wound- and pathogen-induced callose, hereafter referred to as POWDERY MILDEW RESISTANT 4 (PMR4), a name based on its mutant phenotype. *PMR4* was initially identified in a forward genetic screen for increased resistance to the Arabidopsis powdery mildew, *Golovinomyces cichoracearum* (Vogel and Somerville, 2000). The enhanced resistance phenotype of the *pmr4* mutant was counterintuitive given that callose is considered an important component in defense against powdery mildew, but the resistance is apparently explained by hyperactivated salicylic acid defense responses in the *pmr4* mutant (Nishimura et al., 2003). The *pmr4* mutants are devoid of powdery mildew- and flg22-induced callose as well as callose deposited in response to wounding (Jacobs et al., 2003; Nishimura et al., 2003). Notably, chitin-induced callose is drastically reduced in the mutant but the 10% remaining is attributed to another unidentified callose synthase (Luna et al., 2011).

Possible candidates include *GSL6* or *GSL11* as their expression increases in response to powdery mildew but neither has been shown to be involved in the defense response (Jacobs et al., 2003).

The other members of the GSL family have been characterized to varying degrees. GSL1, GSL2, GSL5, GSL8, and GSL10 are proposed to function in various aspects of pollen development (Dong et al., 2005; Enns et al., 2005; Toller et al., 2008). *GSL7* is expressed exclusively in the phloem, and a *gsl7* mutant produces significantly less callose in sieve elements, impacting proper flow through the phloem (Barratt et al., 2011; Xie et al., 2011). GSL6 and GSL8 are involved in deposition of callose during cytokinesis (Hong et al., 2001; Chen et al., 2009). GSL8 and GSL12 deposit callose in the plasmodesmata to regulate cell to cell trafficking (Guseman et al., 2010; Vaten et al., 2011). Although distinct from defense-related callose deposited by PMR4 at the cell wall, callose deposited in the plasmodesmata certainly has implications for pathogen defense, particularly against viruses (Li et al., 2012). The four remaining GSL family members, GSL3, GSL4, GSL9, GSL11 have not been characterized to date. Note that certain callose synthases exhibit multiple biological functions. This is particularly true for GSL8 as it is implicated in cytokinesis, pollen development, as well as plasmodesmatal regulation.

Following its identification as the pathogen and wound-induced callose synthase in 2003, few additional studies focusing specifically on PMR4 were published until relatively recently. Interestingly, overexpression of *PMR4* was also shown to increase resistance to adapted powdery mildew, making it unusual in that both a knockout mutant and an overexpression line exhibit the same phenotype, although the resistance is by different mechanisms (Ellinger et al., 2013). The *PMR4* overexpression line does not constitutively produce callose, but rather produces larger callose deposits and at earlier time points upon elicitation by a pathogen. Moreover, the

overexpressed PMR4-GFP protein is constitutively present at the plasma membrane, but relocalizes to sites of attempted powdery mildew penetration (Ellinger et al., 2013). These findings strongly indicate that PMR4 is regulated post-translationally and that it requires translocation and/or activation before callose is produced.

1.3 Papillae formation and trafficking

While papillae are perhaps most associated with callose, numerous other compounds have been identified as well. Reactive oxygen species, such as H_2O_2, are common and may provide direct antimicrobial activity as well as strength through the peroxidase-catalyzed cross-linking of proteins (Thordal-Christensen et al., 1997). Phenolic compounds including lignin provide additional strength and are resistant to degradation by microbial enzymes (Vance et al., 1980; Nicholson and Hammerschmidt, 1992). Interestingly, the ultrastructure of the papillae remains intact even with the loss of callose in a *pmr4* mutant and is indistinguishable from wild type indicating that callose isn't a required structural component of the papillae (Nishimura et al., 2003).

Much of our understanding of papillae formation and callose is in the context of plant-powdery mildew interactions (Huckelhoven and Panstruga, 2011). Important insights into papillae were gained through a forward genetic screen for increased penetration (*PEN*) of the non-host barley powdery mildew *Blumeria graminis* f. sp. *hordei* (*Bgh*) on Arabidopsis. *PEN1* encodes a syntaxin (*SYP121*) involved in SNARE-mediated exocytosis (Collins et al., 2003). Barley *ROR2* is a functional homolog of *PEN1* and is also required for penetration resistance to adapted powdery mildew, demonstrating a role for SNARE-mediated resistance to both adapted and non-host pathogens. Interestingly, *pen1* mutants still make papillae in response to powdery

mildew, but the response is delayed by approximately two hours, and this delay is considered sufficient to explain the loss of penetration resistance (Assaad et al., 2004). GFP-PEN1 protein strongly accumulates in papillae (Assaad et al., 2004), but the biological relevance of this accumulation is not entirely clear (Nielsen and Thordal-Christensen, 2013).

PEN2 and *PEN3* were identified in the same screen for enhanced penetration of *Bgh*, but they function in an independent pathway from *PEN1* (Lipka et al., 2005; Stein et al., 2006). *PEN2* encodes a β-thioglucoside glucohydrolase and *PEN3* an ATP-binding cassette (ABC) transporter. Both PEN1 and PEN3 proteins relocalize to papillae from the plasma membrane but the proper localization is dependent on different pathways based on studies with pharmacological inhibitors (Underwood and Somerville, 2013). Disruption of the actin cytoskeleton prevents relocalization of PEN3-GFP but not GFP-PEN1. In contrast, relocalization of GFP-PEN1 is dependent on secretary trafficking (Nielsen et al., 2012; Underwood and Somerville, 2013). In response to flg22, both *pen2* and *pen3* mutants exhibit a complete loss of callose deposition (Clay et al., 2009). PEN2 likely acts as a myrosinase catalyzing the hydrolysis of 4-methoxy-indol-3-ylmethylglucosinolate (4-methoxy-I3G), while PEN3 may be involved in the transport of these glucosinolate metabolites. 4-methoxy-I3G itself, as well as upstream glucosinolate biosysnthetic genes and transcription factors are also required for flg22-induced callose deposition (Bednarek et al., 2009; Clay et al., 2009).

The trafficking of papillary materials is dependent on GTPases as well as guanine nucleotide exchange factors (GEFs). The ADP ribosylation factor (ARF) family GTPase ARFA1b/1c in barley is required for papillary localization of the syntaxin ROR2 as well as callose (Bohlenius et al., 2010). As ARFA1b/1c localized to multivesicular bodies, it was suggested that callose may be loaded into papillae via multivesicular bodies. In contrast, no

evidence of multivesicular body involvement in the translocation of PMR4-GFP was identified in Arabidopsis (Ellinger et al., 2013). GNOM, an Arabidopsis ARF-GEF is also involved as callose deposition in a *gnom* mutant is delayed by approximately 30 minutes. Importantly, MIN7 is a related ARF-GEF that is targeted by the *Pseudomonas syringae* effector HopM1 for proteasomal degradation (Nomura et al., 2006). Knockout mutants of *MIN7* are similarly impaired in the deposition of callose in response to *P. syringae*. Together, these finding strongly implicate ARF GTPases in the intracellular trafficking of PMR4/callose and papillary-localized proteins.

1.4 Poly(ADP-ribosyl)ation in plant immunity

Poly(ADP-ribosyl)ation is a post-translational modification in which chains of ADP-ribose are attached to an acceptor protein. Poly(ADP-ribosyl)ation is best recognized for its involvement in DNA damage repair, but roles in chromatin modification, transcriptional regulation, and programmed cell death are known (Schreiber et al., 2006; Gibson and Kraus, 2012; Burkle and Virag, 2013). ADP-ribose units are added by poly(ADP-ribose) polymerases (PARPs), using NAD^+ as the donor of ADP-ribose. The attached poly(ADP-ribose) units are rapidly cleaved from acceptor proteins by poly(ADP-ribose) glycohydrolase (PARG) enzymes. The role of poly(ADP-ribosyl)ation in DNA damage and related responses are largely conserved in animals and plants and have been reviewed (Briggs and Bent, 2011; Lamb et al., 2012). Of particular interest here are the unique roles of poly(ADP)ribosylation in the plant innate immune response.

A microarray study examining *P. syringae*-Arabidopsis interactions provided the first hint that there was a connection between plant immunity and poly(ADP-ribosyl)ation (Adams-

Phillips et al., 2008). Arabidopsis PARG1 and NUDT7, a nudix hydrolase, were both upregulated in response to *P. syringae* or flg22. PARP inhibitors are widely used in the characterization of poly(ADP-ribosyl)ation, both for the purposes of conditional inactivation of the enzymes as well as to overcome the functional redundancy of multiple PARP enzymes. This led to the use of the PARP inhibitor 3-aminobenzamide (3AB) to further characterize the function of poly(ADP-ribosyl)ation in the plant immune response. Intriguingly, 3AB blocks MAMP-induced callose deposition, in addition to an extreme toxicity that is observed in seedlings treated with flg22 and 3AB, much more than with either flg22 or 3AB alone (Adams-Phillips et al., 2008). In a follow-up study, the inhibition of callose deposition by 3AB was revealed to be quite specific, having no impact on other innate immune responses, such as the ROS burst or transcriptional upregulation of defense genes such as FRK1 or WRKY29 (Adams-Phillips et al., 2010).

1.5 Research overview

This project explores the intersection of poly(ADP-ribosyl)ation and the plant innate immune response, with a particular focus on cell wall reinforcement with callose deposition. Chapter 2 focuses on poly(ADP-ribosyl)ation and further characterizes the role of PARP1 and PARP2 in plant immunity as well as in DNA damage responses. Despite clear impacts of poly(ADP-ribosyl)ation on plant immunity, the inhibition of MAMP-induced callose deposition by the PARP inhibitor 3AB appears to be independent of poly(ADP-ribosyl)ation, a project that is investigated in Chapter 3. Finally, Chapter 4 focuses specifically on callose deposition and seeks to identify novel regulators of callose through an Arabidopsis natural variation approach.

1.6 Tables

Table I. The Arabidopsis callose synthase family.

Locus	GSL	CALS	Other Names
AT4G04970	GSL1	CalS11	
AT2G13680	GSL2	CalS5	
AT2G31960	GSL3	CalS2	
AT3G14570	GSL4	CalS8	
AT4G03550	GSL5	CalS12	POWDERY MILDEW RESISTANT 4 (PMR4) ENHANCER OF EDR1 3 (EED3)
AT1G05570	GSL6	CalS1	
AT1G06490	GSL7	CalS7	
AT2G36850	GSL8	CalS10	CHORUS (CHOR) ENLARGED TETRAD 2 (ET2) MASSUE (MAS)
AT5G36870	GSL9	CalS4	
AT3G07160	GSL10	CalS9	
AT3G59100	GSL11	CalS6	
AT5G13000	GSL12	CalS3	

1.7 References

Adams-Phillips L, Briggs AG, Bent AF (2010) Disruption of poly(ADP-ribosyl)ation mechanisms alters responses of Arabidopsis to biotic stress. Plant Physiol **152:** 267-280

Adams-Phillips L, Wan J, Tan X, Dunning FM, Meyers BC, Michelmore RW, Bent AF (2008) Discovery of ADP-ribosylation and other plant defense pathway elements through expression profiling of four different Arabidopsis-Pseudomonas R-avr interactions. Mol Plant Microbe Interact **21:** 646-657

Aist JR (1976) Papillae and Related Wound Plugs of Plant Cells. Annu Rev Phytopathol **14:** 145-163

Assaad FF, Qiu JL, Youngs H, Ehrhardt D, Zimmerli L, Kalde M, Wanner G, Peck SC, Edwards H, Ramonell K, Somerville CR, Thordal-Christensen H (2004) The PEN1 syntaxin defines a novel cellular compartment upon fungal attack and is required for the timely assembly of papillae. Mol Biol Cell **15:** 5118-5129

Barratt DH, Kolling K, Graf A, Pike M, Calder G, Findlay K, Zeeman SC, Smith AM (2011) Callose synthase GSL7 is necessary for normal phloem transport and inflorescence growth in Arabidopsis. Plant Physiol **155:** 328-341

Bednarek P, Pislewska-Bednarek M, Svatos A, Schneider B, Doubsky J, Mansurova M, Humphry M, Consonni C, Panstruga R, Sanchez-Vallet A, Molina A, Schulze-Lefert P (2009) A glucosinolate metabolism pathway in living plant cells mediates broad-spectrum antifungal defense. Science **323:** 101-106

Bohlenius H, Morch SM, Godfrey D, Nielsen ME, Thordal-Christensen H (2010) The multivesicular body-localized GTPase ARFA1b/1c is important for callose deposition and ROR2 syntaxin-dependent preinvasive basal defense in barley. Plant Cell **22:** 3831-3844

Boller T, Felix G (2009) A renaissance of elicitors: perception of microbe-associated molecular patterns and danger signals by pattern-recognition receptors. Annu Rev Plant Biol **60:** 379-406

Briggs AG, Bent AF (2011) Poly(ADP-ribosyl)ation in plants. Trends Plant Sci **16:** 372-380

Burkle A, Virag L (2013) Poly(ADP-ribose): PARadigms and PARadoxes. Mol Aspects Med **34:** 1046-1065

Chen XY, Liu L, Lee E, Han X, Rim Y, Chu H, Kim SW, Sack F, Kim JY (2009) The Arabidopsis callose synthase gene GSL8 is required for cytokinesis and cell patterning. Plant Physiol **150:** 105-113

Clay NK, Adio AM, Denoux C, Jander G, Ausubel FM (2009) Glucosinolate metabolites required for an Arabidopsis innate immune response. Science **323:** 95-101

Collins NC, Thordal-Christensen H, Lipka V, Bau S, Kombrink E, Qiu JL, Huckelhoven R, Stein M, Freialdenhoven A, Somerville SC, Schulze-Lefert P (2003) SNARE-protein-mediated disease resistance at the plant cell wall. Nature **425:** 973-977

De Bary A (1863) Recherches sur le développement de quelques champignons parasites. Annales des Sciences Naturelles Botanique **20:** 5-148

Dong X, Hong Z, Sivaramakrishnan M, Mahfouz M, Verma DP (2005) Callose synthase (CalS5) is required for exine formation during microgametogenesis and for pollen viability in Arabidopsis. Plant J **42:** 315-328

Douglas CM, Foor F, Marrinan JA, Morin N, Nielsen JB, Dahl AM, Mazur P, Baginsky W, Li W, el-Sherbeini M (1994) The Saccharomyces cerevisiae FKS1 (ETG1) gene encodes an integral membrane protein which is a subunit of 1,3-beta-D-glucan synthase. Proc Natl Acad Sci U S A **91:** 12907-12911

Ellinger D, Naumann M, Falter C, Zwikowics C, Jamrow T, Manisseri C, Somerville SC, Voigt CA (2013) Elevated early callose deposition results in complete penetration resistance to powdery mildew in Arabidopsis. Plant Physiol **161:** 1433-1444

Ellinger D, Voigt CA (2014) Callose biosynthesis in Arabidopsis with a focus on pathogen response: what we have learned within the last decade. Ann Bot **114:** 1349-1358

Enns LC, Kanaoka MM, Torii KU, Comai L, Okada K, Cleland RE (2005) Two callose synthases, GSL1 and GSL5, play an essential and redundant role in plant and pollen development and in fertility. Plant Mol Biol **58:** 333-349

Gibson BA, Kraus WL (2012) New insights into the molecular and cellular functions of poly(ADP-ribose) and PARPs. Nat Rev Mol Cell Biol **13:** 411-424

Gomez-Gomez L, Boller T (2000) FLS2: an LRR receptor-like kinase involved in the perception of the bacterial elicitor flagellin in Arabidopsis. Mol Cell **5:** 1003-1011

Guseman JM, Lee JS, Bogenschutz NL, Peterson KM, Virata RE, Xie B, Kanaoka MM, Hong Z, Torii KU (2010) Dysregulation of cell-to-cell connectivity and stomatal patterning by loss-of-function mutation in Arabidopsis chorus (glucan synthase-like 8). Development **137:** 1731-1741

Hong Z, Delauney AJ, Verma DP (2001) A cell plate-specific callose synthase and its interaction with phragmoplastin. Plant Cell **13:** 755-768

Huckelhoven R, Panstruga R (2011) Cell biology of the plant-powdery mildew interaction. Curr Opin Plant Biol **14:** 738-746

Jacobs AK, Lipka V, Burton RA, Panstruga R, Strizhov N, Schulze-Lefert P, Fincher GB (2003) An Arabidopsis Callose Synthase, GSL5, Is Required for Wound and Papillary Callose Formation. Plant Cell **15:** 2503-2513

Jones JD, Dangl JL (2006) The plant immune system. Nature **444:** 323-329

Lamb RS, Citarelli M, Teotia S (2012) Functions of the poly(ADP-ribose) polymerase superfamily in plants. Cell Mol Life Sci **69:** 175-189

Li B, Meng X, Shan L, He P (2016) Transcriptional Regulation of Pattern-Triggered Immunity in Plants. Cell Host Microbe **19:** 641-650

Li W, Zhao Y, Liu C, Yao G, Wu S, Hou C, Zhang M, Wang D (2012) Callose deposition at plasmodesmata is a critical factor in restricting the cell-to-cell movement of Soybean mosaic virus. Plant Cell Rep **31:** 905-916

Lipka V, Dittgen J, Bednarek P, Bhat R, Wiermer M, Stein M, Landtag J, Brandt W, Rosahl S, Scheel D, Llorente F, Molina A, Parker J, Somerville S, Schulze-Lefert P (2005) Pre- and postinvasion defenses both contribute to nonhost resistance in Arabidopsis. Science **310:** 1180-1183

Luna E, Pastor V, Robert J, Flors V, Mauch-Mani B, Ton J (2011) Callose deposition: a multifaceted plant defense response. Mol Plant Microbe Interact **24:** 183-193

Macho AP, Zipfel C (2014) Plant PRRs and the activation of innate immune signaling. Mol Cell **54:** 263-272

Miya A, Albert P, Shinya T, Desaki Y, Ichimura K, Shirasu K, Narusaka Y, Kawakami N, Kaku H, Shibuya N (2007) CERK1, a LysM receptor kinase, is essential for chitin elicitor signaling in Arabidopsis. Proc Natl Acad Sci U S A **104:** 19613-19618

Nicholson RL, Hammerschmidt R (1992) Phenolic Compounds and Their Role in Disease Resistance. Annu Rev Phytopathol **30:** 369-389

Nielsen ME, Feechan A, Bohlenius H, Ueda T, Thordal-Christensen H (2012) Arabidopsis ARF-GTP exchange factor, GNOM, mediates transport required for innate immunity and focal accumulation of syntaxin PEN1. Proc Natl Acad Sci U S A **109:** 11443-11448

Nielsen ME, Thordal-Christensen H (2013) Transcytosis shuts the door for an unwanted guest. Trends Plant Sci **18:** 611-616

Nishimura MT, Stein M, Hou BH, Vogel JP, Edwards H, Somerville SC (2003) Loss of a callose synthase results in salicylic acid-dependent disease resistance. Science **301:** 969-972

Nomura K, Debroy S, Lee YH, Pumplin N, Jones J, He SY (2006) A bacterial virulence protein suppresses host innate immunity to cause plant disease. Science **313:** 220-223

Richmond TA, Somerville CR (2000) The cellulose synthase superfamily. Plant Physiol **124:** 495-498

Schreiber V, Dantzer F, Ame JC, de Murcia G (2006) Poly(ADP-ribose): novel functions for an old molecule. Nat Rev Mol Cell Biol **7:** 517-528

Schwessinger B, Zipfel C (2008) News from the frontline: recent insights into PAMP-triggered immunity in plants. Curr Opin Plant Biol **11:** 389-395

Stein M, Dittgen J, Sanchez-Rodriguez C, Hou BH, Molina A, Schulze-Lefert P, Lipka V, Somerville S (2006) Arabidopsis PEN3/PDR8, an ATP binding cassette transporter, contributes to nonhost resistance to inappropriate pathogens that enter by direct penetration. Plant Cell **18:** 731-746

Stone B, Clarke A (1992) Chemistry and biology of (1, 3)-D-glucans. Victoria, Australia.: La Trobe University Press

Thordal-Christensen H, Zhang Z, Wei Y, Collinge DB (1997) Subcellular localization of H2O2 in plants. H2O2 accumulation in papillae and hypersensitive response during the barley-powdery mildew interaction. Plant J **11:** 1187-1194

Toller A, Brownfield L, Neu C, Twell D, Schulze-Lefert P (2008) Dual function of Arabidopsis glucan synthase-like genes GSL8 and GSL10 in male gametophyte development and plant growth. Plant J **54:** 911-923

Underwood W, Somerville SC (2013) Perception of conserved pathogen elicitors at the plasma membrane leads to relocalization of the Arabidopsis PEN3 transporter. Proc Natl Acad Sci U S A **110:** 12492-12497

Vance CP, Kirk TK, Sherwood RT (1980) Lignification as a Mechanism of Disease Resistance. Annu Rev Phytopathol **18:** 259-288

Vaten A, Dettmer J, Wu S, Stierhof YD, Miyashima S, Yadav SR, Roberts CJ, Campilho A, Bulone V, Lichtenberger R, Lehesranta S, Mahonen AP, Kim JY, Jokitalo E, Sauer N, Scheres B, Nakajima K, Carlsbecker A, Gallagher KL, Helariutta Y (2011) Callose biosynthesis regulates symplastic trafficking during root development. Dev Cell **21:** 1144-1155

Vogel J, Somerville S (2000) Isolation and characterization of powdery mildew-resistant Arabidopsis mutants. Proc Natl Acad Sci U S A **97:** 1897-1902

Voigt CA (2014) Callose-mediated resistance to pathogenic intruders in plant defense-related papillae. Front Plant Sci **5:** 168

Wan J, Zhang XC, Neece D, Ramonell KM, Clough S, Kim SY, Stacey MG, Stacey G (2008) A LysM receptor-like kinase plays a critical role in chitin signaling and fungal resistance in Arabidopsis. Plant Cell **20:** 471-481

Xie B, Wang X, Zhu M, Zhang Z, Hong Z (2011) CalS7 encodes a callose synthase responsible for callose deposition in the phloem. Plant J **65:** 1-14

Zipfel C, Kunze G, Chinchilla D, Caniard A, Jones JD, Boller T, Felix G (2006) Perception of the bacterial PAMP EF-Tu by the receptor EFR restricts Agrobacterium-mediated transformation. Cell **125:** 749-760

Chapter 2: PARP2 is the Predominant Poly(ADP-Ribose) Polymerase in Arabidopsis DNA Damage and Immune Responses

This chapter was previously published as:

Song J, Keppler BD, Wise RR, Bent AF (2015) PARP2 Is the Predominant Poly(ADP-Ribose) Polymerase in Arabidopsis DNA Damage and Immune Responses. PLoS Genet 11(5): e1005200. doi:10.1371/journal.pgen.1005200

Contributions: Junqi Song performed the majority of the work described. I assisted in generating the *parp1parp2* double mutants, performed the callose assays, and wrote portions of the manuscript.

2.1 Abstract

Poly (ADP-ribose) polymerases (PARPs) catalyze the transfer of multiple poly(ADP-ribose) units onto target proteins. Poly(ADP-ribosyl)ation plays a crucial role in a variety of cellular processes including, most prominently, auto-activation of PARP at sites of DNA breaks to activate DNA repair processes. In humans PARP1 (the founding and most characterized member of the PARP family) accounts for more than 90% of overall cellular PARP activity in response to DNA damage. We have found that, in contrast with animals, in *Arabidopsis thaliana* PARP2 (At4g02390) rather than PARP1 (At2g31320) makes the greatest contribution to PARP activity and organismal viability in response to genotoxic stresses caused by bleomycin, mitomycin C or gamma-radiation. Plant PARP2 proteins carry SAP DNA binding motifs rather than the zinc finger domains common in plant and animal PARP1 proteins. PARP2 also makes stronger contributions than PARP1 to plant immune responses including restriction of pathogenic *Pseudomonas syringae* pv. *tomato* growth and reduction of infection-associated DNA double-strand break abundance. For poly(ADP-ribose) glycohydrolase (PARG) enzymes, we find that Arabidopsis PARG1 and not PARG2 is the major contributor to poly(ADP-ribose) removal from acceptor proteins. The activity or abundance of PARP2 is influenced by PARP1 and PARG1. PARP2 and PARP1 physically interact with each other, and with PARG1 and PARG2, suggesting relatively direct regulatory interactions among these mediators of the balance of poly(ADP-ribosyl)ation. As with plant PARP2, plant PARG proteins are also structurally distinct from their animal counterparts. Hence core aspects of plant poly(ADP-ribosyl)ation are mediated by substantially different enzymes than in animals, suggesting the likelihood of substantial differences in regulation.

2.2 Author Summary

All living organisms face constant challenges from environmental factors. Appropriate and rapid responses to external stimuli are crucial for maintenance of genome integrity and cell survival. Poly(ADP-ribosyl)ation is a post-translational modification and contributes to multiple molecular and cellular processes including a prominent role in DNA damage repair. Human PARP1, the founding and most characterized member of the PARP family, accounts for more than 90% of overall molecular and cellular PARP activity in response to DNA damage while PARP2 supplies a minor portion of this PARP activity. Here we show that Arabidopsis PARP2 rather than PARP1 plays the predominant role in poly(ADP-ribosyl)ation and organismal resilience in response to either chemically-induced DNA damage or pathogen infections. We show that the activity and abundance of PARP2 is regulated by both PARP1 and PARG1. We also show that Arabidopsis PARG1 rather than PARG2 is the major contributor to removal poly(ADP-ribose) from acceptor proteins. Core aspects of plant poly(ADP-ribosyl)ation are mediated by substantially different enzymes than in animals, suggesting the likelihood of substantial differences in regulation.

2.3 Introduction

Appropriate and rapid responses to external stimuli can be crucial for maintenance of cellular and organismal viability, especially under stress conditions. Both biotic and abiotic stresses can induce genome DNA damage (Gill and Tuteja, 2010; Chatzinikolaou et al., 2014; Song and Bent, 2014; Weitzman and Weitzman, 2014). Maintenance of genome integrity via DNA damage repair then becomes essential, in both germ-line and somatic cells (Papamichos-Chronakis and Peterson, 2013; Ermolaeva and Schumacher, 2014; Weitzman and Weitzman, 2014).

Poly(ADP-ribosyl)ation is a post-translational modification mediated by poly(ADP-ribose) polymerase (PARP) enzymes, in which negatively charged ADP-ribose units are transferred from donor nicotinamide adenine dinucleotide (NAD^+) molecules onto target proteins (Gibson and Kraus, 2012). PARP enzymes are themselves the most prominent poly(ADP-ribosyl)ation target. Poly(ADP-ribosyl)ation plays a key role in a wide range of cellular responses including DNA repair, chromatin modification, control of transcription and cell death (Gibson and Kraus, 2012; Luo and Kraus, 2012; Burkle and Virag, 2013). Poly(ADP-ribosyl)ation and PARP proteins have been identified in a wide variety of plants and animals as well as bacteria, fungi and double-stranded DNA viruses (Hassa and Hottiger, 2008; Briggs and Bent, 2011; Lamb et al., 2012). In humans, 17 PARP proteins have been identified based on homology to PARP1, the founding member of the PARP family (Schreiber et al., 2006). PARP1 accounts for approximately 90% of the PARP activity in mammalian cells under genotoxic situations, while PARP2 is apparently responsible for the remaining 10% (Shieh et al., 1998; Ame et al., 1999; Schreiber et al., 2002).

The Arabidopsis genome encodes three PARP proteins that carry a PARP signature motif, as well as RCD1 and five SRO ("Similar to RCD One") proteins with a variant form of the PARP signature (Adams-Phillips et al., 2010; Citarelli et al., 2010; Jaspers et al., 2010; Briggs and Bent, 2011). Although the names of plant PARP proteins have in some instances been reversed, the product of the Arabidopsis *At2g31320* gene (NCBI NP_850165.1) is herein called PARP1 and the Arabidopsis *At4g02390* product (NCBI NP_192148.2) is PARP2, based on their relative similarities to the earlier-named and extensively studied animal homologs (S1 Fig) (Briggs and Bent, 2011; Jia et al., 2013). PARP2-like proteins are broadly conserved across diverse plant taxa (S2 Fig), while PARP1 is broadly conserved across plants and animals [11, 18]. Arabidopsis PARP3 contains variant active site residues that suggest lack of PARP catalytic function (Lamb et al., 2012), and expression of Arabidopsis PARP3 is restricted to seed tissues (Rissel et al., 2014). The SROs (including RCD1) are a conserved family of plant-specific proteins that have functions in development and abiotic stress responses (Jaspers et al., 2010). Although a wheat SRO protein that does possesses PARP activity was recently described (Liu et al., 2014), Arabidopsis SROs contain variant PARP motifs that both bioinformatically and biochemically were found to lack ADP-ribosyl transferase activity (Jaspers et al., 2010).

PARPs are widely known for their roles in genotoxic stress, DNA damage repair and programmed cell death in animals (Schreiber et al., 2006; Heeres and Hergenrother, 2007; Krishnakumar and Kraus, 2010). Although additional roles for PARP enzymes are being discovered (Burkle and Virag, 2013), one of the best-known roles of PARPs is their function as DNA damage sensors. PARP1 in particular binds in its poly(ADP-ribosyl)ated form to ssDNA and dsDNA breaks and initiates events that attract DNA damage repair machinery to the sites of damage (Huber et al., 2004; Gibson and Kraus, 2012). A growing body of evidence indicates that

plant PARPs have similar functions. PARP proteins are involved in microhomology mediated back-up non-homologous end joining in Arabidopsis (Jia et al., 2013). Arabidopsis PARP1 and PARP2 accumulate rapidly and strongly in response to ionizing radiation, whereas PARP2 is preferentially induced by dehydration and excess cadmium (Doucet-Chabeaud et al., 2001). PARP in soybean cells is differentially involved in responses to mild and intense oxidative stresses, through regulating DNA repair and programmed cell death (Amor et al., 1998). Knocking down PARP activities in Arabidopsis and oilseed rape plants by chemical inhibition or gene silencing inhibited cell death and made plants more tolerant to a broad range of abiotic stresses including high light, drought and heat (De Block et al., 2005; Vanderauwera et al., 2007). This is due at least in part to induction of specific abscisic acid signaling pathways [29]. PARP inhibition also enhances Arabidopsis growth by promoting the leaf cell number (Schulz et al., 2012; Schulz et al., 2014). In animals, PARP proteins have been implicated in regulation of telomere length, telomere activity and chromosome end protection (Abd Elmageed et al., 2012; De Vos et al., 2012). However, it appears that Arabidopsis PARP proteins make limited contributions to telomere regulation and maintenance, although telomere dysfunction triggers PARP activation (Boltz et al., 2014).

Poly(ADP-ribosyl)ation is reversible; covalently attached poly(ADP-ribose) can be cleaved from acceptor proteins by poly(ADP-ribose) glycohydrolase (PARG) (Gibson and Kraus, 2012; Luo and Kraus, 2012). Mammalian genomes encode a single *PARG* gene (Lin et al., 1997; Ame et al., 1999) and mutation of *PARG* caused enhanced sensitivity to genotoxic stress and elevated accumulation of poly(ADP-ribose), leading to embryonic lethality in mice and *Drosophila* (Hanai et al., 2004; Koh et al., 2004). However, the human *PARG* gene undergoes alternative splicing, resulting in multiple PARG protein isoforms that localize to

different cellular compartments (Meyer-Ficca et al., 2004). Unlike animal models the Arabidopsis genome encodes two *PARG* genes, *PARG1* and *PARG2*, with 52% amino acid identity (S1 Fig) (Briggs and Bent, 2011). *PARG1* and *PARG2*, as well as an inactive pseudogene *At2g31860*, are all located adjacent to each other on Arabidopsis chromosome 2 (Briggs and Bent, 2011). Much less is known about the function of PARGs than PARPs in plant poly(ADP-ribosyl)ation. PARG1 was originally identified to play a role in circadian oscillation in Arabidopsis (Panda et al., 2002). The Arabidopsis *PARG2* gene is robustly induced by pathogen-associated molecular patterns (PAMPs) and numerous different pathogens, but disruption of *PARG1*, not *PARG2*, altered various plant defense responses (Adams-Phillips et al., 2008; Adams-Phillips et al., 2010). Similar to its counterpart, PARP, Arabidopsis PARG1 has also been implicated in drought, osmotic and oxidative stress responses (Li et al., 2011).

Despite the above work, the mechanisms by which PARPs and PARGs regulate diverse cellular processes in plants remain largely unknown. The present study used mutational and biochemical approaches to assess the relative contributions of Arabidopsis PARP1/2 and PARG1/2. We present evidence that, unlike in animals, PARP2 rather than PARP1 plays the major role in plant DNA damage and immune responses. We also demonstrate that PARG1 rather than PARG2 is the primary enzyme that counteracts poly(ADP-ribosyl)ation in Arabidopsis. In addition, we discover that PARP1 associates with PARP2, and that PARP1 and PARP2 interact with both PARG1 and PARG2.

2.4 Results

Mutant *parp2* plants are more sensitive to DNA damage agents than wild-type or *parp1* plants

To examine the functional importance of PARP1 and PARP2 in plant poly(ADP-ribosyl)ation and in effective responses to DNA damage agents, we tested sensitivity to genotoxic agents in Arabidopsis *parp1* and *parp2* single mutants and in *parp1parp2* double mutants. Two Arabidopsis T-DNA insertion lines with mutations in PARP1 (At2g31320) and one for PARP2 (At4g02390) were identified: *parp1-1* (GABI_380E06), *parp1-2* (GABI_382F01) and *parp2-1* (GABI_420G03). Double mutant *parp1parp2* plants were generated by genetic crosses. The chemical bleomycin is a potent inducer of DNA double-strand breaks (DSB), with a mode of action similar to that of ionizing radiation (Povirk, 1996). Plants were grown on MS plates supplemented with bleomycin and organismal-level sensitivity to DNA damage was scored as the number of plants without true leaves 14 days after germination (Durrant et al., 2007; Song et al., 2011). As shown in Fig. 1A, in bleomycin-free MS plates almost all wild-type and mutant plants produced normal true leaves. In MS plates supplemented with 1.5 μg/ml of bleomycin, over 95% of wild-type plants still produced true leaves, whereas approximately 35% of the *parp1-2* plants had no true leaves. Strikingly, more than 50% of the *parp2-1* single mutants failed to generate true leaves, similar to *parp1-2parp2-1* double mutants (Fig. 1A). RT-PCR analysis confirmed that expression of *PARP1* or *PARP2* was abolished in the respective mutants (S3 Fig). Although contributions of PARP1 cannot be ruled out, ANOVA across three replicate experiments indicated that the growth defects on bleomycin were significantly worse than wild-type only for the *parp2* and *parp1parp2* double mutants. The experiments suggest that PARP2 is a more substantial contributor than PARP1 to a successful

response to bleomycin. Similarly, increased sensitivity to the DNA alkylating agent methyl methane sulfonate (MMS) has been observed in a *parp1parp2* double mutant (Jia et al., 2013; Boltz et al., 2014).

To further examine the role of PARP1 and PARP2 in DNA damage repair in Arabidopsis we analyzed sensitivity to mitomycin C, an interstrand DNA crosslinking agent (Dronkert and Kanaar, 2001). Similar to bleomycin treatment, the *parp1-2* and *parp2-1* mutants exhibited moderately or markedly increased sensitivity to mitomycin C, respectively (Fig. 1B). ANOVA across three replicate experiments again indicated that the growth defects, this time in response to mitomycin C, were significantly worse than wild-type only for the *parp2* and *parp1parp2* double mutants. However, the *P*-value for the Col vs. *parp1* contrast was 0.054 (very close to $P < 0.05$ significance), and PARP1 contributions were also indicated because the *parp1parp2* double mutant grew significantly less well than the *parp2* single mutant. Similar results after mitomycin C treatment also were obtained using a second *parp1* mutant allele and *parp1/parp2* double mutant line (S4 Fig). These mitomycin C experiments indicate that PARP1 and PARP2 are both required for effective repair of damaged DNA, but that PARP2 plays a stronger role in tolerance of plant DNA damage.

PARP2 accounts for most of the DNA damage-induced PARP activity in Arabidopsis

To investigate whether disruption of the Arabidopsis *PARP1* or *PARP2* genes disrupts *in planta* poly(ADP-ribosyl)ation of target proteins, wild-type and *parp* mutant plants were treated for 18h with increasing concentrations of bleomycin and poly(ADP-ribosyl)ated proteins were monitored on protein immunoblots using an anti-PAR (anti-poly(ADP-ribose)) antibody (Fig. 2). Greatly increased levels of poly(ADP-ribosyl)ation were observed in wild-type plants after

treatment with bleomycin at concentrations ranging from 2.5 to 10 μg/ml. Substantial amounts of poly(ADP-ribosyl)ated proteins were still detected despite knockout of PARP1 in the *parp1-1* or *parp1-2* single mutants. This is unexpected given that Arabidopsis PARP1 is the zinc finger-containing homolog of animal PARP1, which has been abundantly demonstrated to make the greatest contribution to poly(ADP-ribosyl)ation in response to DNA damage (Shieh et al., 1998; Ame et al., 1999; Schreiber et al., 2002; Hassa and Hottiger, 2008; Gibson and Kraus, 2012). Knockout of PARP2 rather than PARP1 severely depleted detectable PARP activity in Arabidopsis, with only marginal elevation of poly(ADP-ribosyl)ated proteins detected after bleomycin treatment of *parp2-1* mutant plants (Fig. 2). Little or no PARP activity was observed in the *parp1-1parp2-1* or *parp1-2parp2-1* mutants (Fig. 2). Under long exposure conditions residual PARP activity in the *parp1-2parp2-1* double mutants still remained barely detectable.

We had obtained RT-PCR evidence that the *parp2-1* mutation eliminated PARP2 transcript (Fig. 1B) but further tests were then conducted to confirm loss of PARP2 protein production in the *parp2-1* mutant, as well as to confirm the specificity of a custom-raised PARP2 polyclonal antibody. In wild-type Col-0 plants treated with bleomycin, PARP2 protein was detected using the anti-PARP2 antibody (S5 Fig). PARP2 protein was still detected in *parp1-1* and in *parp1-2* mutant plants, but not in the *parp2-1* line or in two separate *parp1parp2* double mutant lines, indicating that *parp2-1* is a null mutant (S5 Fig).

To confirm that the compromised PARP activity in *parp2-1* is due to the T-DNA insertion in the *PARP2* gene, we complemented the *parp2-1* mutant with a construct carrying native Arabidopsis *PARP2* promoter sequences driving expression of Arabidopsis *PARP2* genomic DNA fused to an HA epitope tag. Five independent T2 transgenic lines with different expression levels of PARP2-HA were chosen for complementation analysis. As shown in S6 Fig,

poly(ADP-ribosyl)ation activity was restored in the complemented lines. We further observed that the abundance of poly(ADP-ribosyl)ated proteins present in response to the DNA damaging agent bleomycin correlated with the levels of PARP2 protein in the selected lines (S6 Fig). As a side-matter, the anti-PARP2 antibody was used to detect PARP2 in these complementation experiments. We were not able to detect the PARP2-HA fusion protein using an anti-HA antibody (that worked well with other HA-tagged proteins), possibly due to cleavage or inaccessibility of the C-terminal tag on PARP2. Overall, the above results indicate that PARP1 and PARP2 both contribute to poly(ADP-ribosyl)ation, but that PARP2 is the primary Arabidopsis enzyme responsible for poly(ADP-ribosyl)ation activity in response to DNA damage.

In related experiments we irradiated plants with 150 Gy of γ-radiation, a dose that is sufficient to induce DNA double strand breaks (Friesner et al., 2005), and PARP activity was monitored (Fig. 3A). Markedly increased amounts of poly(ADP-ribosyl)ated proteins were detected in wild-type plants from 20 to 60 min after irradiation. This γ-ray-induced PARP activity was substantially reduced in the *parp1-2* mutant. An even more complete reduction in poly(ADP-ribosyl)ation was observed in the *parp2-1* single mutant, and a similarly complete reduction was observed in the *parp1-2parp2-1* double mutant. With the γ-ray-treated plant samples we also measured the level of phosphorylated histone γ-H2AX, a standard indicator of DNA double-strand breaks (Rogakou et al., 1998; Kinner et al., 2008). Compared to wild-type plants, in the *parp1-2* single mutants elevated DNA damage was detected as an increase in the intensity of the γ-H2AX band (Fig. 3B). More DNA damage was reproducibly detected in the *parp2-1* single mutant than the *parp1-2* mutant, and even more significantly increased DNA damage was observed in the *parp1-2parp2-1* double mutant (Fig. 3B). Hence as in earlier

experiments where plant growth in the face of DNA damage was monitored (Fig. 1), experiments monitoring abundance of γ-ray-induced DNA double-strand breaks (Fig. 3B) detected contributions of PARP1 as well as PARP2. However, these experiments with γ-ray-treated plants again indicated that PARP2 accounts for majority of the cellular PARP activity that is activated in response to DNA damage (Fig. 3A).

Subcellular localization of PARP1/2 and PARG1/2 proteins

To examine whether Arabidopsis PARPs are targeted to the nucleus as in animals, PARP1 and PARP2 proteins fusions to the C-terminus of green fluorescent protein (GFP) were expressed in leaves of *Nicotiana benthamiana* by agroinfiltration. Confocal fluorescence microscopy revealed that both PARP1 and PARP2 predominantly accumulate in the nucleus (Fig. 4A). To determine the subcellular location of PARPs in Arabidopsis, we expressed PARP1-GFP and PARP2-GFP C-terminal fusion proteins in stable transformants of wild-type Col-0. Fluorescence microscopic examination of transgenic Arabidopsis plants expressing *35S:PARP1-GFP* or *35S:PARP2-GFP* detected PARP1 and PARP2 only in the nucleus, in both leaves and roots (Fig. 4B), consistent with a previous report (Babiychuk et al., 2001). Notably, multiple foci were detected throughout the nucleus of root tissues expressing *35S:PARP2-GFP*.

Poly(ADP-ribosyl)ation is impacted by PARP enzymes and also by poly(ADP-ribose) glycohydrolase (PARG) enzymes that remove poly(ADP-ribosyl)ation, so experiments with PARG proteins were also carried out. PARG1-GFP and PARG2-GFP fusion proteins expressed in *N. benthamiana* were reproducibly observed both in the cytoplasm and nucleus (Fig. 4C). PARG2 mRNA abundance was previously shown to be significantly increased in response to virulent or avirulent *Pseudomonas syringae* pv. *tomato* (*Pst*) strains or the PAMPs flg22 or elf18

(Adams-Phillips et al., 2008; Adams-Phillips et al., 2010). In the present study, up-regulation of PARG2 at the protein level was confirmed in transgenic Arabidopsis plants. The abundance of PARG2-GFP protein expressed under control of the *PARG2* promoter sequence was substantially increased in leaves within 8 hr after exposure to *Pst(avrRpt2)* (S7 Fig).

PARG1 **(but not** ***PARG2*****) mediates poly(ADP-ribose) removal in plants responding to bleomycin**

Previous work by our group had detected multiple impacts on plant defense for Arabidopsis *parg1* mutants, unlike Arabidopsis *parg2* mutants (Adams-Phillips et al., 2008; Adams-Phillips et al., 2010). To determine if Arabidopsis *PARG1* and/or *PARG2* confer detectable poly(ADP-ribose) glycohydrolase activity, *parg1-1*, *parg2-1* and Col-0 plants were treated with 2.5 μg/ml bleomycin and the abundance of poly(ADP-ribosyl)ated proteins was examined. Mutation of *PARG1* resulted in significantly elevated presence of poly(ADP-ribosyl)ation in total protein extracts compared with wild-type plants, as might be expected for loss of an active poly(ADP-ribose) glycohydrolase (Fig. 5A). Surprisingly but consistent with the Adams-Philips et al. data (2010), disruption of Arabidopsis *PARG2* caused little or no increase in poly(ADP-ribosyl)ation (Fig. 5A). The data suggest that PARG1 is the primary enzyme that catalyzes the removal of poly(ADP-ribose) from acceptor proteins and that PARG2 makes little or no contribution to this activity. The primary mediator of bleomycin-induced elevation of poly(ADP-ribosyl)ation, PARP2, exhibited increased protein levels in response to bleomycin in all three genetic backgrounds. Notably, the accumulation of PARP2 induced by bleomycin is reduced in the *parg1-2* mutant relative to wild-type (Fig. 5B), suggesting that PARG1 can influence the levels of PARP2 protein.

PARP2 activity is regulated by PARP1 in response to DNA alkylating agent mitomycin C

In further work to characterize the role of PARPs in plant DNA damage responses, wild-type and *parp* mutant plants were treated with mitomycin C to induce DNA cross-linking (Tomasz et al., 1987) and the level of poly(ADP-ribosyl)ated proteins was then monitored. As shown in Fig. 6, mitomycin C caused increased PARP activity in wild-type plants. As with the bleomycin and γ-ray experiments (Figs. 3 and 4), almost no poly(ADP-ribosyl)ation activity was detected after mitomycin C treatment in *parp2-1* mutant plants (Fig. 6). However, increased rather than decreased abundance of poly(ADP-ribosyl)ation was observed in *parp1* mutants, in separate experiments with either the *parp1-1* or *parp1-2* alleles, in response to mitomycin C (Fig. 6). This is unlike the poly(ADP-ribosyl)ation behavior of the same mutants in response to bleomycin or γ-irradiation (Fig. 2). The mitomycin C-induced increase in poly(ADP-ribosyl)ation caused by mutation of PARP1 was eliminated if PARP2 was also mutated (*parp1-1parp2-1* and *parp1-2parp2-1* double mutants, Fig. 6). This interesting finding suggests that loss of PARP1 can in some situations lead to elevated PARP2 activity. Said another way, PARP1 may suppress PARP2 activity under certain stress conditions such as after exposure to mitomycin C.

PARP2 is required for normal basal resistance responses in Arabidopsis

To examine the role of *PARP* genes in plant defense responses, the Arabidopsis *parp* mutants were inoculated with the virulent bacterial pathogen *Pseudomonas syringae* pv. *tomato* (*Pst*) strain DC3000. As shown in Fig. 7A, the *parp2-1* single and *parp1-2parp2-1* double mutants exhibited enhanced susceptibility in comparison to wild-type plants, whereas bacterial

growth in the *parp1-2* single mutant was similar to that in wild-type. This important result demonstrates an impact of loss of poly(ADP-ribosyl)ation activity on the capacity of Arabidopsis to limit the growth of this virulent bacterial pathogen. The finding also suggests that wild-type PARP2 plays a greater role than PARP1 in basal defense against this pathogen.

Experiments with *Pst* DC3000 expressing the effector protein AvrRpt2 (which triggers RPS2-mediated defense in naturally *RPS2*$^{+}$ Arabidopsis Col-0 plants) were also conducted, to test for impacts of poly(ADP-ribosyl)ation on the stronger *R* gene-mediated defense response (also known as effector-triggered immunity) (Jones and Dangl, 2006). No impact of *PARP* mutations was detected (Fig. 7A).

Impacts of *PARP* genes on PAMP-triggered immunity responses (Jones and Dangl, 2006; Boller and Felix, 2009; Dodds and Rathjen, 2010) were also examined. Callose deposition was not detectably affected in *parp1-2* or *parp2-1* single mutants, but callose deposition was significantly enhanced in the *parp1-2parp2-1* double mutant (Fig. 7B). Enhanced callose deposition was also observed in *parp1-1parp2-1* double mutant plants (different *parp1* allele; S8 Fig). Reinforcing rather than antagonistic roles of PARP and PARG activity were suggested by the related observation that, like *parp1parp2* mutants, *parg1* mutant plants exhibited elevated callose deposition in response to flg22 (S9 Fig). Seedling growth inhibition assays (Gomez-Gomez and Boller, 2000), one of the most sensitive indicators of basal defense activation in response to PAMP treatment, also showed that disruption of PARP activity led to a stronger response to flg22 (Fig. 7C). No significant difference in the flg22-induced ROS burst was observed for the *parp* mutants (Fig. 7D).

We recently showed that microbial pathogens including virulent *Pst* DC3000 induce DNA DSBs in plant host genomes (Song and Bent, 2014). To monitor DSB induction in

Arabidopsis *parp* mutants in response to *Pst*, we monitored the accumulation of γ-H2AX. Across replicate experiments, and consistent with the bacterial growth data of Fig. 7A, no impact of *parp* mutations on DSB induction was observed during the strong *R* gene-mediated responses triggered by *Pst* DC3000(*avrRpt2*) (Fig. 7E). However, with virulent *Pst* DC3000 lacking *avrRpt2*, elevated levels of γ-H2AX were observed 4 and 8 hours after infection in leaves of the *parp2-1* and *parp1-2parp2-1* mutants as compared to wild-type plants (Fig. 7E). No increases of γ-H2AX were observed in *parp1-2* plants. These results indicate, as might be predicted (Song and Bent, 2014), that there is a link between plant poly(ADP-ribosyl)ation and prevention or repair of pathogen-induced DNA damage. The results also indicate that in Arabidopsis, PARP2 plays a more significant role than PARP1 in this prevention/repair of pathogen-induced DNA damage.

PARP1 interacts with PARP2; PARG1 interacts with PARG2; PARP1 and PARP2 interact with both PARG1 and PARG2

To determine if plant PARP1 associates with PARP2, we carried out coimmunoprecipitation assays in *N. benthamiana*. As shown in Fig. 8A, myc-tagged PARP1 was coimmunoprecipitated by GFP-tagged PARP2 using an anti-GFP antibody, indicating that at least some PARP1 is present in complexes with PARP2. The interaction was observed without as well as with bleomycin treatment. This readily detectable interaction suggests that PARP2 activity may be regulated in part by physical contact with PARP1. Similarly, PARG1 and PARG2 (the only two PARG proteins in Arabidopsis) also associated with each other (Fig. 8B), although that interaction required longer exposures than the PARP1-PARP2 product of Fig. 8A to detect a co-IP band of similar intensity. We also investigated whether PARPs interact with

PARG1 and/or PARG2. The reproducibly detectable co-immunoprecipitation products in Fig. 8C showed that PARP1 interacts with both PARG1 and PARG2, with or without bleomycin treatment. Similarly, PARP2 also complexes with both PARG1 and PARG2 (Fig. 8D). Hence the regulation of PARP2 abundance and activity by PARG1 may also be achieved via physical interaction between the two proteins.

2.5 Discussion

In mammals, PARP1 is by far the predominant contributor to poly(ADP-ribosyl)ation responses to a variety of cellular stresses, and mammalian PARP1 has received the vast majority of poly(ADP-ribose) polymerase research and pharmaceutical industry attention (Gibson and Kraus, 2012; Luo and Kraus, 2012; Burkle and Virag, 2013). Arabidopsis PARP1 is the poly(ADP-ribose) polymerase with a similar domain structure to mammalian PARP1 (S1 Fig), but the relative roles of the different plant PARPs required investigation (Briggs and Bent, 2011). We used genetic and biochemical approaches to elucidate the contributions to Arabidopsis DNA damage and immune responses made by different poly(ADP-ribose) polymerase and poly(ADP-ribose) glycohydrolase gene products. For both groups of enzymes the predicted proteins have significantly divergent domain structures (S1 Fig). In contrast to the paradigm in mammals, we found that PARP2 rather than PARP1 plays the major role biochemically and in organismal-level responses to DNA damage and pathogen infections. Furthermore, we found that PARG1 rather than PARG2 is the primary enzyme that confers poly(ADP-ribose) glycohydrolase activity in Arabidopsis during the tested responses to DNA damage and pathogen infection.

Arabidopsis PARP1 shares a substantially conserved domain structure with human PARP1, whereas Arabidopsis PARP2 is more analogous to human PARP2. In mice, *parp2*

mutants exhibited some phenotypes similar to *parp1* knockouts, despite the dramatic difference between their respective specific enzymatic activities (de Murcia et al., 1997; Wang et al., 1997; Masutani et al., 2000). Although neither PARP1 nor PARP2 is required for viability in mice, *parp1parp2* double knockouts are embryonic lethal with considerable genomic instability, indicating that the PARP1 and PARP2 gene products together are essential during early embryogenesis and that the deficiency in PARP1 and PARP2 cannot be functionally compensated by other PARP family members (Menissier de Murcia et al., 2003). In contrast, when the functions of Arabidopsis PARP1 and PARP2 both were disrupted plants were developmentally normal, demonstrating that this pair of genes is not essential to viability in Arabidopsis

Overall PARP activity in Arabidopsis is significantly decreased when PARP2 is knocked out, suggesting that Arabidopsis PARP2, unlike its counterpart in animals, is responsible for majority of the PARP activity. The predominant role of Arabidopsis PARP2 was detected at more macroscopic levels by the increased sensitivity of *parp2* mutant plants to genotoxic stresses, and enhanced susceptibility to virulent *Pst* growth and to *Pst*-induced DNA DSB damage. Since poly(ADP-ribosyl)ated proteins were nearly absent in the *parp1parp2* double mutant, it is reasonable to propose that other Arabidopsis PARP-domain containing proteins have either low or no PARP activity under the conditions examined in this study. This is consistent with the bioinformatic prediction that Arabidopsis PARP3, RCD1 and SROs lack conserved active catalytic sites in the PARP domains and possibly have lost the ability to bind NAD (Jaspers et al., 2010; Lamb et al., 2012). We had previously reported that *P. syringae* induces the accumulation of poly(ADP-ribosyl)ated proteins (Adams-Phillips et al., 2010) but we

know of no studies that have identified the suite of proteins that are poly(ADP-ribosyl)ated during plant-pathogen interactions.

PARP1, the primary PARP that mediates responses such as DNA damage repair in human cells, contains zinc-finger DNA binding domains that are crucial to its function (Hassa and Hottiger, 2008; Krishnakumar and Kraus, 2010) (S1 Fig). Known DNA binding domains are absent from human PARP2. The striking finding that core poly(ADP-ribosyl)ation functions of animal PARP1 have been taken on by PARP2 in plants may be less unusual in light of the fact that plant PARP2 proteins carry N-terminal SAP (SAF-A/B, Acinus, and PIAS) domains (S2 Fig). The SAP domain is a highly conserved sequence-specific or structure-specific DNA binding motif with a four-helix bundle, known to contribute to regulation of chromatin structure and transcription (Sahara et al., 1999; Aravind and Koonin, 2000). In contrast to many other DNA recognition protein structures, one end of the helix bundle makes contact with DNA and fits into the minor groove of DNA (Okubo et al., 2004). One to four distinct SAP domains are present in plant PARP2s, depending on the plant species (S2 Fig). Structural differences in DNA binding domains between Arabidopsis PARP1 and PARP2 likely contribute intriguing differences in the substrate specificities of these two enzymes. Arabidopsis PARP1 and PARP2 also exhibit substantial divergence within their areas of shared domain structure (see Fig. 1; for amino acids #130-636 of Arabidopsis PARP2, only 56% are similar (36% identical) to the aligned Arabidopsis PARP1 amino acids #485-982). The substantially divergent structure of plant PARP2 enzymes is likely to be accompanied by substantially divergent mechanisms of regulation.

We found evidence that Arabidopsis PARP2 activity is negatively regulated by PARP1 during responses to mitomycin C, but we did not detect reproducible changes of PARP2 protein

abundance in the *parp1* mutant under the genotoxic stress conditions we examined. However, it has recently been reported that Arabidopsis PARP1 and PARP2 negatively regulate gene expression of each other (Boltz et al., 2014). We observed physical interaction (coimmunoprecipitation) of PARP1 and PARP2 in plants responding to bleomycin. The Boltz et al. data and our data point to an intriguing interplay between PARP1 and PARP2, and also suggest that different modes of action of poly(ADP-ribosyl)ation-mediated regulation may exist in plants that are not observed in animals.

In animals, poly(ADP-ribosyl)ation has recently been found to play a significant role during host-pathogen interactions. For example, *Helicobactor pylori*, a human gastric bacterial pathogen, activates nuclear regulator PARP1 (Nossa et al., 2009). Several proteins produced by pathogenic viruses have been reported to interact directly with and stimulate animal PARP1 enzymatic activity (Gordon-Shaag et al., 2003; Carbone et al., 2006), whereas others prevent PARP1 activation as virulence strategies (Muthumani et al., 2006; Zhou et al., 2009). In plants, there is also an expanding body of evidence that poly(ADP-ribosyl)ation plays critical roles in pathogenicity as well as in immune responses (Bartsch et al., 2006; Jambunathan and Mahalingam, 2006; Ge et al., 2007; Adams-Phillips et al., 2008; Adams-Phillips et al., 2010). The present study found that PARP1/2 are positive regulators in plant immune response. The molecular mechanisms by which PARPs regulate plant immunity remain to be fully discovered, but in light of the γ-H2AX findings summarized in Fig. 7E, it would appear that one important role of Arabidopsis PARP2 is to minimize the host DNA damage elicited by virulent pathogens such as *Pst*.

Over the past 30 years, the function of PARPs in maintenance of genome integrity have been extensively characterized (Gibson and Kraus, 2012; Luo and Kraus, 2012). In contrast,

study of PARG in poly(ADP-ribosyl)ation has been limited, due in part to its low cellular abundance and high sensitivity to proteases (Bonicalzi et al., 2005), but also to the lethality of knockouts of the sole *PARG* gene in metazoans (Hanai et al., 2004; Koh et al., 2004). The presence of two *PARG* genes in plants may offer opportunities for genetic and molecular investigation not available in animal systems. Using Arabidopsis *parg* null mutants, which are viable, we demonstrated that PARG1 mediates removal of poly(ADP-ribose) whereas PARG2 confers limited PARG activity in the examined conditions. This is in line with the observation that *parg1* plants, but not *parg2* plants, exhibit increased sensitivity to PAMP treatment and grow less well than wild-type plants in response to DNA-damaging mitomycin C (Adams-Phillips et al., 2010). Because multiple but divergent copies of *PARG* genes are found in a number of plant species (Briggs and Bent, 2011), in the future it will be interesting to explore if similar divisions of labor among PARG proteins are common in other species, and if PARG proteins from other plant species differ substantially from those of Arabidopsis in their enzymatic activities and cellular roles.

PARPs and PARGs, enzymes with counteracting enzymatic activities, modify target proteins by addition or removal, respectively, of ADP-ribose polymers. Surprisingly, the present and previous studies showed that *parg* and *parp* mutant plants exhibit some unexpectedly similar phenotypes, such as strong seedling growth inhibition and increased callose deposition (Adams-Phillips et al., 2008; Adams-Phillips et al., 2010). This may be attributable to synergistic functions of PARPs and PARGs. There is evidence that in human cells the two enzymes co-localize to target gene promoters and act with a similar rather than antagonistic overall effect to regulate gene expression globally (Frizzell et al., 2009). PARP1 and PARG also function in concert to accelerate single-strand break repair in human cells (Fisher et al., 2007). Intriguingly,

we discovered that the accumulation of PARP2 protein in response to genotoxic agents was reduced relative to wild-type in loss-of-function *parg1* mutant plants, consistent with a recent finding made in human HeLa cells that PARP1 transcript and protein expression levels decreased in the *parg* knockdown. This suggests that PARP1 is regulated by PARG to avoid excess accumulation of poly(ADP-ribose) in a cell (Uchiumi et al., 2013). With our detection of plant PARPs and PARGs in the same *in vivo* complexes, it is plausible to hypothesize that regulation of abundance or activity is achieved in part through physical interactions between PARPs and PARGs (Schreiber et al., 2002; Keil et al., 2006).

In summary, we have found that although plant PARPs and PARGs have partially overlapping functions Arabidopsis PARP2 and PARG1 play the predominant roles in plant poly(ADP-ribosyl)ation during DNA damage and immune responses. Future studies will further identify the molecular mechanism by which PARPs and PARGs regulate various cellular responses, individually or in a concerted manner, and their functional interplay with each other. Identification of the proteins that are poly(ADP-ribosy)ated is another future research direction that may help to elucidate the regulatory functions of plant poly(ADP-ribosyl)ation, both under normal physiological conditions and in response to the stresses of DNA damage or pathogenic infection.

2.6 Materials and Methods

Plant materials and growth conditions

Arabidopsis thaliana plants were grown in Fisons Sunshine Mix #1 soil-less potting mix (Hummert) at 22ºC under 9-h light/15-h dark cycles, or MS-grown plants were cultivated on Murashige-Skoog (MS) agar media at 22ºC under 16-h light/8-h dark cycles.

The homozygous Arabidopsis T-DNA insertion lines *parp1-1* (GABI_380E06), *parp1-2* (GABI_382F01), *parp2-1* (GABI_420G03), all in the Col-0 background (Kleinboelting et al., 2012), were identified as previously described (Enns et al., 2005). Isolation and initial characterization of the *parg1* and *parg2* T-DNA insertion lines was previously described (Adams-Phillips et al., 2010). Homozygous double-mutant lines were obtained as self-fertilized progeny from crosses of single mutants and were identified using PCR-based allele-specific markers.

Mitomycin C and bleomycin sensitivity assay

Seeds were stratified at 4^{o}C for two d and then approximately 100 seeds were grown for 14 d on each MS agar plate containing different concentrations of mitomycin C (0, 15 and 30 μM) and bleomycin (0, 1, 1.5 μg/ml) (both from Sigma-Aldrich), then the number of plants with and without true leaves was recorded. Sensitivity was scored as the percentage of plants without true leaves, using three or four plates for each concentration (or in a few instances two, due to plate contamination) within each experiment, and the entire experiment was repeated three separate times. Mean and standard error for each chemical concentration are reported from within each experiment.

Seedling growth inhibition assay

To monitor plant defense activation in response to the flagellin epitope flg22 peptide, 6 d old seedlings from MS plates were transferred to 1 ml MS liquid medium + 1 μM flg22 in 24-well plates, and seedling fresh weights were recorded 14 d later for 12 seedlings per treatment, as per (Gomez-Gomez and Boller, 2000).

ROS assay

The burst of reactive oxygen species produced in response to the flagellin epitope flg22 peptide was monitored as previously described (Gomez-Gomez et al., 1999). Briefly, leaf discs were taken from 5-week-old plants and incubated in 1% dimethyl sulfoxide (DMSO) solution in a 96-well plate overnight, then treated with 1 μM flg22 in 0.1 mg/ml luminol and 0.1 mg/ml horseradish peroxidase immediately prior to 30 min. of luminescence measurement by plate reader (Centro XS^3 LB 960, Berthold Technology).

Callose deposition

Arabidopsis seedlings were grown on MS agar plates for five days before being transferred to liquid MS containing 1 μM flg22. After 24 h of treatment, seedlings were fixed in FAA solution (10% formaldehyde, 5% acetic acid and 50% ethanol), cleared in 95% ethanol, and stained with 0.01% aniline blue in 67 mM K_2HPO_4 with pH adjusted to 12. The stained seedlings were visualized with an Olympus BX60 Epifluorescence Microscope and images of entire cotyledons were captured with an Olympus DP73 camera (with same settings used throughout single experiment). The callose deposits on entire cotyledons were then quantified automatically using ImageJ software by excluding rare wounded leaves and then analyzing the entire area of all images within an experiment after setting ImageJ hue and brightness cutoff levels using images for positive and negative control leaves.

Bacterial growth assay

Leaves of healthy five-week-old Arabidopsis plants were syringe-inoculated with *Pst* DC3000 or *Pst* DC3000(*avrRpt2*) at 1×10^5 cfu/ml (Whalen et al., 1991). After 3 d, leaf discs were sampled from inoculated plants and macerated in 10 mM $MgCl_2$. Samples were diluted serially, plated on NYGA plates with rifampicin and kanamycin and the number of colonies was recorded after 2 d incubation at 28ºC.

Ionizing radiation and detection of H2AX phosphorylation

For ionizing radiation, Arabidopsis Col-0 plants were irradiated with 150 Gy from a ^{137}Cs source (administered at 2.14 Gy per minute) and tissue samples were collected at the indicated times after removal from the radiation source (Friesner et al., 2005). To detect pathogen-induced DSBs, 5-week-old plants were infiltrated with a 1×10^7 cfu/ml solution of *Pst* bacteria in 10 mM $MgCl_2$ and samples were collected at indicated times. Histone proteins were prepared from leaf tissues as previously described and were subjected to immunoblotting with rabbit anti-human γ-H2AX antibody at 1:5000 dilution (Sigma-Aldrich).

Confocal laser scanning microscopy

The full-length cDNAs of PARP1/2 and PARG1/2 were subcloned into the pDONR 207 vector (Invitrogen) and introduced into the destination vector pGWB405 , resulting in constructs with C-terminal fusions to GFP under the control of 35S promoter. The sequence-verified constructs were transformed into *Agrobacterium tumefaciens* strain GV3101(pMP90) and transiently expressed in *Nicotiana benthamiana* leaves by infiltration. Confocal fluorescence microscopy was carried out at indicated times using a Zeiss 510 Meta confocal laser scanning microscope. *Agrobacterium* strains carrying *35S:PARP1-GFP* and *35S:PARP2-GFP* were also

used to transform wild-type Col-0 Arabidopsis by floral dip (Clough and Bent, 1998). Stable transgenic T2 lines were selected and the subcellular locations of PARP1 and PARP2 were examined by confocal microscopy.

Complementation of the *parp2* mutants

To complement the *parp2* mutants, *PARP2* genomic DNA fragments including its native promoter was cloned into the pDONR207 (Invitrogen). Using LR reactions, PARP2 was cloned into pGWB3300, a modified vector (Y. Cao and A. Bent) carrying in the multiple cloning site of pCambia3300 (http://www.cambia.org) the Gateway cloning site, C-terminal 3xHA and *nos* terminator sequences from pGWB13 (Nakagawa et al., 2007). This resulted in the generation of *PARP2:PARP2-3×HA* construct that was then transformed into the *parp2-1* mutant background.

Immunoblot analysis

Total proteins were prepared from Arabidopsis plants in extraction buffer (50 mM Tris-HCl (pH7.5), 150 mM NaCl, 5 mM EDTA, 0.5% Triton X-100, 10% glycerol, and Sigma-Aldrich plant protease inhibitor cocktail at 1:100). After protein separation by SDS-PAGE, immunoblot analysis was carried out with anti-HA (Roche), anti-poly(ADP-ribose) (anti-PAR) (Trevigen) or anti-PARP2 antibodies. Polyclonal antibodies to Arabidopsis PARP2 protein (custom purchase from Genscript) were raised in rabbit against the synthetic peptide YGKEENDSPVNNDI, which does not share significant homology with PARP1 or other proteins predicted in the Col-0 accession of Arabidopsis. Anti-PARP2 antibodies were purified by peptide affinity chromatography.

Coimmunoprecipitation assays

The cDNAs of PARP1, PARP2, PARG1 and PARG2 were cloned into the GFP-tagged pGWB405 and/or myc-tagged pGWB417 Gateway destination vectors (Nakagawa et al., 2007) and the resulting constructs were transformed into *A. tumefaciens* GV3101(pMP90). Leaves of 4-5 week-old *N. benthamiana* plants were agroinfiltrated with OD_{600} 0.4 of the resulting *A. tumefaciens* strains, and some samples were then infiltrated two days later with 2 μg/ml of bleomycin solution. Tissues were harvested three days after agroinfiltration and total proteins were prepared in extraction buffer (50 mM Tris-HCl (pH7.5), 150 mM NaCl, 5 mM EDTA, 0.2% Triton X-100, 10% glycerol, and Sigma-Aldrich plant protease inhibitor cocktail at 1:100). Immunoprecipitaton was carried out with anti-GFP (Abcam) at 4ºC overnight followed by incubation with protein A beads (Thermo Scientific) for 1-2 h. The beads were washed three times with extraction buffer without protease inhibitors. The precipitated proteins were eluded with the SDS loading buffer, subjected to SDS-PAGE and immunoblotted with anti-myc (Covance) and anti-GFP (Clontech) antibodies, and detected using Supersignal West Pico or Dura chemiluminescent substrates (Thermo Scientific).

2.7 Acknowledgements

We thank Ping He and Libo Shan for sharing results prior to publication, and Sarah Swanson for training and assistance with fluorescence and confocal fluorescence microscopy. The GABI-Kat T-DNA lines GABI_380E06, GABI_382F01, and GABI_420G03 were provided by the Nottingham Arabidopsis Stock Center.

2.8 Figures

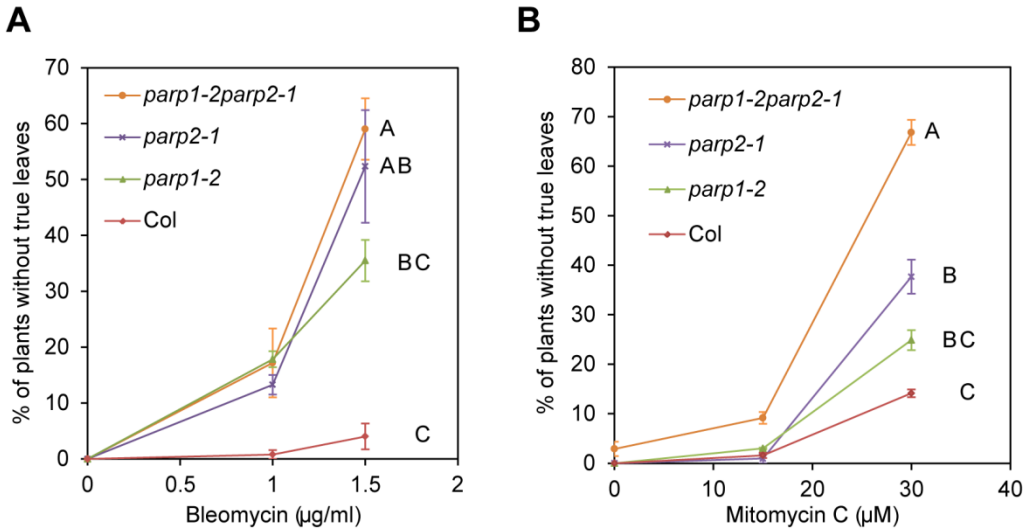

Fig. 1. Arabidopsis *parp* mutants are hypersensitive to DNA damage agents. Wild-type Col-0 and *parp* mutant seeds were grown on MS agar medium supplemented with the genotoxic agents bleomycin (A) or mitomycin C (B). Sensitivity to DNA damage agents was scored as the percentage of plants that had not yet developed true leaves after 14 d. Mean and standard error of the mean are shown for one experiment; experiment was performed three times with similar results. Genotypes not sharing same letter on graph are significantly different at the high concentration (ANOVA Tukey HSD $P < 0.05$ across three experiments).

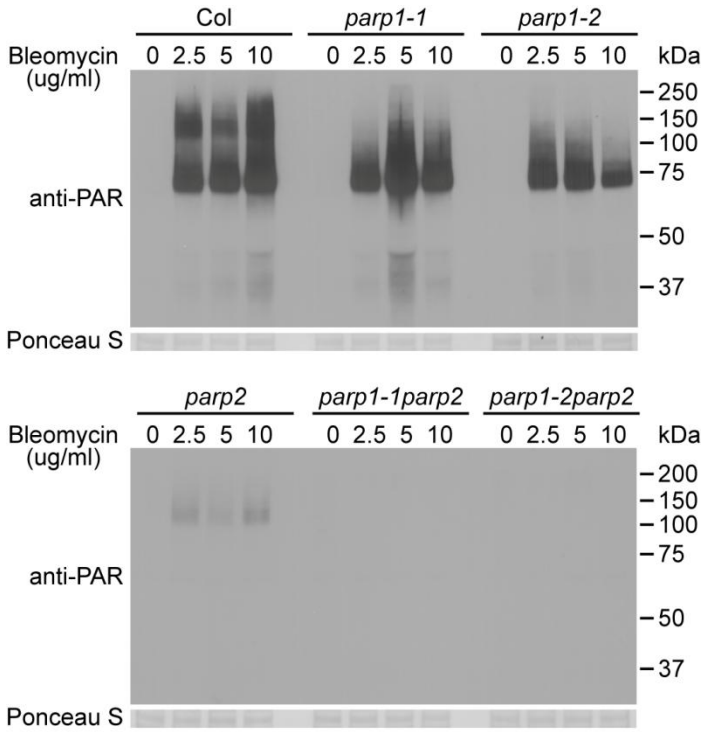

Fig. 2. PARP2 plays a dominant role in DNA damage response after bleomycin treatment. Two-week old *Arabidopsis* plants were transferred to 0, 2.5, 5 or 10 µg/ml of bleomycin for 18 h. Total proteins were extracted, separated by SDS-PAGE and analyzed by immunoblotting using an anti-PAR antibody. Equivalent loading of lanes was verified using Ponceau S stain. All samples shown and both blots were processed in parallel within the same experiment. Similar results were obtained in three separate experiments.

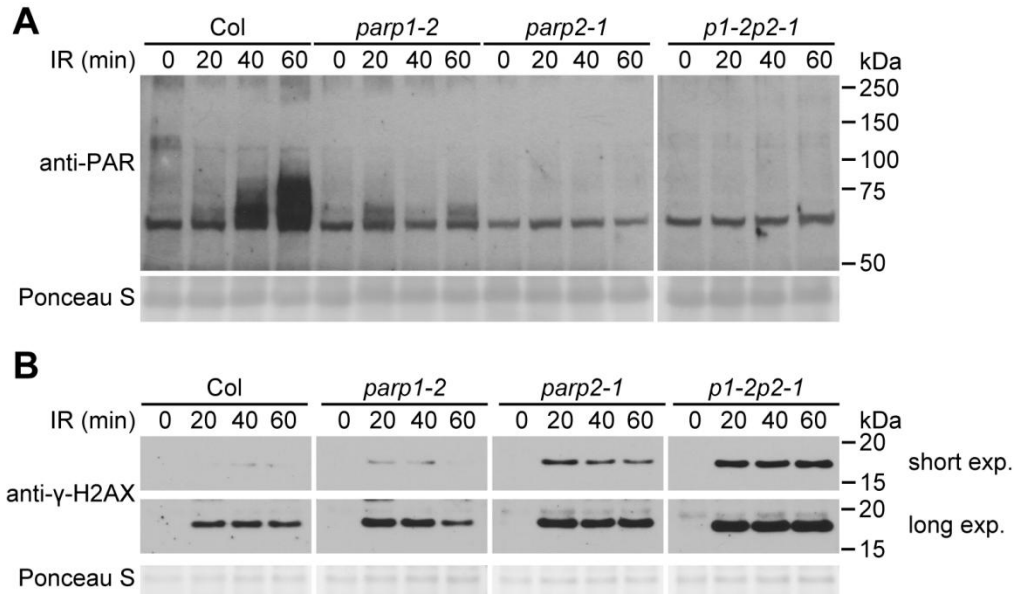

Fig. 3. PARP2 plays a dominant role in response to ionizing irradiation. (A) Two-week old Arabidopsis plants grown on MS plates were irradiated with 150 Gy of γ-radiation and then flash-frozen 20, 40 or 60 min after removal from the radiation source. Total proteins were then extracted, separated by SDS-PAGE and analyzed by immunoblotting with an anti-PAR antibody. 0 min sample not exposed to γ-radiation source. All samples shown in (A) were processed in parallel within the same experiment. (B) The level of γ-H2AX was assessed at 20, 40 and 60 min after irradiation as in (A), using an anti-γ-H2AX antibody. Samples all processed in parallel from same experiment. Shorter and longer time exposures of same immunoblot are shown. Equivalent loading of lanes was verified using Ponceau S stain. Experiments were performed three times with similar results.

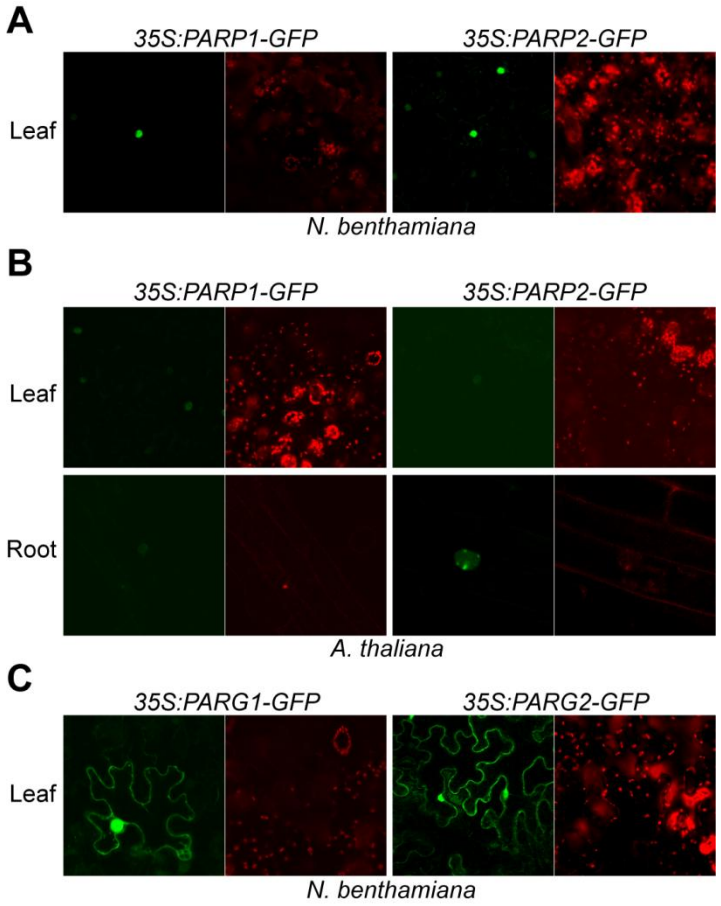

Fig. 4. Subcellular localization of Arabidopsis PARP1/2 and PARG1/2. Paired confocal fluorescence microscopy images show same sample; green wavelengths (GFP) on left and red wavelengths (chlorophyll) on right. (A) Arabidopsis PARP1 and PARP2 localized in the nucleus. *35S:AtPARP1-GFP* and *35S:AtPARP2-GFP* transiently expressed in *N. benthamiana* epidermal cells within leaves were imaged. (B) PARP1 and PARP2 localized in the nucleus in Arabidopsis. Subcellular localization was carried out in stable transgenic lines carrying *35S:AtPARP1-GFP* and *35S:AtPARP2-GFP* in the wild-type Col-0 background. (C) Arabidopsis PARG1 and PARG2 localized in the cytoplasm and nucleus. *35S:AtPARG1-GFP* and *35S:AtPARG2-GFP* were transiently expressed in *N. benthamiana* and the images were taken 2 d after inoculation.

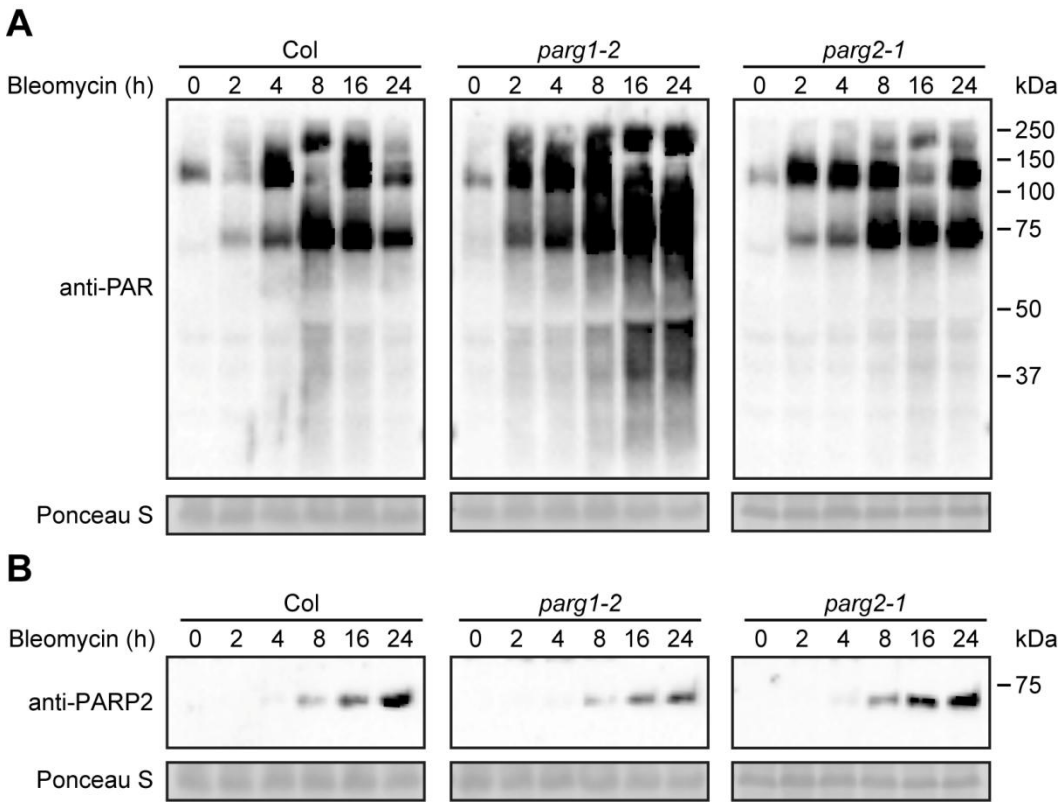

Fig. 5. PARG1 is more active than PARG2 in removal of poly(ADP-ribosyl)ation after bleomycin treatment. Two-week-old *parg1-2*, *parg2-1* and Col-0 Arabidopsis plants were treated with 2.5 μg/ml bleomycin and samples were collected at indicated times. Total proteins were extracted, separated by SDS-PAGE and analyzed by immunoblotting with anti-PAR (A) or anti-PARP2 (B) antibody. Equivalent loading of lanes was verified using Ponceau S stain. Similar results obtained in two separate experiments.

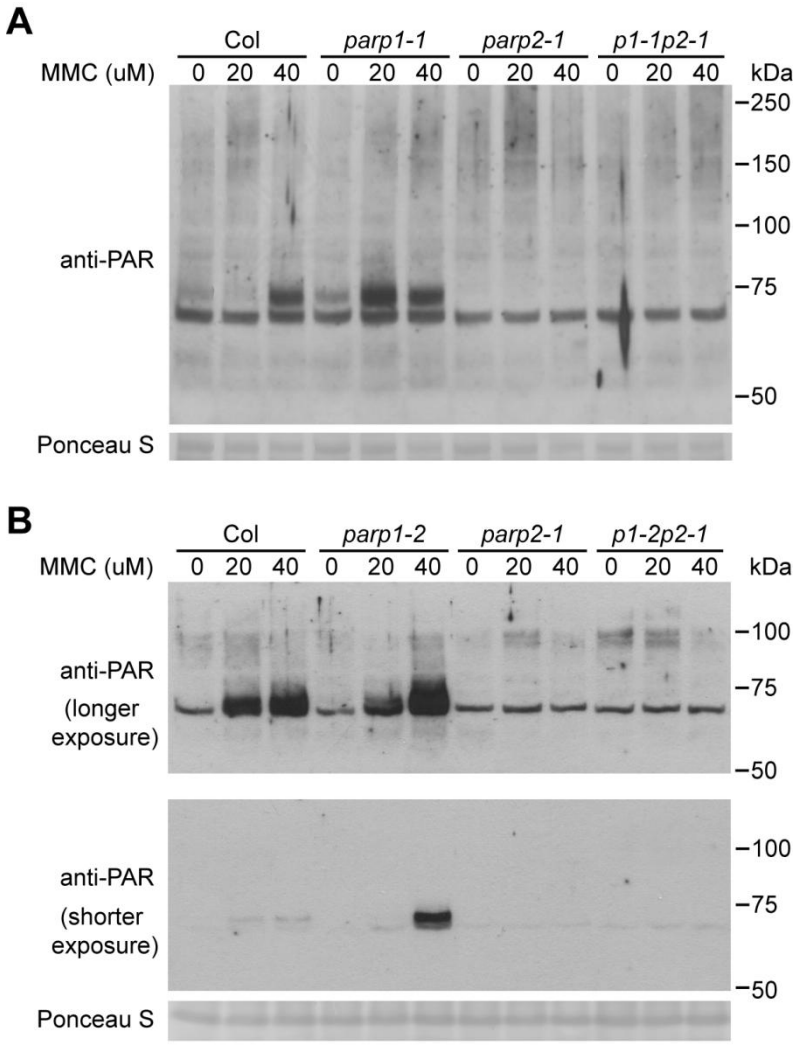

Fig. 6. PARP2 activity is regulated by PARP1 in response to DNA alkylating agent mitomycin C. Arabidopsis plants, including (A) *parp1-1* or (B) *parp1-2* knockout alleles of *PARP1*, were grown on MS plates supplemented with 0, 20 and 40 µM of mitomycin C (MMC) for two weeks. Total proteins were extracted, separated by SDS-PAGE and analyzed by immunoblotting with anti-PAR antibody. Equivalent loading of lanes was verified using Ponceau S stain. Upper and middle panels of (B) are same blot, showing immunoblot signal after longer and shorter exposure times respectively. Similar results obtained in two separate experiments.

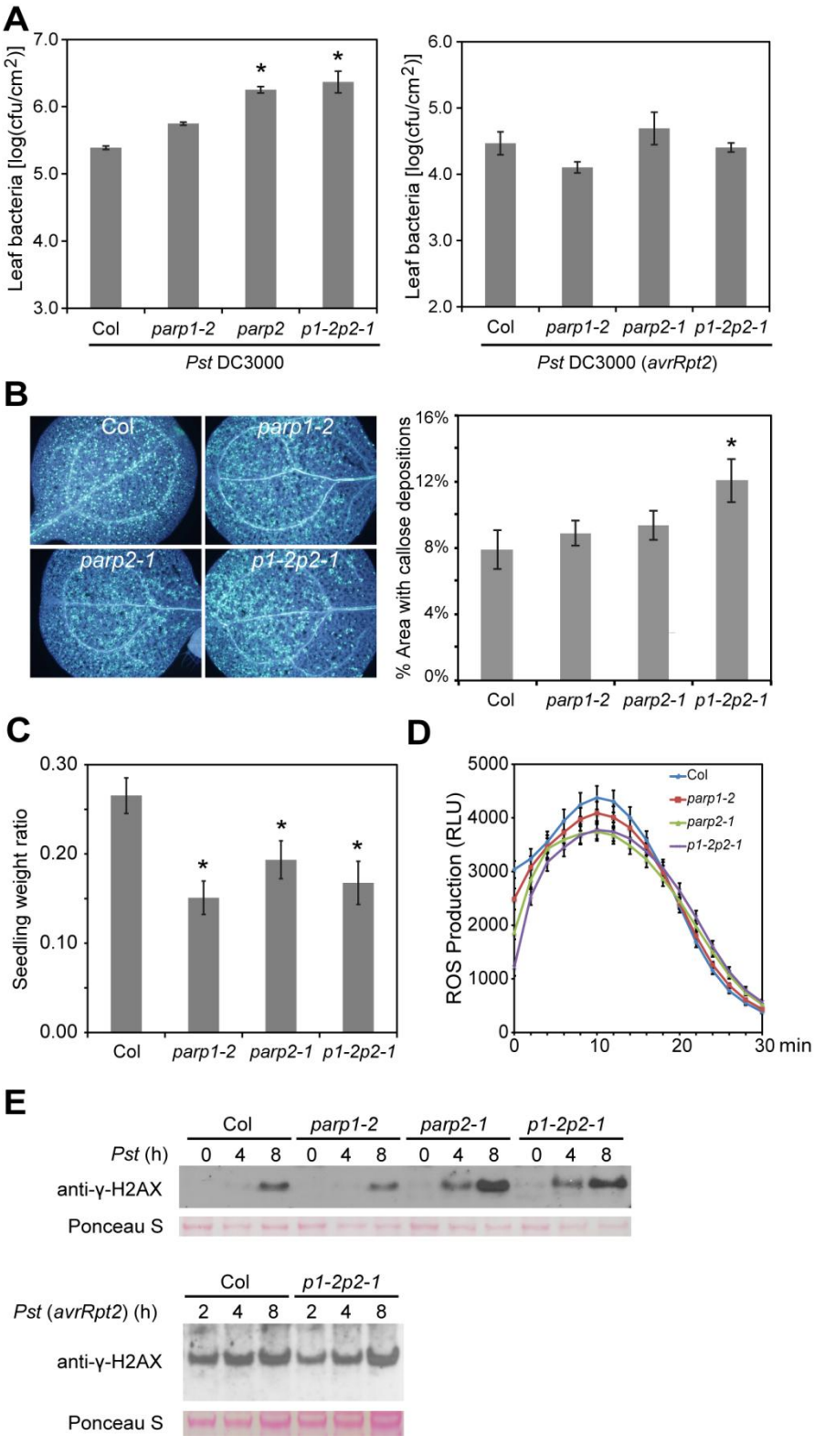
A
Leaf bacteria [log(cfu/cm2)]
7.0
6.0
5.0
4.0
3.0
Col
parp1-2
parp2
p1-2p2-1
Pst DC3000
Leaf bacteria [log(cfu/cm2)]
6.0
5.0
4.0
3.0
2.0
Col
parp1-2
parp2-1
p1-2p2-1
Pst DC3000 (avrRpt2)
B
Col
parp1-2
parp2-1
p1-2p2-1
% Area with callose depositions
16%
12%
8%
4%
0%
Col
parp1-2
parp2-1
p1-2p2-1
C
Seedling weight ratio
0.30
0.20
0.10
0.00
Col
parp1-2
parp2-1
p1-2p2-1
D
ROS Production (RLU)
5000
4000
3000
2000
1000
0
0
10
20
30 min
Col
parp1-2
parp2-1
p1-2p2-1
E
Col
parp1-2
parp2-1
p1-2p2-1
Pst (h)
0 4 8 0 4 8 0 4 8 0 4 8
anti-γ-H2AX
Ponceau S
Col
p1-2p2-1
Pst (avrRpt2) (h)
2 4 8 2 4 8
anti-γ-H2AX
Ponceau S

Fig. 7. Arabidopsis *parp* mutants are compromised in basal resistance. (A) Bacterial population sizes of *Pst* within leaves. *Pst* DC3000 strains with or without *avrRt2* were syringe infiltrated into leaf mesophyll at 1×10^5 cfu/ml and bacterial populations were measured 3 d post-inoculation. Mean ± standard error of mean for one experiment shown. Experiments were performed three times with similar results; * indicates significant difference from Col-0 across the three experiments (ANOVA, Tukey pairwise comparisons, $P < 0.05$). (B) Flg22-induced callose deposition. Seedlings exposed to 1 μM flg22 for 24 h were fixed and stained with aniline blue to highlight callose deposition. Left panel: representative images of the four genotypes; right panel: data summary for all tested leaves (n=24 per genotype). * indicates significant difference from Col-0 across the three experiments (ANOVA, Tukey pairwise comparisons, $P < 0.05$). (C) Seedling growth inhibition due to chronic flg22-induced defense activation. Ratio is weight of individual seedlings grown for 14 d in liquid MS media + 1 μM flg22, divided by mean of seedlings of same genotype grown without flg22 within same experiment (mean ± standard error of mean). * indicates significant difference from Col-0 across the three experiments (ANOVA, Tukey pairwise comparisons, $P < 0.05$). (D) Flg22-triggered oxidative burst. Reactive oxygen species from leaf discs of the indicated genotype were measured for 30 min after treatment with 1 μM flg22. RLU: relative luminescence units. (E) *Pst*-induced γ-H2AX accumulation. Arabidopsis plants of the indicated genotype were vacuum-infiltrated with the indicated *Pst* strain at 1×10^7 cfu/ml. The level of γ-H2AX in leaf samples from the indicated time points after inoculation was assessed by immunoblot using anti-γ-H2AX antibody. Equivalent loading of lanes was verified using Ponceau S stain. Upper and lower blots are from separate experiments. Similar results obtained in two separate experiments.

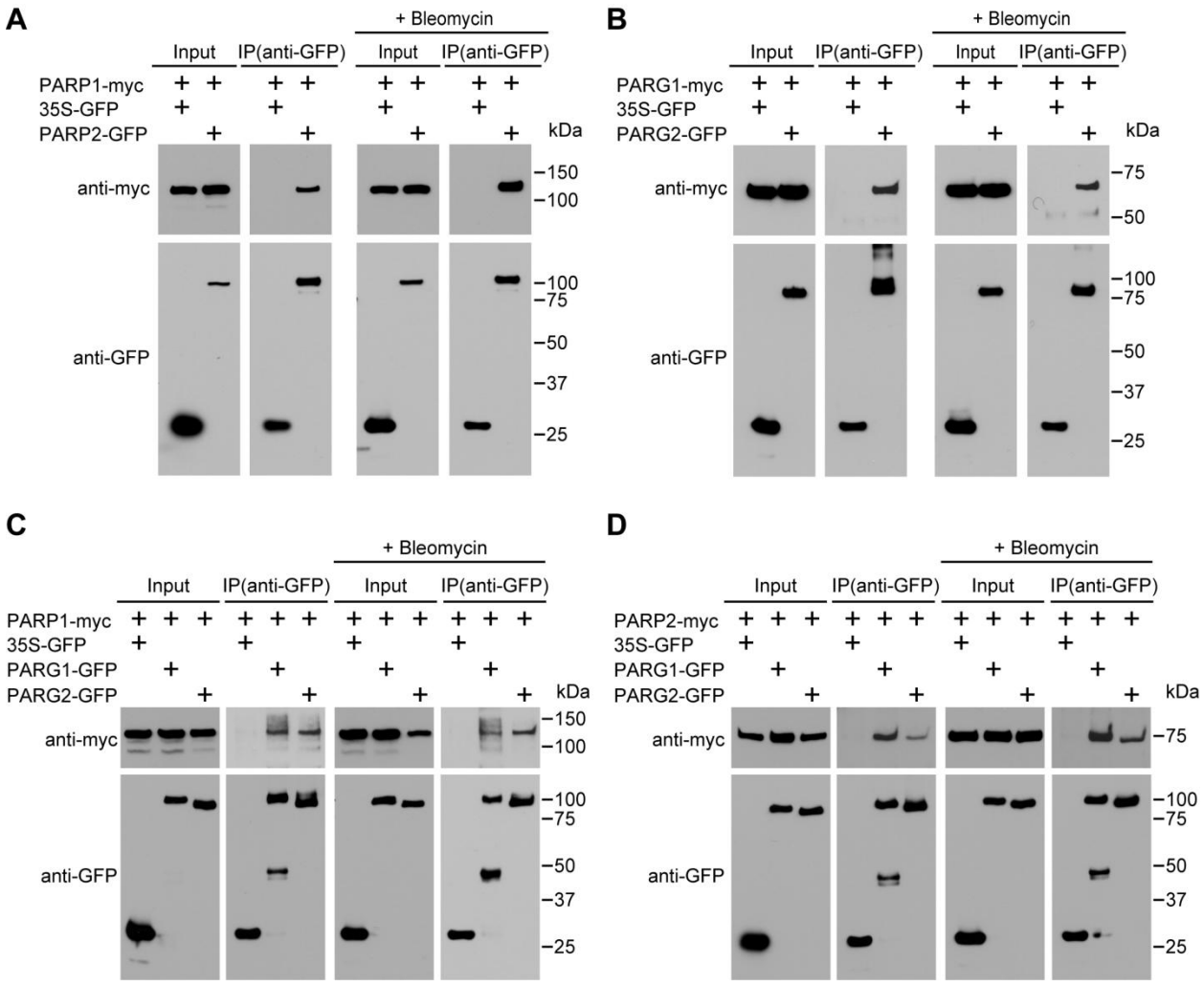

Fig. 8. Interactions between PARPs and PARGs. (A) PARP1 associates *in vivo* with PARP2. (B) PARG1 associates *in vivo* with PARG2. (C) PARP1 associates *in vivo* with PARG1 and PARG2. (D) PARP2 associates *in vivo* with PARG1 and PARG2. The indicated proteins were transiently expressed in *N. benthamiana*. Input lanes were loaded with total protein extracts, IP lanes were loaded with immumoprecipitation products. Immunoprecipitations were performed with anti-GFP antibodies and immunoblots were analyzed with anti-GFP or anti-myc antibodies, as noted. These experiments were repeated twice with similar results.

2.9 Supporting Information

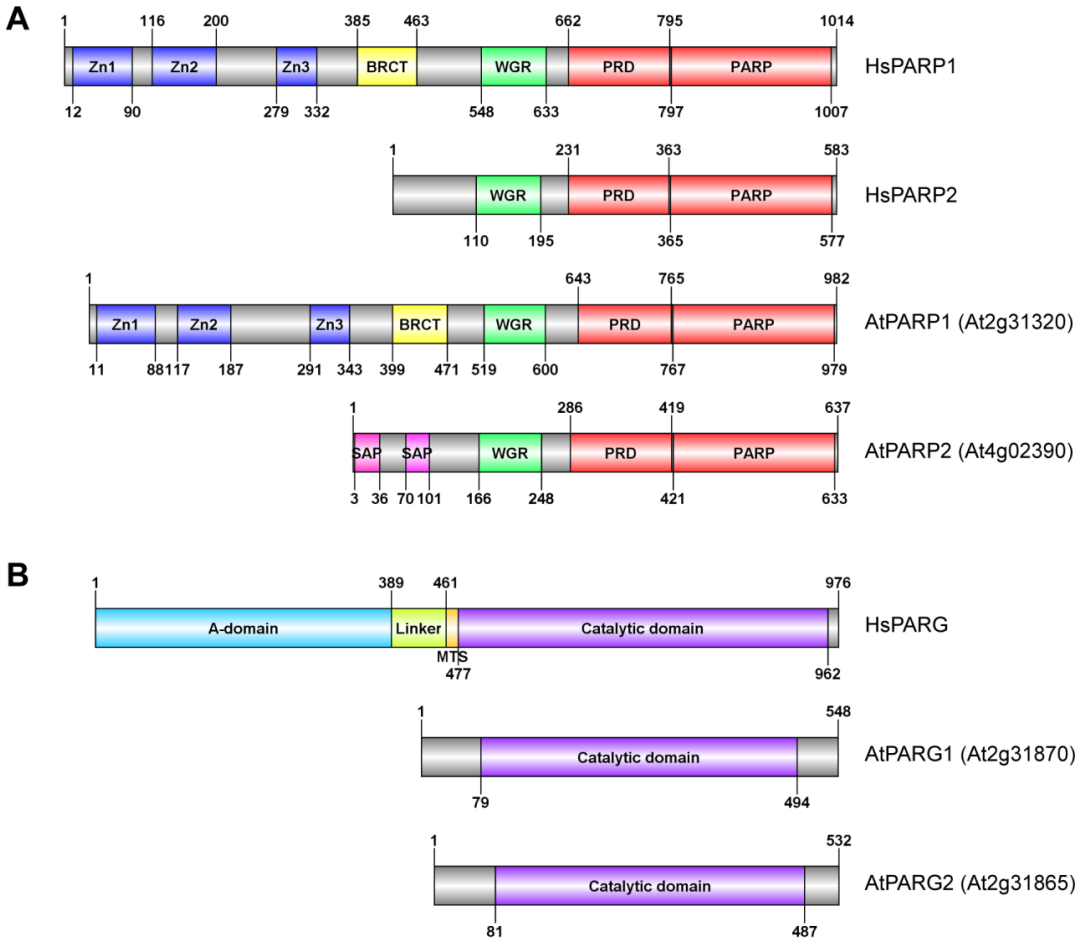

S1 Fig. Domain structures of PARPs and PARGs. (A). Domain structures of human and Arabidopsis poly(ADP-ribose) polymerases. Zn1, Zn2 and Zn3: three zinc binding domains; BRCT: BRCA-1 C-terminal domain for phospho-protein binding. WGR: conserved Trp-Gly-Arg motif for putative nucleic acid binding; PRD: PARP regulatory domain; PARP: PARP catalytic domain; SAP: SAF-A/B, Acinus and PIAS motif for putative DNA/RNA binding. (B) Domain structures of human and Arabidopsis poly(ADP-ribose) glycohydrolases. A-domain: N-terminal regulatory and targeting domain; MTS: mitochondrial targeting sequence; Catalytic domain: PARG catalytic domain. Protein structures were generated using DOG 2.0 software.

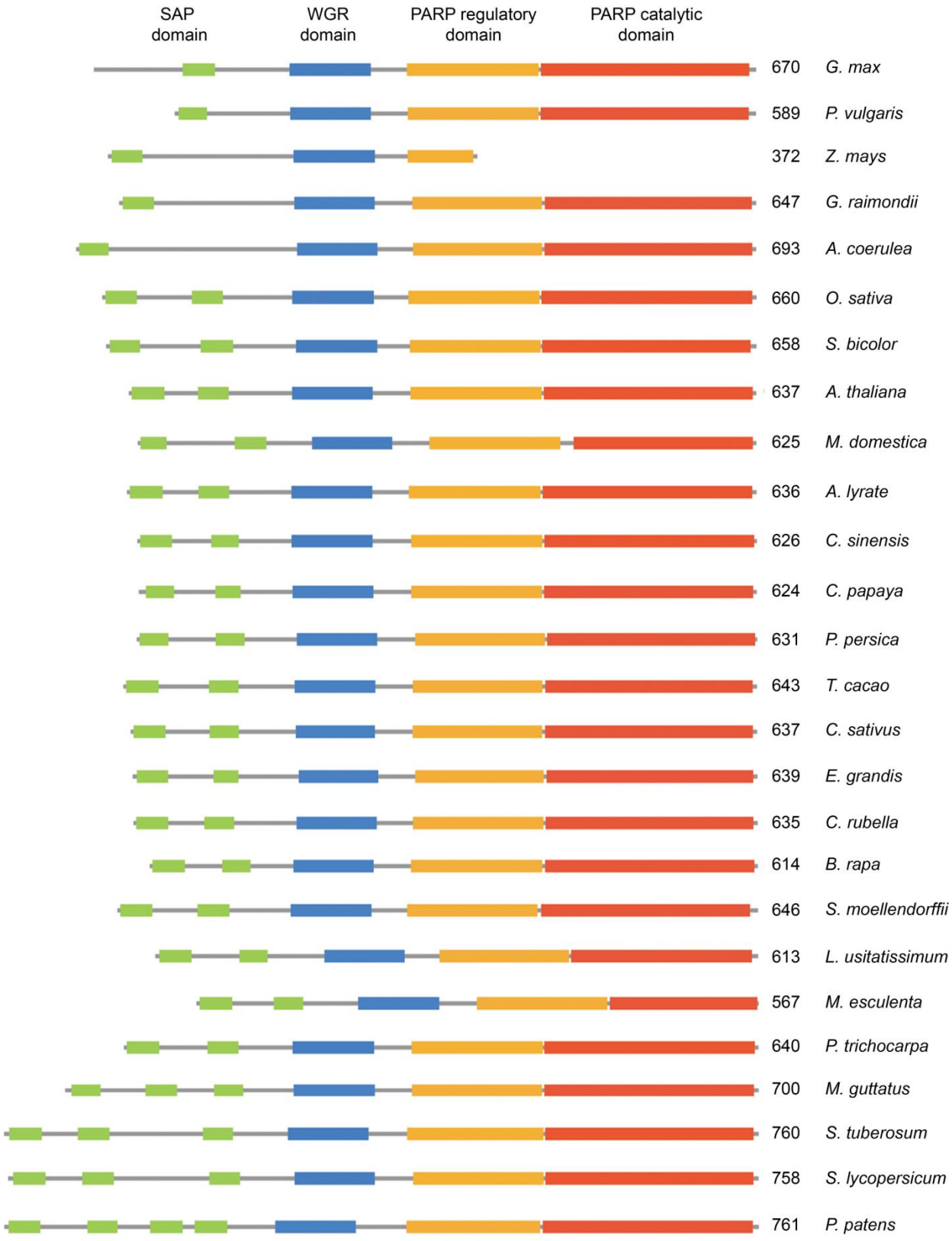
SAP domain
WGR domain
PARP regulatory domain
PARP catalytic domain
670 G. max
589 P. vulgaris
372 Z. mays
647 G. raimondii
693 A. coerulea
660 O. sativa
658 S. bicolor
637 A. thaliana
625 M. domestica
636 A. lyrate
626 C. sinensis
624 C. papaya
631 P. persica
643 T. cacao
637 C. sativus
639 E. grandis
635 C. rubella
614 B. rapa
646 S. moellendorffii
613 L. usitatissimum
567 M. esculenta
640 P. trichocarpa
700 M. guttatus
760 S. tuberosum
758 S. lycopersicum
761 P. patens

S2 Fig. Domain organization of plant PARP2 family. Domain structures of plant PARP2 proteins were identified by Phytozome (http://www.phytozome.net) using Arabidopsis PARP2 as a query. Color codes for domains are: Green for SAF-A/B, Acinus and PIAS (SAP) motif putative DNA/RNA binding domain; Blue for Trp-Gly-Arg (WGR in single letter code) putative PARP nucleic acid binding domain; Orange for PARP regulatory domain; Red for PARP catalytic domain. Number of amino acids in PARP proteins and names of plant species from which they derive are also shown.

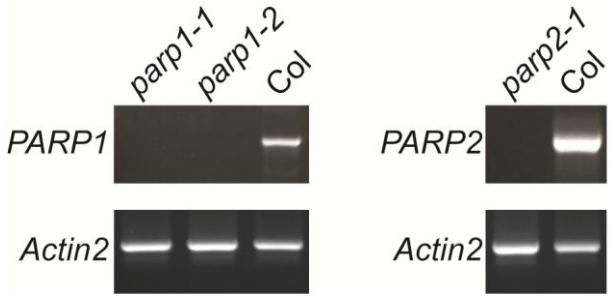

S3 Fig. Characterization of PARP T-DNA insertion lines. RT-PCR analysis of *PARP1* and *PARP2* mRNA in 3-week old wild-type Arabidopsis Col-0, or in *parp1* or *parp2* mutants. *Actin-2* amplified from the same RNA samples served as an RNA isolation and RT-PCR control.

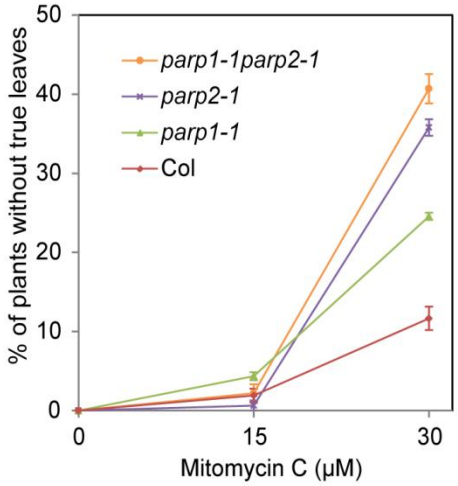

S4 Fig. Arabidopsis *parp* mutants are hypersensitive to DNA damage agents. Wild-type Col-0 and *parp* mutant (including *parp1-1* allele) seeds were grown on MS agar medium supplemented with the genotoxic agent mitomycin C. Sensitivity to DNA damage agents was scored as the percentage of plants that had not yet developed true leaves after 14 d. Mean and standard error of the mean are shown for one experiment; experiment was performed three times with similar results.

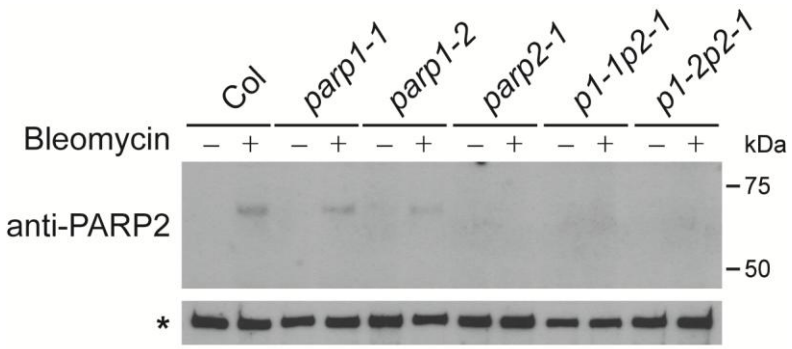

S5 Fig. Analysis of PARP2 proteins in T-DNA insertion lines. PARP2 protein in 2-week old Arabidopsis seedlings of indicated genotypes, left untreated or treated with 5 μg/ml bleomycin for 18 h. Total proteins were extracted, separated by SDS-PAGE and detected with anti-PARP2 antibody. * Equivalent loading of total protein was verified using the signal from a high MW protein recognized by the polyclonal antibody.

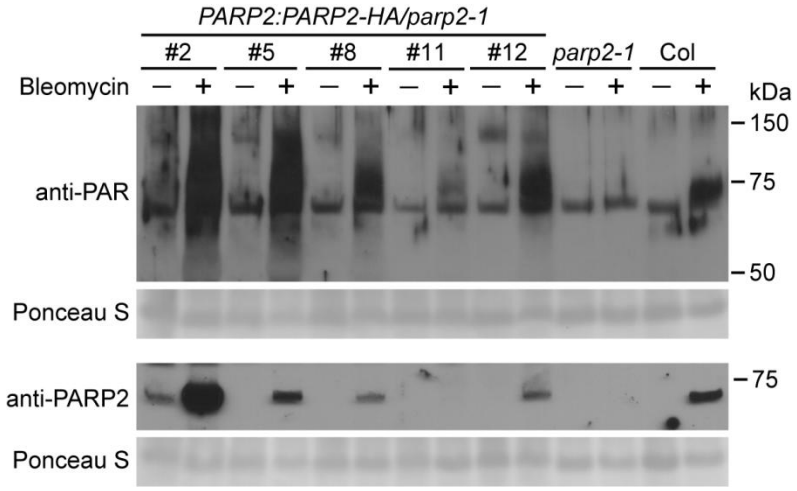

S6 Fig. Complementation of the *parp2-1* mutation with *PARP2:PARP2-HA*. *PARP2:PARP2-HA* was transformed into the *parp2-1* background. Five independent T2 lines, as well as *parp2-1* and wild-type Col-0 plants included as negative and positive controls, were treated with 2.5 μg/ml of bleomycin for 18 h. Total proteins were extracted, separated by SDS-PAGE and detected with anti-poly(ADP-ribose) or anti-PARP2 antibody as indicated. Equivalent loading of lanes was verified using Ponceau S stain.

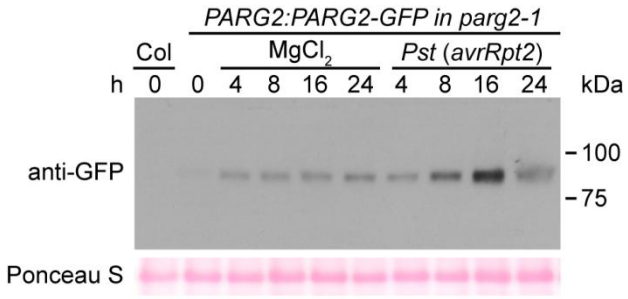

S7 Fig. PARG2 protein is upregulated by *Pst* DC3000(*avrRpt2*). Five-week-old Arabidopsis *parg2-1* mutant plants carrying *PARG2:PARG2-GFP* (2 kb of *PARG2* promoter, *PARG2* coding sequence fused to C-terminal GFP and *nos* terminator) were infiltrated with 10 mM $MgCl_2$, or *Pst* DC3000(*avrRpt2*) at a concentration of 1×10^7 cfu/ml in 10 mM $MgCl_2$. Proteins were extracted at the indicated times, separated by SDS-PAGE and detected with anti-GFP antibody. Equivalent loading of lanes was verified using Ponceau S stain. Hypersensitive response-associated cell death is present in Arabidopsis Col-0 leaf tissues 24 h after infection by *Pst avrRpt2*.

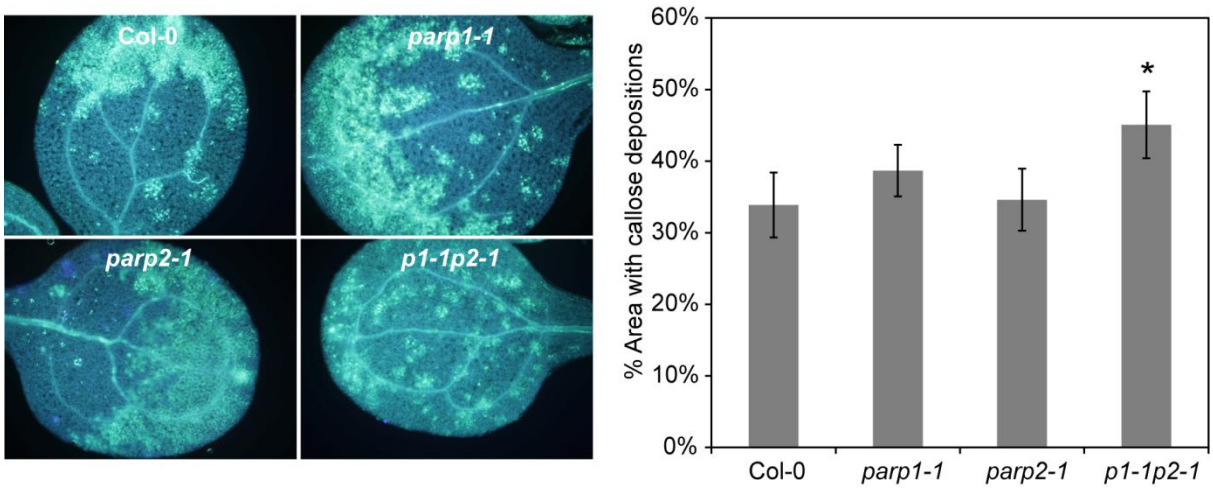

S8 Fig. Callose deposition phenotypes of *parp* mutants. Seedlings exposed to 1 μM flg22 for 24 h were fixed and callose deposits were detected using aniline blue staining and quantified by ImageJ software. * indicates significant difference from Col-0 across the three experiments (ANOVA, Tukey pairwise comparisons, $P < 0.05$).

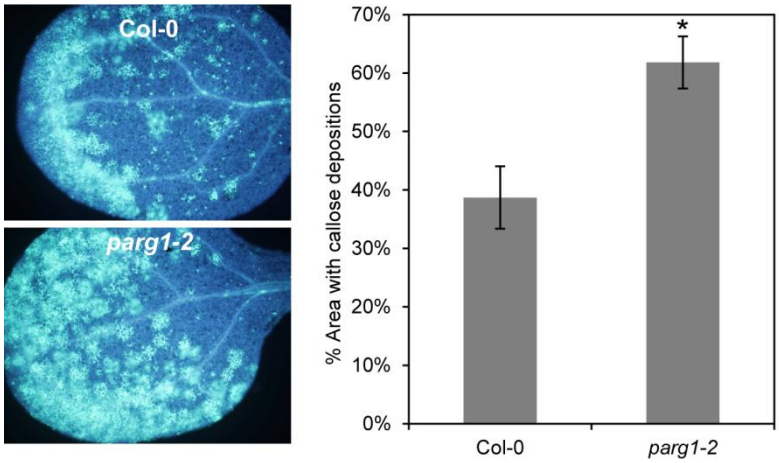

S9 Fig. Callose deposition phenotypes of *parg* mutant. Seedlings exposed to 1 μM flg22 for 24 h were fixed and callose deposits were detected using aniline blue staining and quantified by ImageJ software. * indicates significant difference from Col-0 across the three experiments (ANOVA, Tukey pairwise comparisons, $P < 0.05$).

2.10 References

Abd Elmageed ZY, Naura AS, Errami Y, Zerfaoui M (2012) The poly(ADP-ribose) polymerases (PARPs): new roles in intracellular transport. Cell Signal **24:** 1-8

Adams-Phillips L, Briggs AG, Bent AF (2010) Disruption of poly(ADP-ribosyl)ation mechanisms alters responses of Arabidopsis to biotic stress. Plant Physiol **152:** 267-280

Adams-Phillips L, Wan J, Tan X, Dunning FM, Meyers BC, Michelmore RW, Bent AF (2008) Discovery of ADP-ribosylation and other plant defense pathway elements through expression profiling of four different Arabidopsis-Pseudomonas R-avr interactions. Mol Plant Microbe Interact **21:** 646-657

Ame JC, Apiou F, Jacobson EL, Jacobson MK (1999) Assignment of the poly(ADP-ribose) glycohydrolase gene (PARG) to human chromosome 10q11.23 and mouse chromosome 14B by in situ hybridization. Cytogenet Cell Genet **85:** 269-270

Ame JC, Rolli V, Schreiber V, Niedergang C, Apiou F, Decker P, Muller S, Hoger T, Menissier-de Murcia J, de Murcia G (1999) PARP-2, A novel mammalian DNA damage-dependent poly(ADP-ribose) polymerase. J Biol Chem **274:** 17860-17868

Amor Y, Babiychuk E, Inze D, Levine A (1998) The involvement of poly(ADP-ribose) polymerase in the oxidative stress responses in plants. FEBS Lett **440:** 1-7

Aravind L, Koonin EV (2000) SAP - a putative DNA-binding motif involved in chromosomal organization. Trends Biochem Sci **25:** 112-114

Babiychuk E, Van Montagu M, Kushnir S (2001) N-terminal domains of plant poly(ADP-ribose) polymerases define their association with mitotic chromosomes. Plant J **28:** 245-255

Bartsch M, Gobbato E, Bednarek P, Debey S, Schultze JL, Bautor J, Parker JE (2006) Salicylic acid-independent ENHANCED DISEASE SUSCEPTIBILITY1 signaling in Arabidopsis immunity and cell death is regulated by the monooxygenase FMO1 and the Nudix hydrolase NUDT7. Plant Cell **18:** 1038-1051

Boller T, Felix G (2009) A renaissance of elicitors: perception of microbe-associated molecular patterns and danger signals by pattern-recognition receptors. Annu Rev Plant Biol **60:** 379-406

Boltz KA, Jasti M, Townley JM, Shippen DE (2014) Analysis of poly(ADP-Ribose) polymerases in Arabidopsis telomere biology. PLoS One **9:** e88872

Bonicalzi ME, Haince JF, Droit A, Poirier GG (2005) Regulation of poly(ADP-ribose) metabolism by poly(ADP-ribose) glycohydrolase: where and when? Cell Mol Life Sci **62:** 739-750

Briggs AG, Bent AF (2011) Poly(ADP-ribosyl)ation in plants. Trends Plant Sci **16:** 372-380

Burkle A, Virag L (2013) Poly(ADP-ribose): PARadigms and PARadoxes. Mol Aspects Med **34:** 1046-1065

Carbone M, Reale A, Di Sauro A, Sthandier O, Garcia MI, Maione R, Caiafa P, Amati P (2006) PARP-1 interaction with VP1 capsid protein regulates polyomavirus early gene expression. J Mol Biol **363:** 773-785

Chatzinikolaou G, Karakasilioti I, Garinis GA (2014) DNA damage and innate immunity: links and trade-offs. Trends Immunol

Citarelli M, Teotia S, Lamb RS (2010) Evolutionary history of the poly(ADP-ribose) polymerase gene family in eukaryotes. BMC Evol Biol **10:** 308

Clough SJ, Bent AF (1998) Floral dip: a simplified method for Agrobacterium-mediated transformation of Arabidopsis thaliana. Plant J **16:** 735-743

De Block M, Verduyn C, De Brouwer D, Cornelissen M (2005) Poly(ADP-ribose) polymerase in plants affects energy homeostasis, cell death and stress tolerance. Plant J **41:** 95-106

de Murcia JM, Niedergang C, Trucco C, Ricoul M, Dutrillaux B, Mark M, Oliver FJ, Masson M, Dierich A, LeMeur M, Walztinger C, Chambon P, de Murcia G (1997) Requirement of poly(ADP-ribose) polymerase in recovery from DNA damage in mice and in cells. Proc Natl Acad Sci U S A **94:** 7303-7307

De Vos M, Schreiber V, Dantzer F (2012) The diverse roles and clinical relevance of PARPs in DNA damage repair: current state of the art. Biochem Pharmacol **84:** 137-146

Dodds PN, Rathjen JP (2010) Plant immunity: towards an integrated view of plant-pathogen interactions. Nat Rev Genet **11:** 539-548

Doucet-Chabeaud G, Godon C, Brutesco C, de Murcia G, Kazmaier M (2001) Ionising radiation induces the expression of PARP-1 and PARP-2 genes in Arabidopsis. Mol Genet Genomics **265:** 954-963

Dronkert ML, Kanaar R (2001) Repair of DNA interstrand cross-links. Mutat Res **486:** 217-247

Durrant WE, Wang S, Dong XN (2007) Arabidopsis SNI1 and RAD51D regulate both gene transcription and DNA recombination during the defense response. Proc Natl Acad Sci U S A **104:** 4223-4227

Enns LC, Kanaoka MM, Torii KU, Comai L, Okada K, Cleland RE (2005) Two callose synthases, GSL1 and GSL5, play an essential and redundant role in plant and pollen development and in fertility. Plant Mol Biol **58:** 333-349

Ermolaeva MA, Schumacher B (2014) Systemic DNA damage responses: organismal adaptations to genome instability. Trends Genet **30:** 95-102

Fisher AE, Hochegger H, Takeda S, Caldecott KW (2007) Poly(ADP-ribose) polymerase 1 accelerates single-strand break repair in concert with poly(ADP-ribose) glycohydrolase. Mol Cell Biol **27:** 5597-5605

Friesner JD, Liu B, Culligan K, Britt AB (2005) Ionizing radiation-dependent gamma-H2AX focus formation requires ataxia telangiectasia mutated and ataxia telangiectasia mutated and Rad3-related. Mol Biol Cell **16:** 2566-2576

Frizzell KM, Gamble MJ, Berrocal JG, Zhang T, Krishnakumar R, Cen Y, Sauve AA, Kraus WL (2009) Global analysis of transcriptional regulation by poly(ADP-ribose) polymerase-1 and poly(ADP-ribose) glycohydrolase in MCF-7 human breast cancer cells. J Biol Chem **284:** 33926-33938

Ge X, Li GJ, Wang SB, Zhu H, Zhu T, Wang X, Xia Y (2007) AtNUDT7, a negative regulator of basal immunity in Arabidopsis, modulates two distinct defense response pathways and is involved in maintaining redox homeostasis. Plant Physiol **145:** 204-215

Gibson BA, Kraus WL (2012) New insights into the molecular and cellular functions of poly(ADP-ribose) and PARPs. Nat Rev Mol Cell Biol **13:** 411-424

Gill SS, Tuteja N (2010) Reactive oxygen species and antioxidant machinery in abiotic stress tolerance in crop plants. Plant Physiol Biochem **48:** 909-930

Gomez-Gomez L, Boller T (2000) FLS2: an LRR receptor-like kinase involved in the perception of the bacterial elicitor flagellin in Arabidopsis. Mol Cell **5:** 1003-1011

Gomez-Gomez L, Felix G, Boller T (1999) A single locus determines sensitivity to bacterial flagellin in Arabidopsis thaliana. Plant J **18:** 277-284

Gordon-Shaag A, Yosef Y, Abd El-Latif M, Oppenheim A (2003) The abundant nuclear enzyme PARP participates in the life cycle of simian virus 40 and is stimulated by minor capsid protein VP3. J Virol **77:** 4273-4282

Hanai S, Kanai M, Ohashi S, Okamoto K, Yamada M, Takahashi H, Miwa M (2004) Loss of poly(ADP-ribose) glycohydrolase causes progressive neurodegeneration in Drosophila melanogaster. Proc Natl Acad Sci U S A **101:** 82-86

Hassa PO, Hottiger MO (2008) The diverse biological roles of mammalian PARPS, a small but powerful family of poly-ADP-ribose polymerases. Front Biosci **13:** 3046-3082

Heeres JT, Hergenrother PJ (2007) Poly(ADP-ribose) makes a date with death. Curr Opin Chem Biol **11:** 644-653

Huber A, Bai P, de Murcia JM, de Murcia G (2004) PARP-1, PARP-2 and ATM in the DNA damage response: functional synergy in mouse development. DNA Repair (Amst) **3:** 1103-1108

Jambunathan N, Mahalingam R (2006) Analysis of Arabidopsis growth factor gene 1 (GFG1) encoding a nudix hydrolase during oxidative signaling. Planta **224:** 1-11

Jaspers P, Overmyer K, Wrzaczek M, Vainonen JP, Blomster T, Salojarvi J, Reddy RA, Kangasjarvi J (2010) The RST and PARP-like domain containing SRO protein family: analysis of protein structure, function and conservation in land plants. BMC Genomics **11:** 170

Jia Q, den Dulk-Ras A, Shen H, Hooykaas PJ, de Pater S (2013) Poly(ADP-ribose)polymerases are involved in microhomology mediated back-up non-homologous end joining in Arabidopsis thaliana. Plant Mol Biol **82:** 339-351

Jones JD, Dangl JL (2006) The plant immune system. Nature **444:** 323-329

Keil C, Grobe T, Oei SL (2006) MNNG-induced cell death is controlled by interactions between PARP-1, poly(ADP-ribose) glycohydrolase, and XRCC1. J Biol Chem **281:** 34394-34405

Kinner A, Wu W, Staudt C, Iliakis G (2008) Gamma-H2AX in recognition and signaling of DNA double-strand breaks in the context of chromatin. Nucleic Acids Res **36:** 5678-5694

Kleinboelting N, Huep G, Kloetgen A, Viehoever P, Weisshaar B (2012) GABI-Kat SimpleSearch: new features of the Arabidopsis thaliana T-DNA mutant database. Nucleic Acids Res **40:** D1211-1215

Koh DW, Lawler AM, Poitras MF, Sasaki M, Wattler S, Nehls MC, Stoger T, Poirier GG, Dawson VL, Dawson TM (2004) Failure to degrade poly(ADP-ribose) causes increased sensitivity to cytotoxicity and early embryonic lethality. Proc Natl Acad Sci U S A **101:** 17699-17704

Krishnakumar R, Kraus WL (2010) The PARP side of the nucleus: molecular actions, physiological outcomes, and clinical targets. Mol Cell **39:** 8-24

Lamb RS, Citarelli M, Teotia S (2012) Functions of the poly(ADP-ribose) polymerase superfamily in plants. Cell Mol Life Sci **69:** 175-189

Li G, Nasar V, Yang Y, Li W, Liu B, Sun L, Li D, Song F (2011) Arabidopsis poly(ADP-ribose) glycohydrolase 1 is required for drought, osmotic and oxidative stress responses. Plant Sci **180:** 283-291

Lin W, Ame JC, Aboul-Ela N, Jacobson EL, Jacobson MK (1997) Isolation and characterization of the cDNA encoding bovine poly(ADP-ribose) glycohydrolase. J Biol Chem **272:** 11895-11901

Liu S, Liu S, Wang M, Wei T, Meng C, Wang M, Xia G (2014) A wheat SIMILAR TO RCD-ONE gene enhances seedling growth and abiotic stress resistance by modulating redox homeostasis and maintaining genomic integrity. Plant Cell **26:** 164-180

Luo X, Kraus WL (2012) On PAR with PARP: cellular stress signaling through poly(ADP-ribose) and PARP-1. Genes Dev **26:** 417-432

Masutani M, Nozaki T, Nakamoto K, Nakagama H, Suzuki H, Kusuoka O, Tsutsumi M, Sugimura T (2000) The response of Parp knockout mice against DNA damaging agents. Mutat Res **462:** 159-166

Menissier de Murcia J, Ricoul M, Tartier L, Niedergang C, Huber A, Dantzer F, Schreiber V, Ame JC, Dierich A, LeMeur M, Sabatier L, Chambon P, de Murcia G (2003) Functional interaction between PARP-1 and PARP-2 in chromosome stability and embryonic development in mouse. EMBO J **22:** 2255-2263

Meyer-Ficca ML, Meyer RG, Coyle DL, Jacobson EL, Jacobson MK (2004) Human poly(ADP-ribose) glycohydrolase is expressed in alternative splice variants yielding isoforms that localize to different cell compartments. Exp Cell Res **297:** 521-532

Muthumani K, Choo AY, Zong WX, Madesh M, Hwang DS, Premkumar A, Thieu KP, Emmanuel J, Kumar S, Thompson CB, Weiner DB (2006) The HIV-1 Vpr and glucocorticoid receptor complex is a gain-of-function interaction that prevents the nuclear localization of PARP-1. Nat Cell Biol **8:** 170-179

Nakagawa T, Kurose T, Hino T, Tanaka K, Kawamukai M, Niwa Y, Toyooka K, Matsuoka K, Jinbo T, Kimura T (2007) Development of series of gateway binary vectors, pGWBs, for realizing efficient construction of fusion genes for plant transformation. J Biosci Bioeng **104:** 34-41

Nakagawa T, Suzuki T, Murata S, Nakamura S, Hino T, Maeo K, Tabata R, Kawai T, Tanaka K, Niwa Y, Watanabe Y, Nakamura K, Kimura T, Ishiguro S (2007) Improved Gateway binary vectors: high-performance vectors for creation of fusion constructs in transgenic analysis of plants. Biosci Biotechnol Biochem **71:** 2095-2100

Nossa CW, Jain P, Tamilselvam B, Gupta VR, Chen LF, Schreiber V, Desnoyers S, Blanke SR (2009) Activation of the abundant nuclear factor poly(ADP-ribose) polymerase-1 by Helicobacter pylori. Proc Natl Acad Sci U S A **106:** 19998-20003

Okubo S, Hara F, Tsuchida Y, Shimotakahara S, Suzuki S, Hatanaka H, Yokoyama S, Tanaka H, Yasuda H, Shindo H (2004) NMR structure of the N-terminal domain of SUMO ligase PIAS1 and its interaction with tumor suppressor p53 and A/T-rich DNA oligomers. J Biol Chem **279:** 31455-31461

Panda S, Poirier GG, Kay SA (2002) tej defines a role for poly(ADP-ribosyl)ation in establishing period length of the arabidopsis circadian oscillator. Dev Cell **3:** 51-61

Papamichos-Chronakis M, Peterson CL (2013) Chromatin and the genome integrity network. Nat Rev Genet **14:** 62-75

Povirk LF (1996) DNA damage and mutagenesis by radiomimetic DNA-cleaving agents: bleomycin, neocarzinostatin and other enediynes. Mutat Res **355:** 71-89

Rissel D, Losch J, Peiter E (2014) The nuclear protein Poly(ADP-ribose) polymerase 3 (AtPARP3) is required for seed storability in Arabidopsis thaliana. Plant Biol (Stuttg)

Rogakou EP, Pilch DR, Orr AH, Ivanova VS, Bonner WM (1998) DNA double-stranded breaks induce histone H2AX phosphorylation on serine 139. J Biol Chem **273:** 5858-5868

Sahara S, Aoto M, Eguchi Y, Imamoto N, Yoneda Y, Tsujimoto Y (1999) Acinus is a caspase-3-activated protein required for apoptotic chromatin condensation. Nature **401:** 168-173

Schreiber V, Ame JC, Dolle P, Schultz I, Rinaldi B, Fraulob V, Menissier-de Murcia J, de Murcia G (2002) Poly(ADP-ribose) polymerase-2 (PARP-2) is required for efficient base excision DNA repair in association with PARP-1 and XRCC1. J Biol Chem **277:** 23028-23036

Schreiber V, Dantzer F, Ame JC, de Murcia G (2006) Poly(ADP-ribose): novel functions for an old molecule. Nat Rev Mol Cell Biol **7:** 517-528

Schulz P, Jansseune K, Degenkolbe T, Meret M, Claeys H, Skirycz A, Teige M, Willmitzer L, Hannah MA (2014) Poly(ADP-ribose)polymerase activity controls plant growth by promoting leaf cell number. PLoS One **9:** e90322

Schulz P, Neukermans J, Van der Kelen K, Muhlenbock P, Van Breusegem F, Noctor G, Teige M, Metzlaff M, Hannah MA (2012) Chemical PARP inhibition enhances growth of Arabidopsis and reduces anthocyanin accumulation and the activation of stress protective mechanisms. PLoS One **7:** e37287

Shieh WM, Ame JC, Wilson MV, Wang ZQ, Koh DW, Jacobson MK, Jacobson EL (1998) Poly(ADP-ribose) polymerase null mouse cells synthesize ADP-ribose polymers. J Biol Chem **273:** 30069-30072

Song J, Bent AF (2014) Microbial pathogens trigger host DNA double-strand breaks whose abundance is reduced by plant defense responses. PLoS Pathog **10:** e1004030

Song J, Durrant WE, Wang S, Yan S, Tan EH, Dong X (2011) DNA repair proteins are directly involved in regulation of gene expression during plant immune response. Cell Host Microbe **9:** 115-124

Tomasz M, Lipman R, Chowdary D, Pawlak J, Verdine GL, Nakanishi K (1987) Isolation and structure of a covalent cross-link adduct between mitomycin C and DNA. Science **235:** 1204-1208

Uchiumi F, Watanabe T, Ohta R, Abe H, Tanuma S (2013) PARP1 gene expression is downregulated by knockdown of PARG gene. Oncol Rep **29:** 1683-1688

Vanderauwera S, De Block M, Van de Steene N, van de Cotte B, Metzlaff M, Van Breusegem F (2007) Silencing of poly(ADP-ribose) polymerase in plants alters abiotic stress signal transduction. Proc Natl Acad Sci U S A **104:** 15150-15155

Wang ZQ, Stingl L, Morrison C, Jantsch M, Los M, SchulzeOsthoff K, Wagner EF (1997) PARP is important for genomic stability but dispensable in apoptosis. Genes Dev **11:** 2347-2358

Weitzman MD, Weitzman JB (2014) What's the damage? The impact of pathogens on pathways that maintain host genome integrity. Cell Host Microbe **15:** 283-294

Whalen MC, Innes RW, Bent AF, Staskawicz BJ (1991) Identification of *Pseudomonas syringae* pathogens of Arabidopsis and a bacterial locus determining avirulence on both Arabidopsis and soybean. Plant Cell **3:** 49-59

Zhou J, Huang JD, Poon VK, Chen DQ, Chan CC, Ng F, Guan XY, Watt RM, Lu L, Yuen KY, Zheng BJ (2009) Functional dissection of an IFN-alpha/beta receptor 1 promoter variant that confers higher risk to chronic hepatitis B virus infection. J Hepatol **51:** 322-332

Chapter 3: 3-Aminobenzamide inhibits callose deposition and alters PMR4 callose synthase abundance independently of poly(ADP-ribosyl)ation

The material in this chapter is currently being prepared for publication.

Authors: Brian D. Keppler, Junqi Song, Jackson Nyman, Andrew F. Bent

Contributions: I performed all experiments with the exception of Figure 3B and Supplemental Figure 1.

3.1 Abstract

Cell wall reinforcement with callose is a common feature of plant responses to infection. Poly(ADP-ribosyl)ation is a post-translational modification in which chains of ADP-ribose are added to a target protein by poly(ADP-ribose) polymerases (PARPs). Poly(ADP-ribosyl)ation is well known for its roles in DNA damage repair and has more recently been shown to contribute to plant immune responses. 3-aminobenzamide (3AB) is an established PARP inhibitor and it blocks the callose deposition elicited by flg22 or elf18, two microbe-associated molecular patterns (MAMPs, also termed PAMPs). However, we report that an Arabidopsis *parp1parp2parp3* triple mutant does not exhibit loss of flg22- or elf18-induced callose deposition. Additionally, the more potent and specific PARP inhibitors PJ-34 and INH_2BP inhibit PARP activity in Arabidopsis, but do not block MAMP-induced callose deposition. These data demonstrate off-target activity of 3AB, and indicate that 3AB inhibits callose deposition through a mechanism other than poly(ADP-ribosyl)ation. POWDERY MILDEW RESISTANT 4 (PMR4) is the callose synthase responsible for the majority of MAMP and wound-induced callose deposition in Arabidopsis. 3AB does not block wound-induced callose deposition, and 3AB does not reduce *PMR4* mRNA abundance in response to flg22. Levels of PMR4-HA protein (under control of *PMR4* promoter sequences) increase in response to flg22 and interestingly, PMR4-HA levels after flg22 treatment increase even more in the presence of 3AB, despite no callose being produced. The callose synthase inhibitor 2-deoxy-D-glucose does not cause similar impacts on PMR4-HA protein levels after flg22 treatment. 3AB thus reveals the presence of one or more presently unknown pathways that regulate PMR4 activity and MAMP-induced callose deposition in plants.

3.2 Introduction

Plants face numerous potential bacterial, oomycete, and fungal invaders, yet they are able to effectively prevent the large majority of these encounters from progressing to disease. Once a microbe has overcome preformed physical or chemical barriers in the plant, this disease resistance is due in large part to the plant's innate immune system. Plants have evolved pattern recognition receptors (PRRs) that induce defense responses after recognizing certain characteristic compounds of microbes, known as microbe- or pathogen-associated molecular patterns (MAMPs, or PAMPs)(Jones and Dangl, 2006; Boller and Felix, 2009). Upon the binding of MAMPs to PRRs, an innate immune response known as pattern-triggered immunity (PTI) is initiated. PTI involves a variety of plant defense responses, including deposition of the β-(1,3)-glucan callose (Dodds and Rathjen, 2010; Macho and Zipfel, 2014; Li et al., 2016).

Callose serves a variety of specialized functions in the cell walls of higher plants. Callose is one of the most abundant compounds in papillae, cell wall thickenings formed in response to pathogen attack (Aist, 1976). In addition to its roles in pathogen defense, callose plays critical roles in pollen development (Dong et al., 2005; Enns et al., 2005), formation of the cell plate during cytokinesis (Chen et al., 2009; Thiele et al., 2009), and regulation of cell-to-cell trafficking through the plasmodesmata (Lee and Lu, 2011; Vaten et al., 2011). The Arabidopsis genome encodes a total of twelve callose synthase enzymes (Richmond and Somerville, 2000; Hong et al., 2001). PMR4 (POWDERY MILDEW RESISTANT 4; also known as GLUCAN SYNTAHSE-LIKE 5 [GSL5] and CALS12) accounts for nearly all wound- and pathogen-induced callose, as both responses are absent in *pmr4* mutants (Jacobs et al., 2003; Nishimura et al., 2003; Clay et al., 2009; Luna et al., 2011)**.**

PMR4 was initially identified in a screen to identify mutants with increased resistance to the Arabidopsis powdery mildew pathogen, *Erysiphe cichoracearum* (now known as *Golovinomyces cichoracearum* (Vogel and Somerville, 2000). Given that callose deposition was regarded as a cell wall reinforcement to prevent further pathogen ingress, the finding that a mutant lacking callose was more resistant to a pathogen was counterintuitive and initially cast doubt on the importance of callose deposition in the plant innate immune response, but *pmr4* mutants exhibit constitutively elevated or primed defenses that apparently account for the increased resistance (Nishimura et al., 2003). More recently, overexpression of *PMR4* was shown to enhance callose deposition and also increases resistance to adapted powdery mildew (Ellinger et al., 2013). Despite the ubiquitous presence of callose deposition in plant innate immune responses, much remains to be understood about the regulation of pathways between MAMP perception by PRRs or wounding and the PMR4 callose synthase, including the activation of PMR4 and its relocalization to sites of pathogen attack.

Poly(ADP-ribosyl)ation is a post-translational modification of proteins in which chains of ADP-ribose are added to a target protein by enzymes known as poly-ADP-ribose polymerases (PARPs) (Gibson and Kraus, 2012). Poly-ADP-ribose moieties in turn can be removed by poly-ADP-ribose glycohydralase (PARG) enzymes. Poly(ADP-ribosyl)ation has been studied extensively in animal systems because of its involvement in DNA damage repair and an increasing number of other important processes (Schreiber et al., 2006; Kalisch et al., 2012) and due to the potential use of therapeutic PARP inhibitors in cancer treatment (Virag and Szabo, 2002; Ellisen, 2011). Poly(ADP-ribosyl)ation and related processes, including DNA damage, also have been demonstrated to play important roles in plant immune system responses to

infection (Lucht et al., 2002; Briggs and Bent, 2011; Yan et al., 2013; Yao et al., 2013; Song and Bent, 2014; Feng et al., 2015; Song et al., 2015).

The Arabidopsis genome encodes three PARP genes similar in structure to those found in mammalian systems, namely PARP1, PARP2, and PARP3 (Briggs and Bent, 2011; Lamb et al., 2012). PARP2 plays a more important role than PARP1 in DNA damage responses and plant immune responses (Song et al., 2015), while PARP3 is expressed primarily in seeds and may promote seed viability (Rissel et al., 2014). In addition, six plant-specific proteins with PARP domains were previously identified: the SRO (SIMILAR TO RCD ONE) family, consisting of the founding member RCD1 as well the related SRO1 through SRO5 (Overmyer et al., 2000; Ahlfors et al., 2004). RCD1 has been confirmed experimentally to lack PARP activity and bioinformatics-based sequence analysis indicated the remaining members are unlikely to possess PARP activity (Jaspers et al., 2010). However, wheat SRO1 was confirmed to exhibit PARP activity and play a role in abiotic stress resistance (Liu et al., 2014).

In order to study poly(ADP-ribosyl)ation and overcome the potential functional redundancy of multiple PARP enzymes, chemical inhibitors of PARP are often utilized. 3-aminobenzamide (3AB) is a well characterized inhibitor of poly(ADP-ribosyl)ation that has been used in studies with mammalian systems since the early 1980s (Purnell and Whish, 1980; Virag and Szabo, 2002; Ellisen, 2011). Notably, 3AB blocks some plant innate immune responses while others remain intact. In general, the early steps following recognition of a MAMP remain intact, while later events are disrupted (Adams-Phillips et al., 2010). Specifically, expression of early MAMP-induced genes such as *WRKY29* and *FRK1* are still upregulated and reactive oxygen species (ROS) production still occurs even in the presence of 3AB. However, flg22-

induced callose deposition, which is typically apparent 12 to 24 hours following MAMP perception, is inhibited by 3AB (Adams-Phillips et al., 2010).

Here we further characterize the impact of 3AB on MAMP-induced callose deposition. Surprisingly, we find that the inhibition of callose by 3AB is largely independent of poly(ADP-ribosyl)ation. However, 3AB does impact PMR4 protein abundance in the presence of flg22, suggesting novel mechanisms of PMR4 regulation. Hence 3AB is a valuable chemical genetic tool to probe the unique pathways that regulate pathogenesis-related plant callose deposition.

3.3 Results

3AB blocks flg22-induced callose but not wound-induced callose

In Arabidopsis, flg22 and wound-induced callose are the product of the same PMR4 callose synthase enzyme, as both are absent in a *pmr4* mutant (Jacobs et al., 2003; Nishimura et al., 2003; Luna et al., 2011). Interestingly, while 3AB blocks flg22-induced callose, wound-induced callose is unaffected (Adams-Phillips et al., 2010). Even within a single seedling exposed to flg22 and with one cotyledon wounded, we found that 3AB blocks the flg22-induced callose but not the wound-induced callose (**Figure 1**). This intriguing specificity strongly suggests that 3AB does not inhibit callose synthase activity directly. Rather, the target of 3AB is likely to be upstream of PMR4 callose synthase catalytic activity and specific to the flg22-activated (or other MAMP-activated) callose deposition pathways, but downstream of initial MAMP detection, because early plant innate immune responses such as MAP kinase activation and ROS production were previously shown to occur in even the presence of 3AB (Adams-Phillips et al., 2010).

***parp1parp2parp3* triple mutants still produce flg22-induced callose**

Given that 3AB is a well-characterized inhibitor of PARP-mediated poly(ADP-ribosyl)ation, we hypothesized that 3AB blocks callose deposition by inhibiting the activity of one or more of the three enzymes with predicted PARP activity in Arabidopsis, namely PARP1, PARP2, and PARP3, and that this PARP activity is required for flg22-induced callose deposition. We constructed a *parp1parp2parp3* triple mutant to investigate the role of all three PARP enzymes in callose deposition. Surprisingly, the *parp1parp2parp3* triple mutant does not exhibit a loss of callose as is observed with 3AB, or even a reduction, and if anything exhibits a slight increase in callose deposition compared to wild type (**Figure 2**). We have demonstrated that the *parp1parp2* double mutant that was used to make this triple mutant already exhibits little or no poly(ADP-ribosyl)ation activity (Song et al., 2015). The differing callose response phenotypes with the PARP inhibitor 3AB as opposed to the *parp1parp2parp3* triple mutant brings up known issues about the specificity of 3AB as an inhibitor of poly(ADP-ribosyl)ation (Virag and Szabo, 2002).

One hypothesis for the differing results with 3AB and the triple mutant is that 3AB may be blocking callose as a PARP inhibitor but the target is a previously unidentified protein with PARP enzymatic activity. Alternatively, the impact of 3AB on callose could be an off-target effect unrelated to PARP inhibition and poly(ADP-ribosyl)ation. To test the first hypothesis, we studied *SRO2* and *SRO5*. RCD1 and the SRO family are the only other Arabidopsis proteins with predicted similarity to PARPs, but have been shown experimentally or bioinformatically to be unlikely to have PARP activity (Jaspers et al., 2010). However, we tested *SRO2* and *SRO5* because they are upregulated by flg22 and pathogen infection in the Genevestigator V3 microarray database (Hruz et al., 2008). We generated RNAi knockdown lines targeting either

the *SRO2* or *SRO5* transcript, but neither altered levels of flg22-induced callose deposition (**Supplemental Figure 1**).

INH_2BP and PJ-34 are bona fide PARP inhibitors in Arabidopsis but do not impact callose deposition

Other known PARP inhibitors were tested to determine if they also block flg22-induced callose as is observed with 3AB. Numerous PARP inhibitors have been developed to target mammalian PARPs in recent years as research tools as well as for potential chemotherapeutic uses (Rouleau et al., 2010), but these have not previously been reported as inhibitors of plant PARPs. The more specific PARP inhibitor PJ-34, which is considered 10,000 times more potent than 3AB, and INH_2BP were obtained (Abdelkarim et al., 2001). Both PJ-34 and INH_2BP were tested but failed to inhibit callose as is observed with 3AB (**Figure 3A**). Only the PARP inhibitor 3-methoxybenzamide (3MB), which is structurally related to 3AB, behaved similarly to 3AB and blocked flg22-induced callose (**Figure 3A**).

In order to confirm that INH_2BP and PJ-34 are bona fide PARP inhibitors in Arabidopsis, plants were treated with the DNA damage reagent bleomycin in the presence or absence of the inhibitors. Use of an anti-PAR antibody after bleomycin treatment showed that bleomycin strongly induces poly(ADP-ribosyl)ation of target proteins, including the PARP enzymes themselves. At either 16 or 24 hours following bleomycin treatment, poly(ADP-ribosyl)ation is strongly induced. Poly(ADP-ribosyl)ation was inhibited not only by 3AB but also by INH_2BP and PJ-34 (**Figure 3B**). These results demonstrate that INH_2BP and PJ-34 are bona fide PARP inhibitors in Arabidopsis, yet do not inhibit flg22-induced callose deposition, supporting the conclusion that the impact of 3AB on callose is independent of PARP activity.

3AB does not reduce *PMR4* gene expression

Despite questions about the target of 3AB, its intriguing impact on callose deposition makes it a powerful tool to elucidate regulatory mechanisms that control pathogenesis-responsive callose deposition. As such, we investigated the impacts of 3AB on PMR4. Quantitative real time (qRT)-PCR was utilized to monitor *PMR4* gene expression following flg22 treatment in the presence or absence of 3AB. We observed a two- to three-fold induction of *PMR4* gene expression at two and four hours following flg22 treatment (**Figure 4**). A similar induction of *PMR4* was observed even in the presence of 3AB, demonstrating that 3AB does not block, either directly or indirectly, *PMR4* gene expression. At 16 and 24 hours following flg22 treatment, a slight increase in *PMR4* expression was observed in the presence of 3AB, suggesting possible upregulation of *PMR4* as a compensatory response to the inhibition of callose deposition.

3AB increases PMR4-HA protein abundance in the presence flg22

In order to monitor PMR4 protein levels following flg22 and/or 3AB treatments, an HA-tagged *PMR4* construct under control of the *PMR4* native promoter (*PMR4pro::PMR4-HA*) was generated and transformed into the *pmr4* mutant background. The *pmr4* mutant line transformed with *PMR4pro::PMR4-HA* regained the capacity to deposit callose in response to flg22 at wild type levels. Flg22-induced callose deposition is also blocked by 3AB in this line, confirming that the construct successfully rescues the *pmr4* mutant phenotypes (**Supplemental Figure 2**).

The abundance of the PMR4-HA protein was monitored at 24 hours after treatments with flg22 and 3AB. Consistent with observations in the above gene expression study, an increase in

PMR4-HA protein levels was observed in flg22-treated samples as compared to untreated controls (**Figure 5**). Intriguingly, samples treated with flg22 and 3AB exhibit greater PMR4-HA abundance even compared to those treated with flg22 alone, despite the fact that no callose is produced. Apparently, 3AB inhibits callose production and the plant responds by upregulating *PMR4* mRNA and PMR4 protein abundance, but because 3AB continues to inhibit through an unknown mechanism, no callose is produced. Similar results were also observed with an independent GFP-tagged PMR4 line (**Supplemental Figure 3**). As wound induced callose is a product of the same PMR4 callose synthase but is not blocked, PMR4-HA was also monitored with 3AB and wounding. As predicted, unlike for flg22, an increase in PMR4-HA protein was not observed with 3AB and wounding compared to wounding alone (**Supplemental Figure 4**). We also observed that samples treated with 3AB in the absence of flg22 sometimes exhibited decreased PMR4-HA abundance as compared to untreated controls, but this phenomenon was not consistently observed across all biological replicates.

Inhibition of callose synthase activity does not alter PMR4 levels

2-Deoxy-D-glucose (2-DDG) is a non-metabolizable form of glucose widely used as a direct inhibitor of callose synthase activity (Jaffe and Leopold, 1984; Bayles et al., 1990; Li et al., 2012). At a concentration of 3mM 2-DDG, flg22-induced callose deposition was blocked (**Figure 6**). However unlike 3AB, 2-DDG treatment did not alter PMR4 protein levels (**Figure 6**), suggesting that the mechanism of inhibition of callose by 3AB is not the product of direct inhibition of callose synthase activity.

3AB-induced changes in PMR4 abundance are unlikely to be due to PARP inhibition

While the loss of callose deposition caused by 3AB appears unlikely to be due to PARP inhibition, we also wanted to exclude the possibility that the changes in PMR4 abundance were due to inhibition of poly(ADP-ribosyl)ation. In order to do so, the impact of the more potent and specific PARP inhibited PJ-34 was also examined. Indeed, the increase in PMR4-HA observed with flg22+3AB is not apparent when seedlings are treated with flg22+PJ-34 (**Figure 7**). Given that PJ-34 is a more potent and specific PARP inhibitor than 3AB (Abdelkarim et al., 2001), and an inhibitor that more effectively blocks DNA damage induced poly(ADP-ribosyl)ation in Arabidopsis (**Figure 3B**), this provides evidence that the impact of 3AB on both callose deposition and PMR4 protein abundance are independent of poly(ADP-ribosyl)ation.

Protein levels of PEN1 and PEN3, which are required for callose deposition, are not altered by 3AB

Additional experiments assessed if the impact of 3AB on protein abundance is specific to PMR4 or if it impacts the abundance other proteins, in particular proteins associated with callose deposition. Levels of GFP-tagged PENETRATION1 and PENETRATION3 (GFP-PEN1 and PEN3-GFP) were therefore examined. *PEN1* encodes a syntaxin, while *PEN3* encodes an ABC transporter, and each is required for an independent pathway leading to penetration resistance to powdery mildew (Collins et al., 2003; Stein et al., 2006). Importantly, *pen1* and *pen3* mutants lack flg22-induced callose deposition (Clay et al., 2009). We observed that PEN3-GFP is strongly induced by flg22, but additional PEN3-GFP protein is not induced by 3AB as is observed with PMR4-HA (**Figure 8**). Similarly, GFP-PEN1 levels remained relatively constant whether treated with flg22 or 3AB **(Figure 8)**.

3.4 Discussion

Poly(ADP-ribosyl)ation is best characterized for its roles in DNA damage repair, cell death, chromatin remodeling, and transcriptional regulation in mammals (Schreiber et al., 2006; Gibson and Kraus, 2012). Roles for poly(ADP-ribosyl)ation in plant immunity have also become increasingly clear (Adams-Phillips et al., 2008; Adams-Phillips et al., 2010; Briggs and Bent, 2011; Feng et al., 2015; Song et al., 2015). Despite the roles of poly(ADP-ribosyl)ation in plant immunity demonstrated by other means such as mutational studies, the present work shows that the inhibition of MAMP-induced callose by the PARP inhibitor 3AB is independent of poly(ADP-ribosyl)ation. While the structurally related 3MB also blocks callose, other more potent and specific PARP inhibitors, such as INH_2BP and PJ-34 do not. Moreover, *parp1parp2parp3* knockout mutants still produce callose near wild type levels. The activity of 3AB as a PARP inhibitor and an inhibitor of poly(ADP-ribosyl)ation has been widely and conclusively documented in animal and plant studies (Chen et al., 1994; Panda et al., 2002; Virag and Szabo, 2002; Rouleau et al., 2010). However, despite common statements about 3AB as a specific inhibitor of poly(ADP-ribosyl)ation, several off-target impacts have been reported in mammalian systems. For instance, 3AB protects primary human keratinocytes from UV-induced cell death, but this phenotype was not reproduced with the inhibitor PJ-34 or with silencing of PARP1, indicating a poly(ADP-ribosyl)ation independent mechanism (Lakatos et al., 2013). In other studies 3AB has been shown to inhibit protein kinase C (Ricciarelli et al., 1998), certain cytochrome P450s (Eriksson et al., 1996), and to act as a hydroxyl radical scavenger (Czapski et al., 2004). Our study adds to this list, and demonstrates a new off-target effect of 3AB in plants.

Despite these non-specific impacts, 3AB is still frequently used as an inhibitor of poly(ADP-ribosyl)ation. Numerous Arabidopsis studies have utilized 3AB, where it helped implicate roles for poly(ADP-ribosyl)ation in the regulation of apoptosis, circadian rhythms, and stress responses (Tian et al., 2000; Panda et al., 2002; Ishikawa et al., 2009; Schulz et al., 2012). Given this possibility of non-specific targets, reports utilizing 3AB to demonstrate a role for poly(ADP-ribosyl)ation in a given process should be treated with caution and should be accompanied by other inhibitors or, preferably, genetic evidence through the use of *parp* knockout lines.

The unique impact of 3AB on PMR4 protein abundance is intriguing. We investigated the hypothesis that the lack of flg22-induced callose could be explained by reduced PMR4 protein abundance in the presence of 3AB, but instead observed that 3AB increases PMR4 protein abundance after flg22 treatment, despite a near-complete absence of callose. The presence of abundant PMR4 protein but no callose production suggests that 3AB is impacting the localization or subsequent activation of the PMR4 protein. Importantly, the target of inhibition is unique to MAMP-induced callose, because wound-induced callose is not altered by 3AB. Moreover, the 3AB-induced increase in PMR4 abundance after MAMP treatment is not due to inhibition of callose synthase activity, because 3AB does not block wound-induced callose deposition and because similar alterations were not observed with the callose synthase inhibitor 2-DDG.

Possible targets of 3AB include disrupting PMR4 localization at the plasma membrane, relocalization of PMR4 to the site of pathogen attack, or activation of the PMR4 protein itself (Bohlenius et al., 2010; Nielsen et al., 2012; Ellinger et al., 2014). We constructed *PMR4pro::PMR4-GFP* lines that successfully rescued the *pmr4* mutant for flg22-induced callose

deposition, as one possible avenue to investigate the MAMP- or pathogen-induced relocalization of the PMR4 in the presence and absence of 3AB. However, GFP fluorescence was not detectable above background in those lines using a sensitive Zeiss Elyra PS1 confocal microscopy system, possibly due to the low expression of *PMR4* from the *PMR4* promoter. Overexpression of PMR4-GFP might overcome the GFP detection issue, but the biological validity of PMR4 localization results in strong overexpression lines would remain unclear. Much remains to be understood about the regulation of PMR4 and callose deposition following pathogen perception, particularly in contrast to wound-induced callose, and 3AB provides a useful tool for this research. Studies with 3AB have revealed the presence of one or more presently unknown pathways that regulate PMR4 activity and MAMP-induced callose deposition in plants.

3.5 Materials and Methods

Plant growth conditions

Arabidopsis thaliana seedlings were grown for callose assays as previously described with some modifications (Clay et al., 2009; Luna et al., 2011). Briefly, 15 seeds per well were distributed into each well of a 12-well plate. 1mL of liquid Murashige-Skoog (MS) media was added to each well, plates were sealed with micropore tape and cold treated for 2-3 days at 4°C. Following cold treatment, plates were moved to growth chambers at 22°C under 16-h light/8-h dark cycles. The media was replaced on day 7 and then on day 9 seedlings were treated with elicitors (1µM flg22) and/or inhibitors (1mM 3AB, 1mM 3MB, 100µM PJ-34, 100µM INH_2BP, 3mM 2-DDG). Unless otherwise noted, seedlings were collected after 24 hours of treatment.

Plant material

The previously described *parp1-2* (GABI_382F01) *parp2-1* (GABI_420G03) double mutant (Song et al., 2015) was crossed with a *parp3* (SALK_108092) mutant and progeny were genotyped to identify a *parp1parp2parp3* triple mutant. GFP-PEN1 and PEN3-GFP lines were previously described and kindly provided by William Underwood (Collins et al., 2003; Stein et al., 2006). The *pmr4-1* seeds (CS3858) were obtained from the Arabidopsis Biological Resource Center (ABRC).

Callose deposition assays and epifluorescence microscopy

Following elicitor/inhibitor treatment, seedlings were fixed in an FAA solution (10% formaldehyde, 5% acetic acid, and 50% ethanol) overnight, cleared in 95% ethanol, and stained with aniline blue (0.01% aniline blue in 67 mM K_2HPO_4 with pH adjusted to 12). The stained seedlings were visualized with an Olympus BX60 Epifluorescence Microscope and images of entire cotyledons were captured with an Olympus DP73 camera. At least 12 cotyledons were imaged per line per treatment and callose deposits were quantified automatically using ImageJ software and compared to total cotyledon area in order to calculate a percent area with callose deposits.

Generating tagged PMR4 lines

The full length genomic sequence of *PMR4* along with 2000 base pairs upstream promoter region and excluding the stop codon were amplified (5'-CGGGCAAGTTCCAAAGTTTTG-3' and 5'- GACATCGCCTTTTGATTTCTTCC -3') by PCR and cloned into the pCR8/GW/TOPO vector according to the manufacturer's protocol (Thermo

Fisher Scientific). The fragment was then recombined by LR cloning into pGWB13 (for C-terminal HA tag) and pGWB4 (for C-terminal GFP tag), which were then transformed into Arabidopsis *pmr4-1* mutant lines by agrobacterium-mediated floral drip transformation (Clough and Bent, 1998). Transformants were selected by antibiotic selection and all experiments were performed on homozygous T3 plants.

RNA extraction and gene expression analysis

RNA was extracted using TRIzol reagent (Thermo Fisher Scientific) with DNA removed with the DNA-free DNA Removal Kit (Thermo Fisher Scientific) . RNA concentrations were determined using the NanoDrop 1000 spectrophotometer (Thermo Fisher Scientific). cDNA was synthesized from RNA using iScript cDNA synthesis kit (Bio-Rad) according to the manufacturer's protocol. Quantitative PCR was performed with a CFX96 real-time PCR detection system (Bio-Rad). Primers used for PMR4 (5' - CTGGAATGCTGTTGTCTCTGTTG - 3' and 5'- TCGCCTTTTGATTTCTTCCCAGT-3') were previously described (Jacobs et al., 2003). Primers for TIP41-like family protein (At4g34270) were used as an internal control (Czechowski et al., 2005).

Protein extraction and western blot analysis

Total protein extracts were prepared from Arabidopsis plants in extraction buffer (50mM Tris-HCl pH7.5, 150mM NaCl, 5mM EDTA, 0.5% Triton X-100, 10% glycerol, and Sigma-Aldrich plant protease inhibitor cocktail at 1:100) as described previously (Song et al., 2015). Given the multiple transmembrane domains of PMR4, samples were heated in sample buffer at 37°C for 30 minutes to avoid protein aggregation. Following protein separation by SDS-PAGE,

western blot analysis was performed with anti-poly(ADP-ribose) (anti-PAR), anti-HA, or anti-GFP antibodies.

3.6 Figures

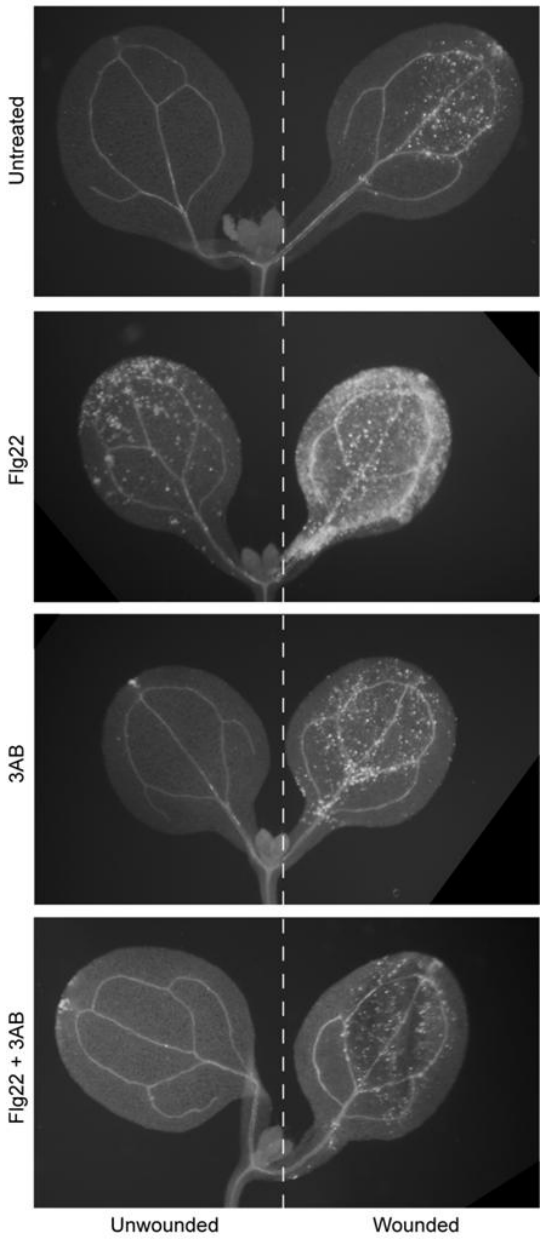

Figure 1. The poly(ADP-ribosyl)ation inhibitor 3AB blocks callose deposition in response to flg22, but not in response to wounding. Intact Arabidopsis seedlings were treated with flg22 and/or 3AB, and also were wounded on one cotyledon (right half of figure) but not the other (left half).

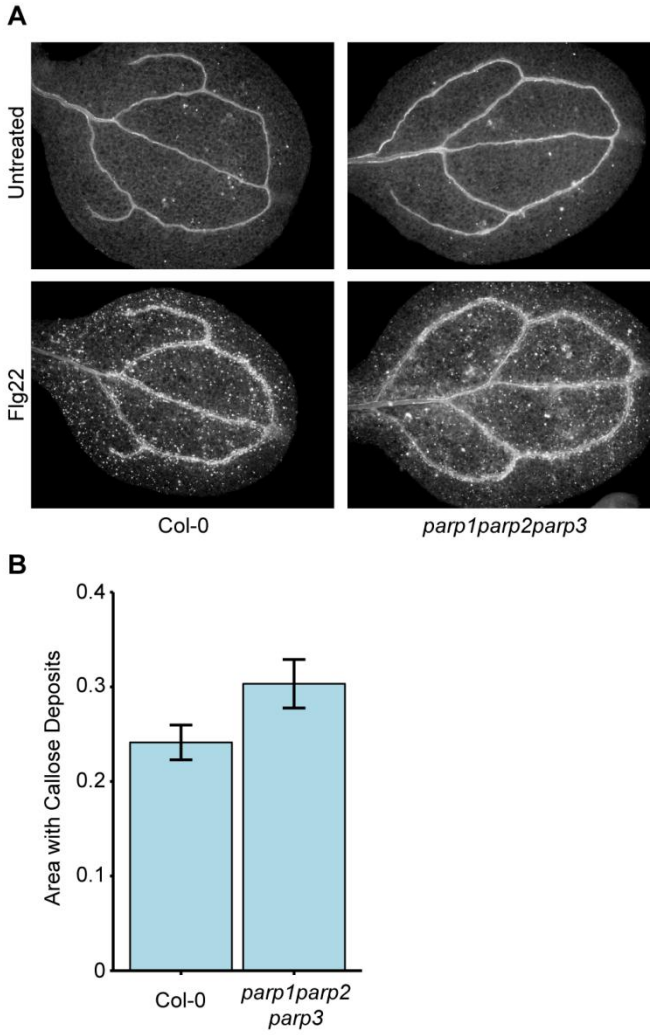

Figure 2. Col-0 and *parp1parp2parp3* triple mutants produce similar levels of flg22-induced callose. A, Representative images from Col-0 and the *parp1parp2parp3* triple mutant untreated or treated with flg22. B, Quantification of callose in cotyledons treated with flg22. Area represents total area with callose divided by total cotyledon area. Experiment repeated three times with twelve cotyledons per line per experiment. Bars indicate standard error. No significant differences (t-test, $p > 0.05$).

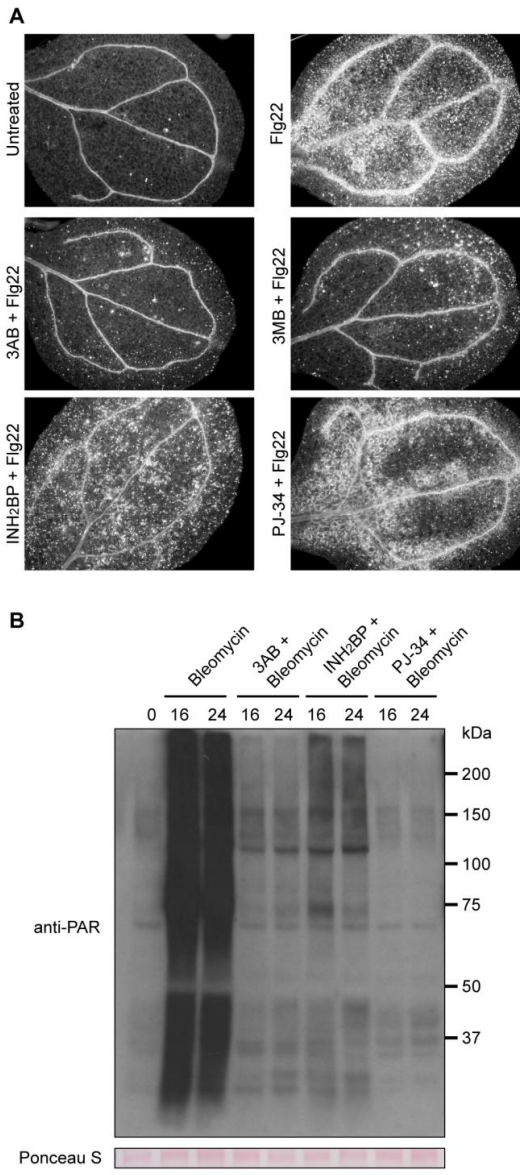

Figure 3. INH_2BP and PJ-34 inhibit PARP activity but do not impact flg22-induced callose deposition. A, Representative images of cotyledons treated with flg22 alone, or flg22 with the inhibitors 3AB, 3MB, INH_2BP, or PJ-34. B, Total protein extracts from seedlings treated with the DNA damage reagent bleomycin for 16 or 24 hours with or without PARP inhibitors were analyzed by immunoblotting with an anti-PAR antibody to detect poly(ADP-ribosyl)ed proteins. Equivalent loading of lanes was verified using Ponceau S stain.

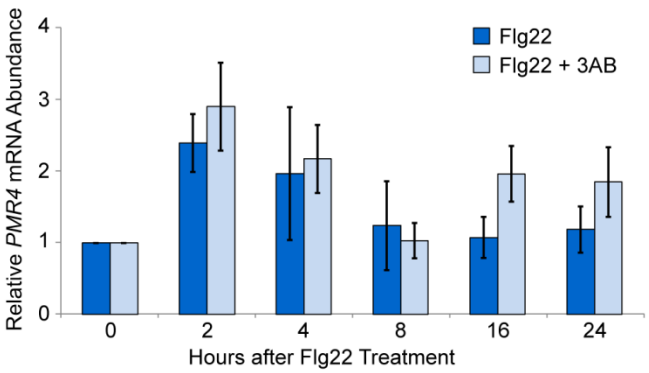

Figure 4. *PMR4* mRNA abundance is not reduced by 3AB. qRT-PCR analysis of *PMR4* mRNA abundance at various time points following flg22 or flg22+3AB treatment. Data are the average of two independent biological replicates. Bars indicate standard error.

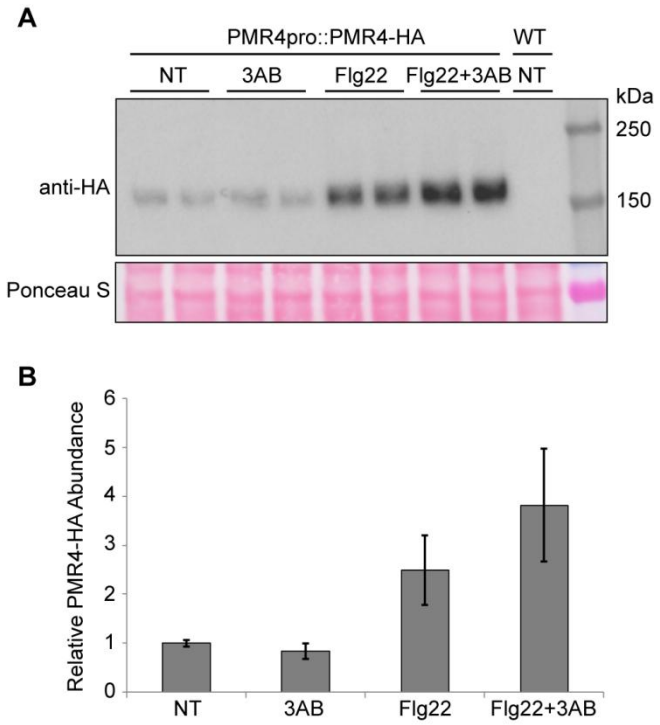

Figure 5. Inhibition of callose by 3AB increases the abundance of PMR4-HA in the presence flg22. A, Total protein extracts from seedlings analyzed by immunoblotting with an anti-HA antibody. Treatments were performed in duplicate. Equivalent loading of lanes was verified using Ponceau S stain. NT indicates no treatment. WT is a Col-0 wild type negative control.

B, Quantification of panel A and two additional biological replicates. Bars indicate standard error.

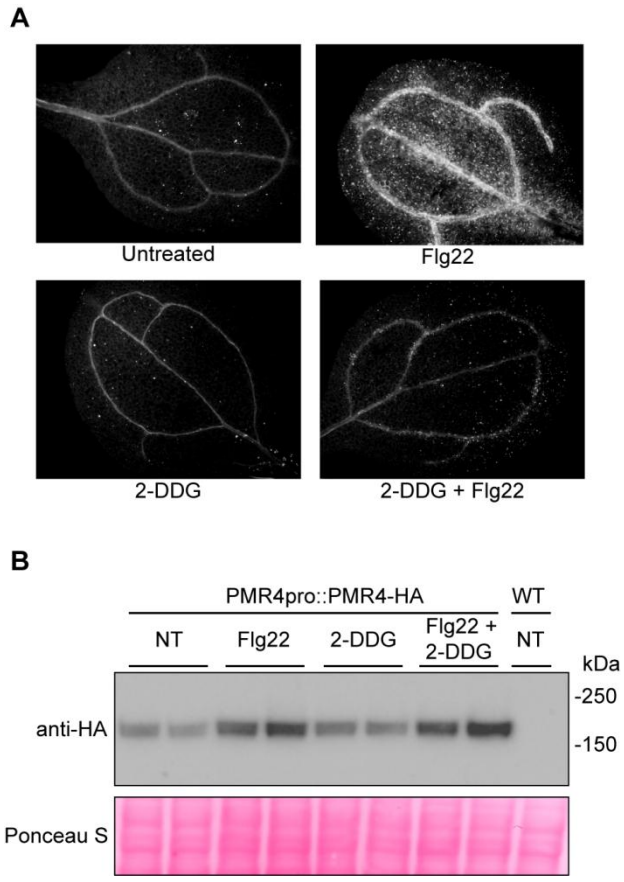

Figure 6. The callose synthase inhibitor 2-DDG blocks flg22-induced callose deposition but does not impact PMR4-HA abundance. A, Representative cotyledons untreated or treated with flg22, 3mM 2-DDG, or 3mM 2-DDG and flg22. B, Total protein extracts from seedlings untreated (NT) or treated as indicated were analyzed by immunoblotting with an anti-HA antibody. Treatments were performed in duplicate. Equivalent loading of lanes was verified using Ponceau S stain. WT is a Col-0 wild type negative control. Similar results were obtained in two separate experiments.

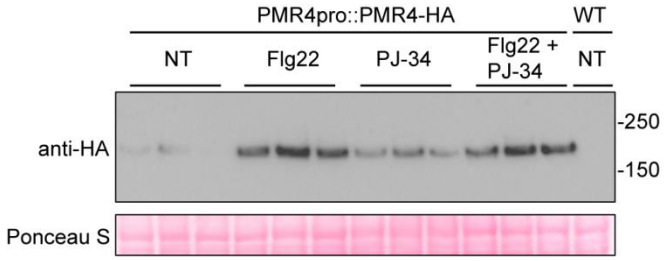

Figure 7. The more potent and specific PARP inhibitor PJ-34 does not cause alterations in PMR4-HA abundance. Total protein extracts from seedlings were analyzed by immunoblotting with an anti-HA antibody. Treatments were performed in triplicate. Equivalent loading of lanes was verified using Ponceau S stain. WT is a Col-0 wild type negative control. Similar results were obtained in two separate experiments.

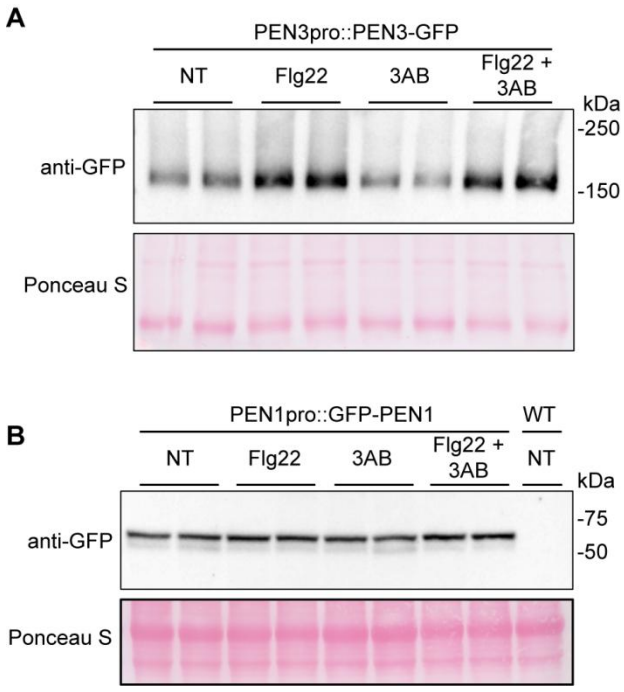

Figure 8. 3AB does not alter PEN3-GFP or GFP-PEN1 protein abundance as is observed for PMR4-HA. Total protein extracts from (A) PEN3-GFP or (B) GFP-PEN1 seedlings were analyzed by immunoblotting with an anti-GFP antibody. Treatments were performed in duplicate. Equivalent loading of lanes was verified using Ponceau S stain. NT indicates no treatment. WT is a Col-0 wild type negative control.

3.7 Supplemental Figures

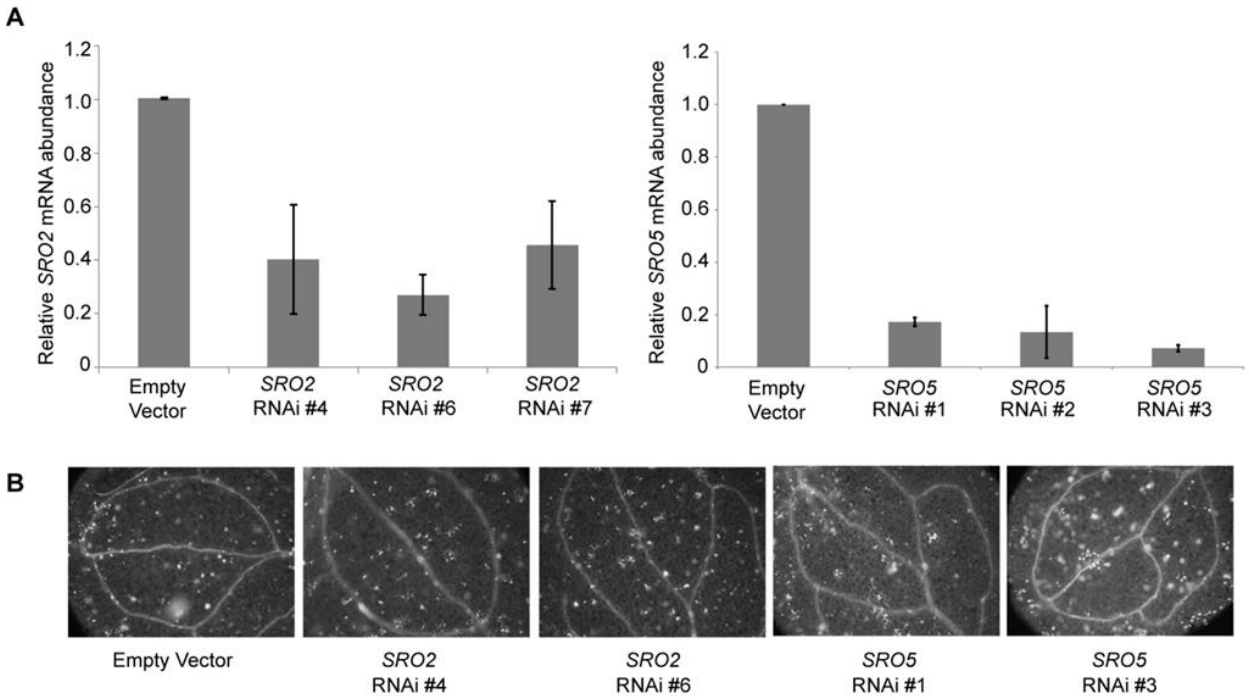

Supplemental Figure 1. *SRO2* and *SRO5* RNAi knockdown lines do not impact flg22-induced callose deposition. A, Quantitative real-time PCR analysis comparing *SRO2* or *SRO5* RNAi lines to empty vector controls. Average of two biological replicates. Bars indicate standard error. B, Representative images of flg22-induced callose in the *SRO2* and *SRO5* RNAi lines.

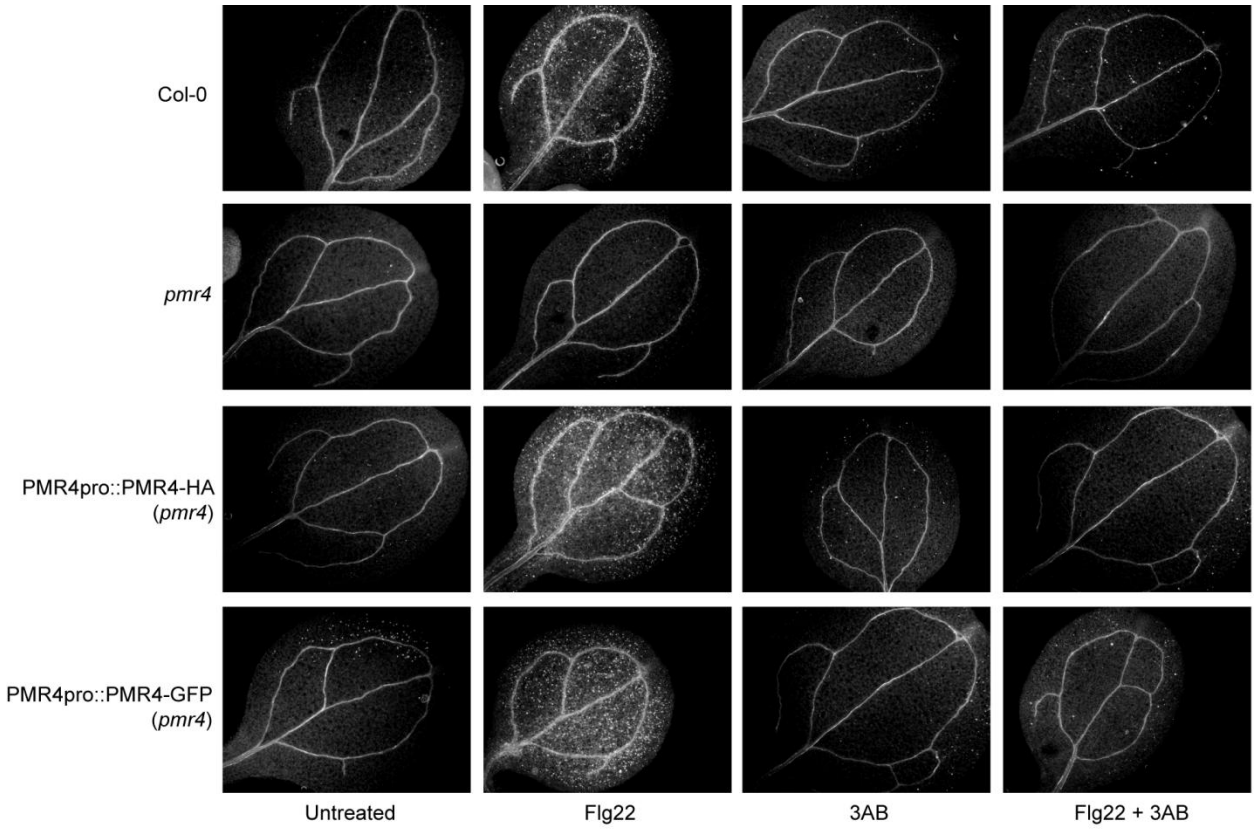

Supplemental Figure 2. PMR4-HA and PMR4-GFP lines successfully complement the *pmr4* knockout mutant. Representative images of Col-0 wild type, *pmr4* mutant, and PMR4-HA or PMR4-GFP lines (transformed in the *pmr4* mutant background) cotyledons untreated or treated with flg22, 3AB, or flg22+3AB.

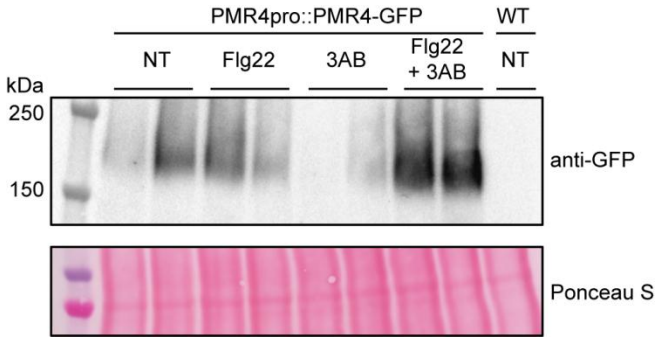

Supplemental Figure 3. As with PMR4-HA (Figure 5), 3AB increases the abundance of PMR4-GFP protein in the presence flg22. Total protein extracts from PMR4-GFP seedlings were analyzed by immunoblotting with an anti-GFP antibody. Treatments were performed in duplicate. Equivalent loading of lanes was verified using Ponceau S stain. NT indicates no treatment. WT is a Col-0 wild type negative control.

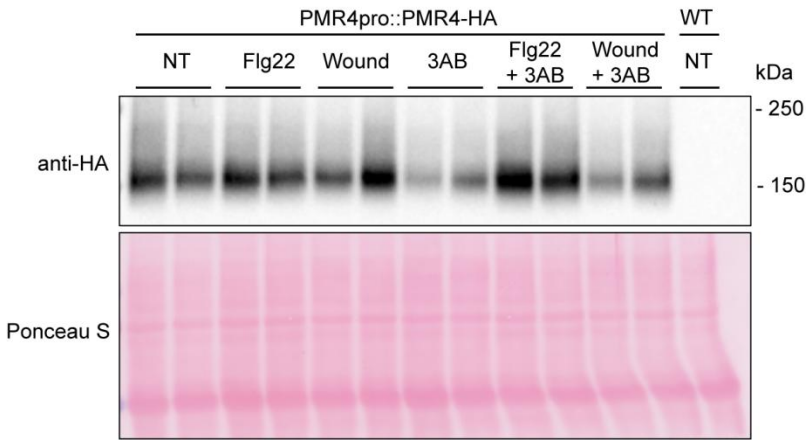

Supplemental Figure 4. Wounding in the presence of 3AB does not increase PMR4 protein abundance as with flg22. Total protein extracts from PMR4-HA seedlings analyzed by immunoblotting with an anti-HA antibody. Treatments were performed in duplicate. Equivalent loading of lanes was verified using Ponceau S stain. NT indicates no treatment. WT is a Col-0 wild type negative control.

3.8 References

Abdelkarim GE, Gertz K, Harms C, Katchanov J, Dirnagl U, Szabo C, Endres M (2001) Protective effects of PJ34, a novel, potent inhibitor of poly(ADP-ribose) polymerase (PARP) in in vitro and in vivo models of stroke. Int J Mol Med **7:** 255-260

Adams-Phillips L, Briggs AG, Bent AF (2010) Disruption of poly(ADP-ribosyl)ation mechanisms alters responses of Arabidopsis to biotic stress. Plant Physiol **152:** 267-280

Adams-Phillips L, Wan J, Tan X, Dunning FM, Meyers BC, Michelmore RW, Bent AF (2008) Discovery of ADP-ribosylation and other plant defense pathway elements through expression profiling of four different Arabidopsis-Pseudomonas R-avr interactions. Mol Plant Microbe Interact **21:** 646-657

Ahlfors R, Lang S, Overmyer K, Jaspers P, Brosche M, Tauriainen A, Kollist H, Tuominen H, Belles-Boix E, Piippo M, Inze D, Palva ET, Kangasjarvi J (2004) Arabidopsis RADICAL-INDUCED CELL DEATH1 belongs to the WWE protein-protein interaction domain protein family and modulates abscisic acid, ethylene, and methyl jasmonate responses. Plant Cell **16:** 1925-1937

Aist JR (1976) Papillae and Related Wound Plugs of Plant Cells. Annu Rev Phytopathol **14:** 145-163

Bayles CJ, Ghemawat MS, Aist JR (1990) Inhibition by 2-deoxy-D-glucose of callose formation, papilla deposition, and resistance to powdery mildew in an ml-o barley mutant. Physiol Mol Plant Pathol **36:** 63-72

Bohlenius H, Morch SM, Godfrey D, Nielsen ME, Thordal-Christensen H (2010) The multivesicular body-localized GTPase ARFA1b/1c is important for callose deposition and ROR2 syntaxin-dependent preinvasive basal defense in barley. Plant Cell **22:** 3831-3844

Boller T, Felix G (2009) A renaissance of elicitors: perception of microbe-associated molecular patterns and danger signals by pattern-recognition receptors. Annu Rev Plant Biol **60:** 379-406

Briggs AG, Bent AF (2011) Poly(ADP-ribosyl)ation in plants. Trends Plant Sci **16:** 372-380

Chen XY, Liu L, Lee E, Han X, Rim Y, Chu H, Kim SW, Sack F, Kim JY (2009) The Arabidopsis callose synthase gene GSL8 is required for cytokinesis and cell patterning. Plant Physiol **150:** 105-113

Chen Y-M, Shall S, O'Farrell M (1994) Poly(ADP-Ribose) Polymerase in Plant Nuclei. Eur J Biochem **224:** 135-142

Clay NK, Adio AM, Denoux C, Jander G, Ausubel FM (2009) Glucosinolate metabolites required for an Arabidopsis innate immune response. Science **323:** 95-101

Clough SJ, Bent AF (1998) Floral dip: a simplified method for Agrobacterium-mediated transformation of Arabidopsis thaliana. Plant J **16:** 735-743

Collins NC, Thordal-Christensen H, Lipka V, Bau S, Kombrink E, Qiu JL, Huckelhoven R, Stein M, Freialdenhoven A, Somerville SC, Schulze-Lefert P (2003) SNARE-protein-mediated disease resistance at the plant cell wall. Nature **425:** 973-977

Czapski GA, Cakala M, Kopczuk D, Strosznajder JB (2004) Effect of poly(ADP-ribose) polymerase inhibitors on oxidative stress evoked hydroxyl radical level and macromolecules oxidation in cell free system of rat brain cortex. Neurosci Lett **356:** 45-48

Czechowski T, Stitt M, Altmann T, Udvardi MK, Scheible WR (2005) Genome-wide identification and testing of superior reference genes for transcript normalization in Arabidopsis. Plant Physiol **139:** 5-17

Dodds PN, Rathjen JP (2010) Plant immunity: towards an integrated view of plant-pathogen interactions. Nat Rev Genet **11:** 539-548

Dong X, Hong Z, Sivaramakrishnan M, Mahfouz M, Verma DP (2005) Callose synthase (CalS5) is required for exine formation during microgametogenesis and for pollen viability in Arabidopsis. Plant J **42:** 315-328

Ellinger D, Glockner A, Koch J, Naumann M, Sturtz V, Schutt K, Manisseri C, Somerville SC, Voigt CA (2014) Interaction of the Arabidopsis GTPase RabA4c with its effector PMR4 results in complete penetration resistance to powdery mildew. Plant Cell **26:** 3185-3200

Ellinger D, Naumann M, Falter C, Zwikowics C, Jamrow T, Manisseri C, Somerville SC, Voigt CA (2013) Elevated early callose deposition results in complete penetration resistance to powdery mildew in Arabidopsis. Plant Physiol **161:** 1433-1444

Ellisen LW (2011) PARP inhibitors in cancer therapy: promise, progress, and puzzles. Cancer Cell **19:** 165-167

Enns LC, Kanaoka MM, Torii KU, Comai L, Okada K, Cleland RE (2005) Two callose synthases, GSL1 and GSL5, play an essential and redundant role in plant and pollen development and in fertility. Plant Mol Biol **58:** 333-349

Eriksson C, Busk L, Brittebo EB (1996) 3-Aminobenzamide: effects on cytochrome P450-dependent metabolism of chemicals and on the toxicity of dichlobenil in the olfactory mucosa. Toxicol Appl Pharmacol **136:** 324-331

Feng B, Liu C, de Oliveira MV, Intorne AC, Li B, Babilonia K, de Souza Filho GA, Shan L, He P (2015) Protein poly(ADP-ribosyl)ation regulates arabidopsis immune gene expression and defense responses. PLoS Genet **11:** e1004936

Gibson BA, Kraus WL (2012) New insights into the molecular and cellular functions of poly(ADP-ribose) and PARPs. Nat Rev Mol Cell Biol **13:** 411-424

Hong Z, Delauney AJ, Verma DP (2001) A cell plate-specific callose synthase and its interaction with phragmoplastin. Plant Cell **13:** 755-768

Hruz T, Laule O, Szabo G, Wessendorp F, Bleuler S, Oertle L, Widmayer P, Gruissem W, Zimmermann P (2008) Genevestigator v3: a reference expression database for the meta-analysis of transcriptomes. Adv Bioinformatics **2008:** 420747

Ishikawa K, Ogawa T, Hirosue E, Nakayama Y, Harada K, Fukusaki E, Yoshimura K, Shigeoka S (2009) Modulation of the Poly(ADP-ribosyl)ation Reaction via the Arabidopsis ADP-Ribose/NADH Pyrophosphohydrolase, AtNUDX7, Is Involved in the Response to Oxidative Stress. Plant Physiol **151:** 741-754

Jacobs AK, Lipka V, Burton RA, Panstruga R, Strizhov N, Schulze-Lefert P, Fincher GB (2003) An Arabidopsis Callose Synthase, GSL5, Is Required for Wound and Papillary Callose Formation. Plant Cell **15:** 2503-2513

Jaffe MJ, Leopold AC (1984) Callose deposition during gravitropism ofZea mays andPisum sativum and its inhibition by 2-deoxy-D-glucose. Planta **161:** 20-26

Jaspers P, Overmyer K, Wrzaczek M, Vainonen JP, Blomster T, Salojarvi J, Reddy RA, Kangasjarvi J (2010) The RST and PARP-like domain containing SRO protein family: analysis of protein structure, function and conservation in land plants. BMC Genomics **11:** 170

Jones JD, Dangl JL (2006) The plant immune system. Nature **444:** 323-329

Kalisch T, Ame JC, Dantzer F, Schreiber V (2012) New readers and interpretations of poly(ADP-ribosyl)ation. Trends Biochem Sci **37:** 381-390

Lakatos P, Szabo E, Hegedus C, Hasko G, Gergely P, Bai P, Virag L (2013) 3-Aminobenzamide protects primary human keratinocytes from UV-induced cell death by a poly(ADP-ribosyl)ation independent mechanism. Biochim Biophys Acta **1833:** 743-751

Lamb RS, Citarelli M, Teotia S (2012) Functions of the poly(ADP-ribose) polymerase superfamily in plants. Cell Mol Life Sci **69:** 175-189

Lee JY, Lu H (2011) Plasmodesmata: the battleground against intruders. Trends Plant Sci **16:** 201-210

Li B, Meng X, Shan L, He P (2016) Transcriptional Regulation of Pattern-Triggered Immunity in Plants. Cell Host Microbe **19:** 641-650

Li W, Zhao Y, Liu C, Yao G, Wu S, Hou C, Zhang M, Wang D (2012) Callose deposition at plasmodesmata is a critical factor in restricting the cell-to-cell movement of Soybean mosaic virus. Plant Cell Rep **31:** 905-916

Liu S, Liu S, Wang M, Wei T, Meng C, Wang M, Xia G (2014) A wheat SIMILAR TO RCD-ONE gene enhances seedling growth and abiotic stress resistance by modulating redox homeostasis and maintaining genomic integrity. Plant Cell **26:** 164-180

Lucht JM, Mauch-Mani B, Steiner HY, Metraux JP, Ryals J, Hohn B (2002) Pathogen stress increases somatic recombination frequency in Arabidopsis. Nat Genet **30:** 311-314

Luna E, Pastor V, Robert J, Flors V, Mauch-Mani B, Ton J (2011) Callose deposition: a multifaceted plant defense response. Mol Plant Microbe Interact **24:** 183-193

Macho AP, Zipfel C (2014) Plant PRRs and the activation of innate immune signaling. Mol Cell **54:** 263-272

Nielsen ME, Feechan A, Bohlenius H, Ueda T, Thordal-Christensen H (2012) Arabidopsis ARF-GTP exchange factor, GNOM, mediates transport required for innate immunity and focal accumulation of syntaxin PEN1. Proc Natl Acad Sci U S A **109:** 11443-11448

Nishimura MT, Stein M, Hou BH, Vogel JP, Edwards H, Somerville SC (2003) Loss of a callose synthase results in salicylic acid-dependent disease resistance. Science **301:** 969-972

Overmyer K, Tuominen H, Kettunen R, Betz C, Langebartels C, Sandermann H, Jr., Kangasjarvi J (2000) Ozone-sensitive arabidopsis rcd1 mutant reveals opposite roles for ethylene and jasmonate signaling pathways in regulating superoxide-dependent cell death. Plant Cell **12:** 1849-1862

Panda S, Poirier GG, Kay SA (2002) tej Defines a Role for Poly(ADP-Ribosyl)ation in Establishing Period Length of the Arabidopsis Circadian Oscillator. Dev Cell **3:** 51-61

Purnell MR, Whish WJ (1980) Novel inhibitors of poly(ADP-ribose) synthetase. Biochem J **185:** 775-777

Ricciarelli R, Palomba L, Cantoni O, Azzi A (1998) 3-Aminobenzamide inhibition of protein kinase C at a cellular level. FEBS Lett **431:** 465-467

Richmond TA, Somerville CR (2000) The cellulose synthase superfamily. Plant Physiol **124:** 495-498

Rissel D, Losch J, Peiter E (2014) The nuclear protein Poly(ADP-ribose) polymerase 3 (AtPARP3) is required for seed storability in Arabidopsis thaliana. Plant Biol (Stuttg) **16:** 1058-1064

Rouleau M, Patel A, Hendzel MJ, Kaufmann SH, Poirier GG (2010) PARP inhibition: PARP1 and beyond. Nat Rev Cancer **10:** 293-301

Schreiber V, Dantzer F, Ame JC, de Murcia G (2006) Poly(ADP-ribose): novel functions for an old molecule. Nat Rev Mol Cell Biol **7:** 517-528

Schulz P, Neukermans J, Van der Kelen K, Muhlenbock P, Van Breusegem F, Noctor G, Teige M, Metzlaff M, Hannah MA (2012) Chemical PARP inhibition enhances growth of Arabidopsis and reduces anthocyanin accumulation and the activation of stress protective mechanisms. PLoS One **7:** e37287

Song J, Bent AF (2014) Microbial pathogens trigger host DNA double-strand breaks whose abundance is reduced by plant defense responses. PLoS Pathog **10:** e1004030

Song J, Keppler BD, Wise RR, Bent AF (2015) PARP2 Is the Predominant Poly(ADP-Ribose) Polymerase in Arabidopsis DNA Damage and Immune Responses. PLoS Genet **11:** e1005200

Stein M, Dittgen J, Sanchez-Rodriguez C, Hou BH, Molina A, Schulze-Lefert P, Lipka V, Somerville S (2006) Arabidopsis PEN3/PDR8, an ATP binding cassette transporter, contributes to nonhost resistance to inappropriate pathogens that enter by direct penetration. Plant Cell **18:** 731-746

Thiele K, Wanner G, Kindzierski V, Jurgens G, Mayer U, Pachl F, Assaad FF (2009) The timely deposition of callose is essential for cytokinesis in Arabidopsis. Plant J **58:** 13-26

Tian R-H, Zhang G-Y, Yan C-H, Dai Y-R (2000) Involvement of poly(ADP-ribose) polymerase and activation of caspase-3-like protease in heat shock-induced apoptosis in tobacco suspension cells. FEBS Lett **474:** 11-15

Vaten A, Dettmer J, Wu S, Stierhof YD, Miyashima S, Yadav SR, Roberts CJ, Campilho A, Bulone V, Lichtenberger R, Lehesranta S, Mahonen AP, Kim JY, Jokitalo E, Sauer N, Scheres B, Nakajima K, Carlsbecker A, Gallagher KL, Helariutta Y (2011) Callose biosynthesis regulates symplastic trafficking during root development. Dev Cell **21:** 1144-1155

Virag L, Szabo C (2002) The therapeutic potential of poly(ADP-ribose) polymerase inhibitors. Pharmacol Rev **54:** 375-429

Vogel J, Somerville S (2000) Isolation and characterization of powdery mildew-resistant Arabidopsis mutants. Proc Natl Acad Sci U S A **97:** 1897-1902

Yan S, Wang W, Marques J, Mohan R, Saleh A, Durrant WE, Song J, Dong X (2013) Salicylic acid activates DNA damage responses to potentiate plant immunity. Mol Cell **52:** 602-610

Yao Y, Kathiria P, Kovalchuk I (2013) A systemic increase in the recombination frequency upon local infection of Arabidopsis thaliana plants with oilseed rape mosaic virus depends on plant age, the initial inoculum concentration and the time for virus replication. Front Plant Sci **4:** 61

Chapter 4: Identification of QTL underlying the MAMP-induced callose response in Arabidopsis

4.1 Abstract

Callose deposition is a ubiquitous plant immune response, yet much remains unknown about the pathways from pathogen perception to callose production. We identified naturally occurring genetic variation for microbe-associated molecular pattern (MAMP)-induced callose deposition in Arabidopsis. Quantitative trait loci (QTL) analysis of the MAMP-induced callose response, using the existing Bayreuth (Bay-0) x Shahdara (Sha) recombinant inbred line population, was performed in order to identify genes involved directly in callose deposition or the upstream PTI response. We detected three QTL for variation in the flg22-induced callose response compared to two QTL for elf18. One QTL was identified in both flg22 and elf18 treatments and was confirmed by heterogeneous inbred family analysis. Recombinants were generated and used for fine mapping. By comparing known genes involved in PTI or callose deposition to those in the genomic region, several candidate genes are proposed.

4.2 Introduction

Callose is a β-1,3-glucan deposited between the plasma membrane and the pre-existing cell wall at sites of pathogen attack for the purposes of cell wall reinforcement (Aist, 1976; Stone and Clarke, 1992). Cell wall reinforcement with callose is one downstream response when pathogens, or more specifically microbe-associated molecular patterns (MAMPs), are perceived by plant pattern recognition receptors (PRRs). Callose deposition combined with other immune responses including the production of a reactive oxygen species (ROS) burst, activation of MAP kinase signaling cascades, ion fluxes, and induction of defense gene expression make up pattern-triggered immunity (PTI) (Dodds and Rathjen, 2010). Callose deposition is ubiquitous in plant innate immunity yet remains poorly understood (Ellinger and Voigt, 2014).

The best-characterized PRRs are the receptor-like kinases (RLKs) FLS2 and EFR that recognize bacterial flagellin (flg22) and elongation factor Tu (elf18), respectively (Gomez-Gomez and Boller, 2000; Zipfel et al., 2006). The components of early PTI signaling are increasingly well understood (Macho and Zipfel, 2014; Li et al., 2016). Following ligand binding, FLS2 forms a complex with BAK1 leading to the rapid phosphorylation of both proteins (Chinchilla et al., 2007; Heese et al., 2007; Schulze et al., 2010). The receptor-like cytoplasmic kinase BIK1, which interacts with FLS2 and other PRRs, is phosphorylated following MAMP perception and dissociates from the complex (Lu et al., 2010; Zhang et al., 2010). BIK1 is considered a central regulator of immunity as it appears to integrate the signals from multiple PRRs. BIK1 was demonstrated to interact with and phosphorylate RBOHD (Kadota et al., 2014; Li et al., 2014), which is responsible for the MAMP-induced ROS burst (Torres et al., 2002). Additional genes that impact FLS2 and/or EFR signaling have been identified (Macho and Zipfel, 2014; Li et al., 2016).

POWERDY MILDREW RESISTANT 4 (PMR4), also known as GLUCAN SYNTHASE LIKE 5 (GSL5), is the callose synthase involved in MAMP-induced callose deposition (Jacobs et al., 2003; Nishimura et al., 2003; Luna et al., 2011). The pathway from pathogen perception and early PTI signaling to the deposition of callose by PMR4 remains largely unknown. Callose deposition is likely downstream of the ROS burst as *rbohd* mutants exhibited reduced flg22-induced callose (Zhang et al., 2007; Luna et al., 2011). Of course mutants in upstream signaling often exhibit reduced callose and, indeed, MAMP-induced callose deposition is a popular assay to indicate impairment of PTI signaling (Luna et al., 2011). For instance, *bik1* mutants as well as the related *pbs1* exhibit reduced callose deposition (Zhang et al., 2010). In contrast, negative regulators of PTI often have enhanced callose deposition phenotypes, as is the case for mutants of *BIR2,* another RLK that interacts with BAK1 (Halter et al., 2014). Surprisingly, indole glucosinolate metabolites, well characterized for their role in herbivore defense, were demonstrated to be required for MAMP-induced callose deposition and involves the myrosinase PENETRATION2 (PEN2) (Bednarek et al., 2009; Clay et al., 2009).

While various aspects of PTI were elucidated through–mutational studies or through protein-protein interactions, use of natural variation has been less widely reported. Identifying natural variation followed by quantitative trait loci (QTL) analysis is an unbiased approach and has the potential to identify novel aspects of the PTI response, whether in upstream PTI signaling or the specific regulation of callose deposition by PMR4. Such studies can also reveal the natural variation for those PTI functions present within a plant species. In this study, we identify natural variation in the MAMP-induced callose response. Furthermore, we utilize QTL analysis and the existing Bayreuth (Bay-0) x Shahdara (Sha) recombinant inbred (RIL) population to identify the QTL controlling this aspect of plant immunity.

4.3 Results

The flg22-induced callose response varies in Arabidopsis natural accessions

The flg22-induced callose response was quantified in 48 Arabidopsis natural accessions. All accessions produced callose to some extent aside from Cvi-1, which was included as a negative control and lacks a functional FLS2 receptor (Dunning et al., 2007). The area with callose deposits was detected and compared to the total area of the cotyledon to give a percent area with callose. Interestingly, the callose response varies widely across different accessions, from a low of approximately 10% to as high as 60% as measured by the present method (**Figure 1**). Natural variation in MAMP-induced callose or the PTI response in general has not previously received extensive study, aside from variation in FLS2 abundance and flg22 perception (Vetter et al., 2012). As such, we sought to identify the factors that impact the MAMP-induced callose response in Arabidopsis.

The MAMP-induced callose response is stronger in Bay-0 than Sha with flg22 or elf18

From among the accessions tested, we identified Bay-0 and Sha as two accessions that exhibit divergent flg22-induced callose responses, and that also have a well-developed population of recombinant inbred lines (RILs) available (Loudet et al., 2002). To exclude the possibility that the differences observed in Bay-0 and Sha are primarily due to differences in FLS2 abundance or flg22 perception, the elf18-induced callose response was also examined. Indeed, Bay-0 also produces significantly more elf18-induced callose than Sha, perhaps indicating that the genes responsible for the variation are largely downstream of the FLS2 and EFR receptors (**Figure 2**).

QTL analysis identifies four loci impacting the MAMP-induced callose response

In order to identify QTL responsible for variation in the callose responses of Bay-0 and Sha, we examined a total of 198 lines from the Bay-0 x Sha RIL population for levels of flg22- and elf18-induced callose deposition (**Supplemental Figure 1**). QTL analysis was performed in R/qtl (Broman et al., 2003) utilizing the available "Map2" genetic data with 69 microsatellite markers (publiclines.versailles.inra.fr/page/33). Between flg22 and elf18 treatments, a total of four unique QTL impacting the callose response were identified, designated crQTL1 (callose response QTL 1) through crQTL4 (**Figure 3 and Table 1**). For flg22, three loci were identified explaining 25.2% of the callose response variation. Only two loci explained 27.7% of the phenotypic variation for the elf18-induced callose response. Notably, only crQTL3 on chromosome 5 was identified for both the flg22 and elf18 treatments, explaining 15.7% of the phenotypic variation for elf18 treatment compared to 5.4% for flg22. Based on its identification in both flg22 and elf18 treatments, further confirmation and analysis was focused on crQTL3.

crQTL3 confirmed with heterogenous inbred families

We confirmed the impact of crQTL3 on the MAMP-induced callose response by utilizing a heterogenous inbred family (HIF) approach (Tuinstra et al., 1997). HIF analysis takes advantage of the residual heterozygosity in the RILs to obtain near isogenic lines with a genetic background that is a mix of homozygous Bay-0 and homozygous Sha regions, but segregating at the markers of interest. Residual heterozygosity at MSAT5.19, the marker corresponding to crQTL3, was identified in RIL47, RIL103, RIL199, and RIL286. RIL199, with residual heterozygosity at markers MSAT5.19 and K9I9, was ultimately used for developing HIFs.

Screening of RIL199 F8 plants at MSAT5.19 and K9I9 identified plants fixed for Bay-0 and Sha, designated $HIF199_{Bay\text{-}0}$ and $HIF199_{Sha}$.

For further experiments, we exclusively utilized the MAMP elf18 because the variation in callose abundance observed in Bay-0 and Sha is more distinct with elf18 than flg22. Elf18-induced callose abundance was significantly higher in $HIF199_{Bay\text{-}0}$ compared to $HIF199_{Sha}$, confirming the impact of crQTL3 on the MAMP-induced callose response (**Figure 4**). In order to assess if crQTL3 is specific to the callose response or if it impacts the larger PTI response, elf18-induced seedling growth inhibition was also examined in $HIF199_{Bay\text{-}0}$ and $HIF199_{Sha}$. $HIF199_{Bay\text{-}0}$ exhibits a significantly stronger growth inhibition phenotype in response to elf18, suggesting the locus may impact multiple PTI responses.

Recombinants for fine mapping

Additional markers were utilized to further define the genomic region of interest in RIL199. The region covers approximately 2 Mbp from 24.5 to 26.6 Mbp on chromosome 5, corresponding to the markers 61060 and 67590 (**Figure 5**). Markers were named based on the nearest gene (e.g. 61060 is near At5g61060). This region encompasses a maximum of about 740 genes. In order to identify recombinants for fine mapping, we selected progeny from RIL199 F8 individuals that were heterozygous across this genomic region. We screened 384 of these F9 progeny with markers flanking the region (62170 and 67590) and identified 70 recombinants (**Figure 5**).

Elf18-induced callose deposition in selected recombinants

To begin the process of fine mapping the gene underlying crQTL3, six recombinants were selected with recombination events between the markers 64990 and 66390, essentially dividing the region of interest in half (**Figure 6**). The recombinants 7C2,7F8, and 7G8 were genotyped as Sha at 64990 while 6A7,6D2, and 10D1 were Bay-0. All six recombinants were heterozygous at 66390. The elf18-induced callose response was similar in all six recombinants and corresponded to an intermediate segregating phenotype, as opposed to a phenotype similar to $HIF199_{Bay\text{-}0}$ or $HIF199_{Sha}$. This result strongly indicated the gene of interest is between 64990 and 67590, reducing the region of interest to 0.6 Mbp, an area containing approximately 300 genes.

4.4 Discussion

Natural variation is a powerful resource to dissect complex traits, such as the Arabidopsis PTI response and specifically MAMP-induced callose deposition. The availability of numerous well developed RIL populations in Arabidopsis provides an effective means to conduct QTL analyses, which provides starting point for the identification of the underlying genes (Koornneef et al., 2004). Analysis of natural genetic variation in the plant immune response can also suggest the evolutionary mechanisms by which plants adapt to pathogenesis, and the range of immune capacities that have been maintained in viable natural accessions (ecotypes). Furthermore, natural variation often provides novel alleles not previously isolated in mutational studies that can help to further elucidate gene function (Mitchell-Olds and Schmitt, 2006; Weigel, 2012).

QTL analyses in Arabidopsis relating to defense tend to focus on natural genetic variation in resistance to a particular pathogen (Ahmad et al., 2010). These include previous studies on *Botrytis cinerea* (Denby et al., 2004; Rowe and Kliebenstein, 2008), partial resistance to

Pseudomonas syringae (Perchepied et al., 2006), the necrotrophic fungus *Plectosphaerella cucumerina* (Llorente et al., 2005), and the downy mildew pathogen *Hyaloperonospora arabidopsidis* (Nemri et al., 2010). In contrast, in this study we sought to identify variation in a particular immune response, namely MAMP-induced callose deposition (Gómez-Gómez et al., 1999; Dunning et al., 2007).

As the gene underlying crQTL3 is of particular interest, we sought to identify candidate genes within this interval with known or predicted roles in callose deposition or PTI signaling. Furthermore, we utilized flg22 and elf18 transcriptomics data (Briggs, 2010) to identify genes upregulated by MAMP treatment (**Table II**).

One such candidate gene is *CALCIUM-DEPENDENT PROTEIN KINASE 28* (*CPK28*). CPK28 is a known negative regulator of the plant immune response (Monaghan et al., 2014). CPK28 interacts with and phosphorylates BIK1 leading to BIK1 turnover. Natural variation in CPK28 could certainly affect levels of BIK1 and result in downstream alterations in the callose response. No nonsynonymous substitutions were identified in the *CPK28* coding sequence based on the full genome sequences of Bay-0 and Sha, but variation in *CPK28* expression could possibly account for the difference. As CPK28 is a negative regulator, we would predict higher *CPK28* expression in Sha, dampening the immune response through BIK1 turnover and resulting in less callose production.

Natural variation in glucosinolate production and structural diversity has been extensively studied and numerous QTL have been identified impacting glucosinolates (Kliebenstein, 2001; Koornneef et al., 2004). Interestingly, tryptophan-derived indole glucosinolates, but not alphatic glucosinolates, are required for flg22-induced callose deposition (Clay et al., 2009). The cytochrome P450 monooxygenase *CYP81F2* underlies the QTL Indole Glucosinolate Modifier1

(IGM1) and is required for production of 4-hydroxy-indole-3-yl-methyl and 4-methoxy-indole-3-yl-methyl (4-methoxy-I3G) (Pfalz et al., 2009). *CYP81F2* is positioned on chromosome 5 near crQTL3, but it is outside the mapped region. A related cytochrome P450, *CYP81G1*, is within the genomic region of interest and is upregulated in response to both flg22 (11.9 fold) and elf18 (4.5 fold). Moreover, analysis of the genome sequences of Bay-0 and Sha identified approximately 500 bp of the *CYP81G1* coding region where no sequencing reads mapped in the Sha data set, potentially indicating a large deletion in the gene (**Supplemental Figure 2**). It remains to be investigated if a *cyp81g1* mutant impacts callose deposition or if it is involved in the biosynthetic pathway of 4-methoxy-I3G or related secondary metabolites required for MAMP-induced callose deposition.

Although we focused on confirming and identifying the gene underlying crQTL3, the identity of the other three QTL indentified are certainly of interest. crQTL2 was detected only in the flg22 treatment and its position is very close to the flg22 receptor FLS2. Indeed, natural variation in FLS2 protein abundance and flg22 perception has been previously reported and likely accounts for some of the downstream impacts on callose abundance (Vetter et al., 2012). Notably, no QTL corresponding to the location of EFR was detected for the elf18 treated samples. Although FLS2 is a strong candidate, this is unconfirmed and other genes potentially impacting the callose response are in the general vicinity, including *RBOHD*.

In summary, we discovered natural genetic variation in the MAMP-induced callose response and demonstrated differences in the accession Bay-0 and Sha. One identified QTL, crQTL3, was detected with both flg22 and elf18 treatments. We confirmed crQTL3 by HIF analysis and generated recombinants for fine-mapping and to date we have refined the interval to a 0.6 Mbp genomic region with approximately 300 genes. Future work will involve further fine

mapping to narrow the genomic region as well as mutational studies of candidate genes to confirm their impact on callose deposition and the PTI response.

4.5 Materials and Methods

Plant material

All Arabidopsis accessions used in this study were from the Arabidopsis Biological Resource Center (ABRC): Aitba-1 (CS76649), An-1 (CS76091), Bay-0 (CS76094), Bur-0 (CS6643), Cal-0 (CS76460), Can-0 (CS6660), Col-0 (CS6673), Col-4 (CS933), Ct-1 (CS6674), Cvi-1 (CS8580), Da(1)-12 (CS28201), Edi-0 (CS6688), Ei-2 (CS76478), Eri-1 (CS97471), Est-1 (CS22629), Fei-0 (CS76412), Hi-0 (CS6736), Kas-1 (CS3880), Kas-2 (CS76150), Kondara (CS76532), Ler-0 (CS20), Ler-2 (CS8581), Mt-0 (CS1380), Nd-1 (CS22619), NFA-8 (CS76199), No-0 (CS6805), Nok-0 (CS28567), Ob-0 (CS76566), Oy-0 (CS6824), Po-0 (CS6839), Rovero-1 (CS76351), Rsch-4 (CS6850), Sav-0 (CS28725), Sf-2 (CS28731), Sha (CS76227), Sq-8 (CS76230), St-0 (CS76231), Tac-1 (CS97578), Toufl-1 (CS76348), Tsu-1 (CS6874), Uk-1 (CS76620), Uk-3 (CS28789), Van-0 (CS22694), Wa-1 (CS28804), Wil-2 (CS6889), Ws-0 (CS6891), Wu-0 (CS6897), Zu-0 (CS6902).

The complete set of 411 Bay-0 x Sha recombinant inbred lines (Stock # CS57920) were also obtained from ABRC. HIFs to confirm crQTL3 were derived from RIL199 by screening F8 plants at the markers MSAT5.19 and K9I9 to identify lines fixed for Bay-0 or Sha. Additional Cleaved Amplified Polymorphic Sequence (CAPS) markers utilized to select recombinants are described in Supplemental Table II.

Plant growth conditions

Arabidopsis seedlings were grown hydroponically at 22°C under long-day conditions (16 h of light / 8 h of dark). Approximately 15 surface-sterilized seeds per well were added to each well in a 12-well plate with 1mL of 1x Murashige and Skoog (MS) media with 0.5% sucrose, 0.5% MES, and 1x Gamborg's vitamins. After seven days of growth, the media was removed and replaced with fresh.

Callose deposition assays

MAMPs, either flg22 or elf18, were added to hydroponically grown Arabidopsis seedlings after nine days of growth. After 24 hours of treatment, seedlings were transferred to an FAA fixative solution (10% formaldehyde, 5% acetic acid, and 50% ethanol) overnight, cleared in 95% ethanol, and stained with aniline blue (0.01% aniline blue in 67 mM K_2HPO_4 with pH adjusted to 12). The stained seedlings were visualized with an Olympus BX60 Epifluorescence Microscope and images captured with an Olympus DP73 camera. At least 12 cotyledons were imaged per line per treatment and callose deposits were quantified automatically using ImageJ software.

Seedling growth inhibition assays

Surface-sterilized seeds were germinated on 0.5x MS agar plates (1% sucrose, 1x Gamborg's vitamins). After five days of growth, seedlings were transferred to 500µL liquid MS in 24-well plates with 100nM elf18 or no treatment. The fresh weight at least 12 seedlings per treatment were recorded after 14 days.

QTL analysis

QTL analysis was performed with the R/qtl package (Broman et al., 2003) in R (http://www.r-project.org) using the multiple imputation method (step size =1, draws = 256, error probability = 0.001). The automatic stepwiseqtl procedure to generate the mutiple QTL models was used after the calculation of LOD penalties with permutation tests (1,000 permutations). Confidence intervals for QTL positions were obtained as Bayesian credible intervals (bayesesint) with a probability of 0.95.

Genome sequence analysis

Bay-0 and Sha sequence data were produced by the DOE Joint Genome Institute (JGI). Sequencing data were downloaded from the 1001 Genomes Data Center (www.1001genomes.org) and viewed in the Integrative Genomics Viewer (IGV)(Robinson et al., 2011).

4.6 Tables

Table I: QTLs controlling the MAMP-induced callose response in the Bay-0 x Sha RIL population.

Treatment	QTL	Chromosome	Position (cM)	Marker	Confidence Interval	% Variation
Flg22	crQTL1	4	66	MSAT4.37	52-69	7.13
	crQTL2	5	61	MSAT518662	53-67	9.06
	crQTL3	5	85	MSAT5.19	81-91	5.42
	crQTL1:crQTL2					3.63
Elf18	crQTL3	5	85	MSAT5.19	81-87	15.67
	crQTL4	1	60	NGA128	51-73	6.92
	crQTL3:crQTL4					5.15

Table II. Genes within the crQTL3 interval that are up-regulated (FDR < 0.05 and fold-change > 1.3) by flg22 and elf18 treatments relative to untreated.

Locus ID	Description	Flg22 Fold-Change	Elf18 Fold-Change
AT5G65600	Concanavalin A-like lectin protein kinase	79.09	36.75
AT5G66020	Suppressor of Actin 1B (SAC1B)	58.87	8.72
AT5G66640	DA1-related protein 3 (DAR3)	10.78	9.40
AT5G67450	Zinc-finger Protein 1 (ZF1)	5.48	11.53
AT5G67310	Cytochrome P450, CYP81G1	11.86	4.49
AT5G67340	ARM repeat superfamily protein	9.75	5.44
AT5G66620	DA1-related protein 6 (DAR6)	7.72	4.56
AT5G66650	Protein of unknown function (DUF607)	7.98	2.91
AT5G66480	Unknown protein	6.79	3.99
AT5G66220	Chalcone isomerase	8.33	2.45
AT5G66790	Protein kinase superfamily protein	5.93	4.46
AT5G67640	Unknown protein	4.39	4.29
AT5G66070	RING/U-box superfamily protein	4.95	3.45
AT5G66210	Calcium Dependent Protein Kinase 28 (CPK28)	4.09	3.65
AT5G66630	DA1-related protein 5 (DAR5)	4.63	3.08
AT5G67080	MAP Kinase Kinase Kinase 19 (MAPKKK19)	4.68	3.02
AT5G66675	Protein of unknown function (DUF677)	4.25	3.13
AT5G65300	Unknown protein	4.50	2.08
AT5G66900	Disease resistance protein (CC-NBS-LRR class)	3.83	2.68
AT5G67350	Unknown protein	4.12	2.39
AT5G65200	Plant U-BOX 38 (PUB38)	2.97	2.33
AT5G65925	Unknown protein	1.70	3.35
AT5G66670	Protein of unknown function (DUF677)	3.22	1.60
AT5G66310	ATP binding microtubule motor family protein	2.17	2.35
AT5G66600	Protein of unknown function (DUF547)	2.24	2.24
AT5G67245	Unknown protein	2.29	2.18
AT5G65920	ARM repeat superfamily protein	2.35	1.90
AT5G67250	SKP1 interacting partner (SKIP2)	2.33	1.79
AT5G66490	Unknown protein	1.91	2.07
AT5G66850	MAP Kinase Kinase Kinase 5 (MAPKKK5)	2.13	1.68
AT5G65165	Succinate dehydrogenase (SDH2-3)	1.84	1.63
AT5G66658	Unknown protein	1.87	1.59
AT5G67630	P-loop containing nucleoside triphosphate hydrolase	1.64	1.59
AT5G66080	Protein phosphatase 2C family protein	1.43	1.41
AT5G67540	Arabinanase/levansucrase/invertase	1.42	1.33

4.7 Figures

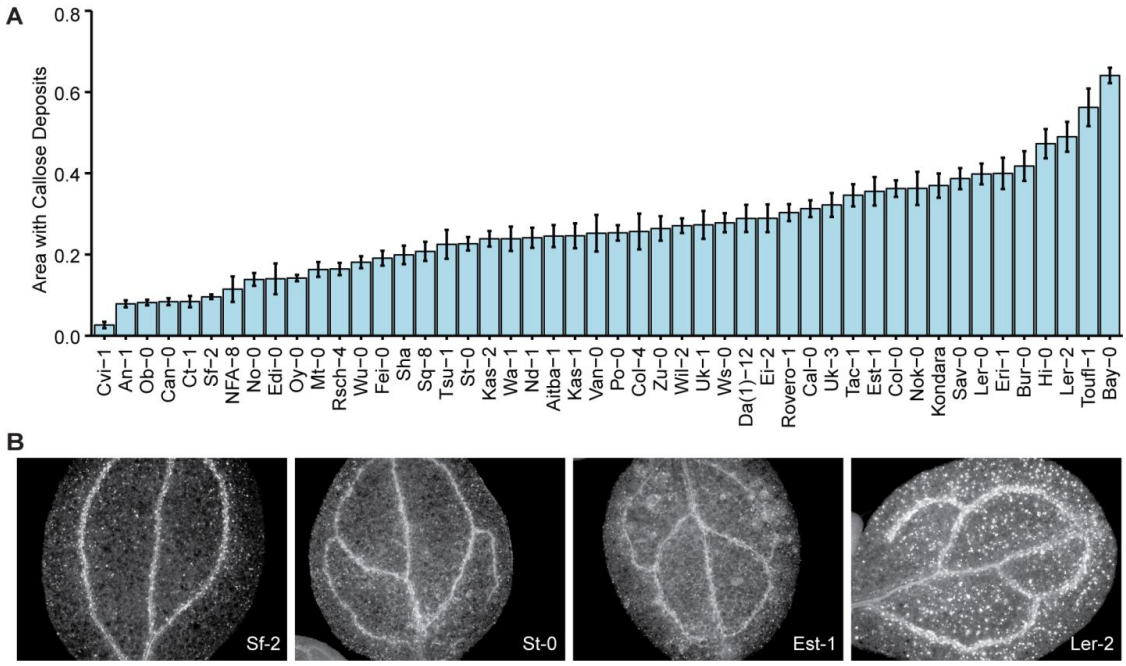

Figure 1. The flg22-induced callose response varies significantly in Arabidopsis accessions. (A) Flg22-induced callose deposition in 48 Arabidopsis accessions. Average of at least two biological replicates for each accession. Bars indicate standard error. (B) Representative images of callose deposition in the indicated accession.

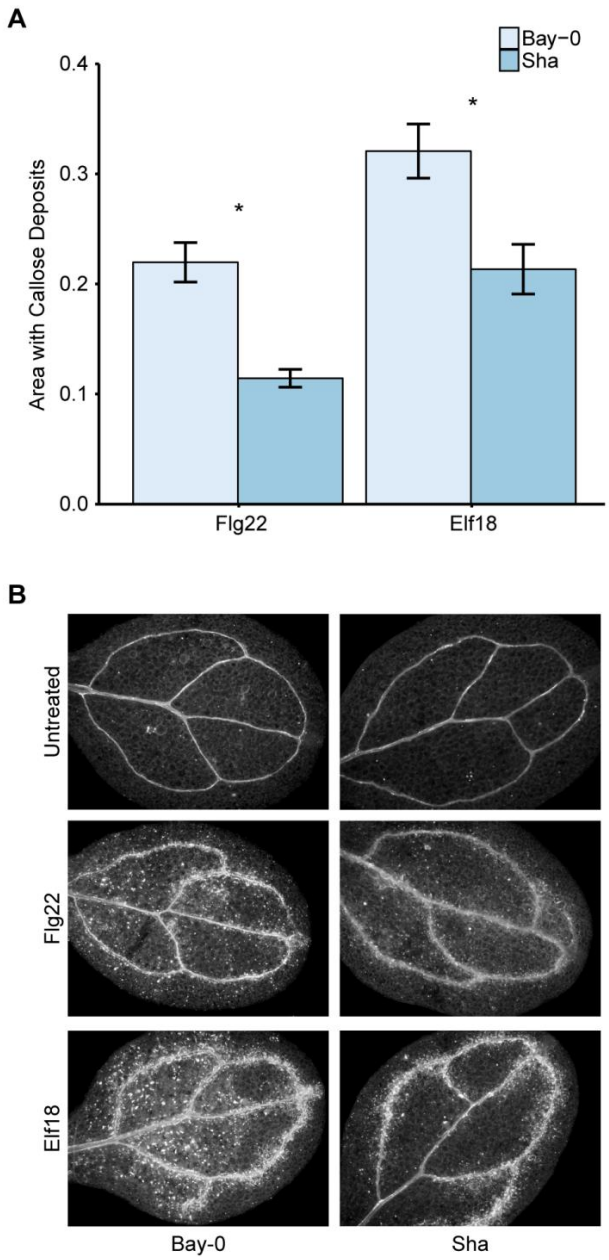

Figure 2. A stronger callose response occurs in Bay-0 than Sha in response to flg22 or elf18. (A) Quantification of flg22- and elf18-induced callose in Bay-0 and Sha cotyledons. Average of twelve cotyledons per line per treatment. Bars indicate standard error. * indicates significant differences (t-test, $p < 0.05$). Experiment repeated three times with similar results. (B) Representative images of untreated or MAMP-treated Bay-0 and Sha cotyledons.

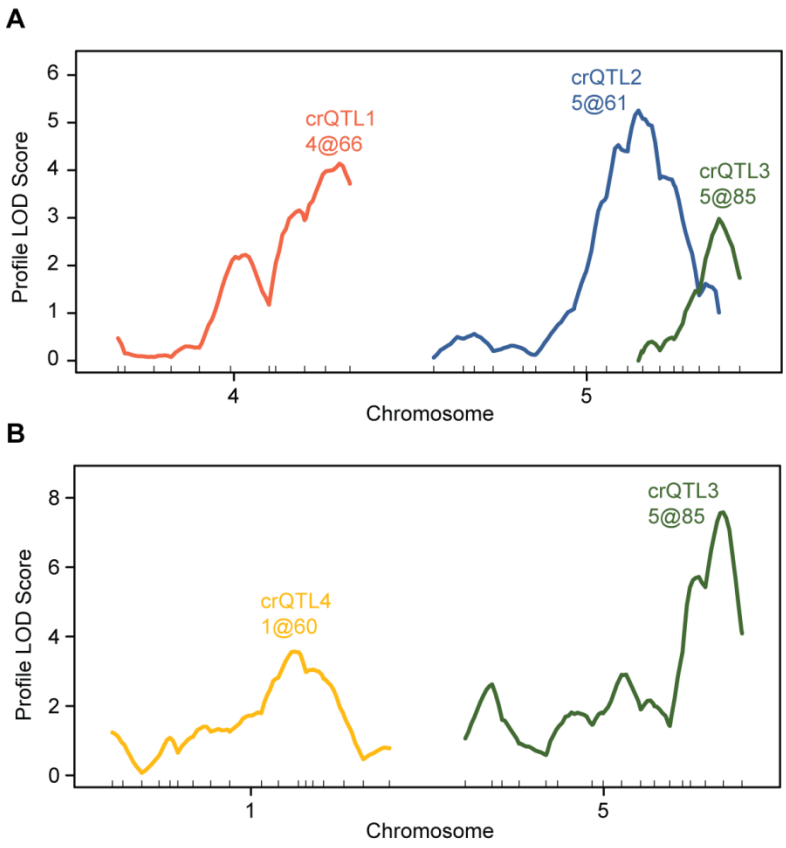

Figure 3. QTL analysis indentified four loci controlling the MAMP-induced callose response in the Bay-0 x Sha RIL population. Profile LOD scores for models generated from stepwise QTL analysis to explain variability of the flg22- (A) or elf18-induced (B) callose response. Only chromosomes with significant QTL are shown.

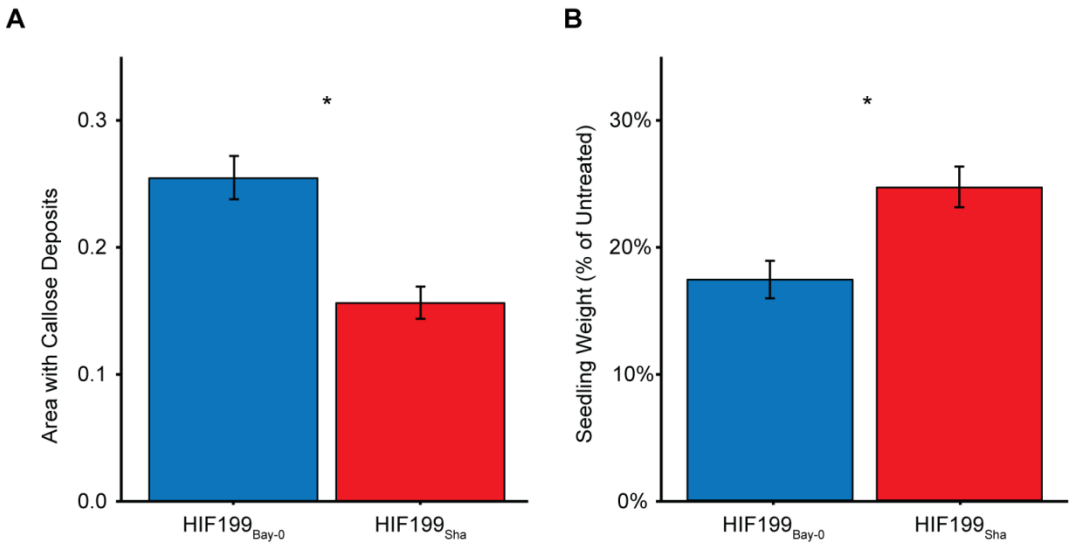

Figure 4. Validation of crQTL3 with heterogeneous inbred families (HIFs). (A) The elf18-induced callose response in HIFs fixed for Bay-0 ($HIF199_{Bay\text{-}0}$) or Sha ($HIF199_{Sha}$). Thirty six cotyledons were imaged and quantified per line. (B) Seedling growth inhibition assay in response to elf18 for $HIF199_{Bay\text{-}0}$ and $HIF199_{Sha}$. * indicates significant differences (t-test, $p < 0.05$). Bars indicate standard error.

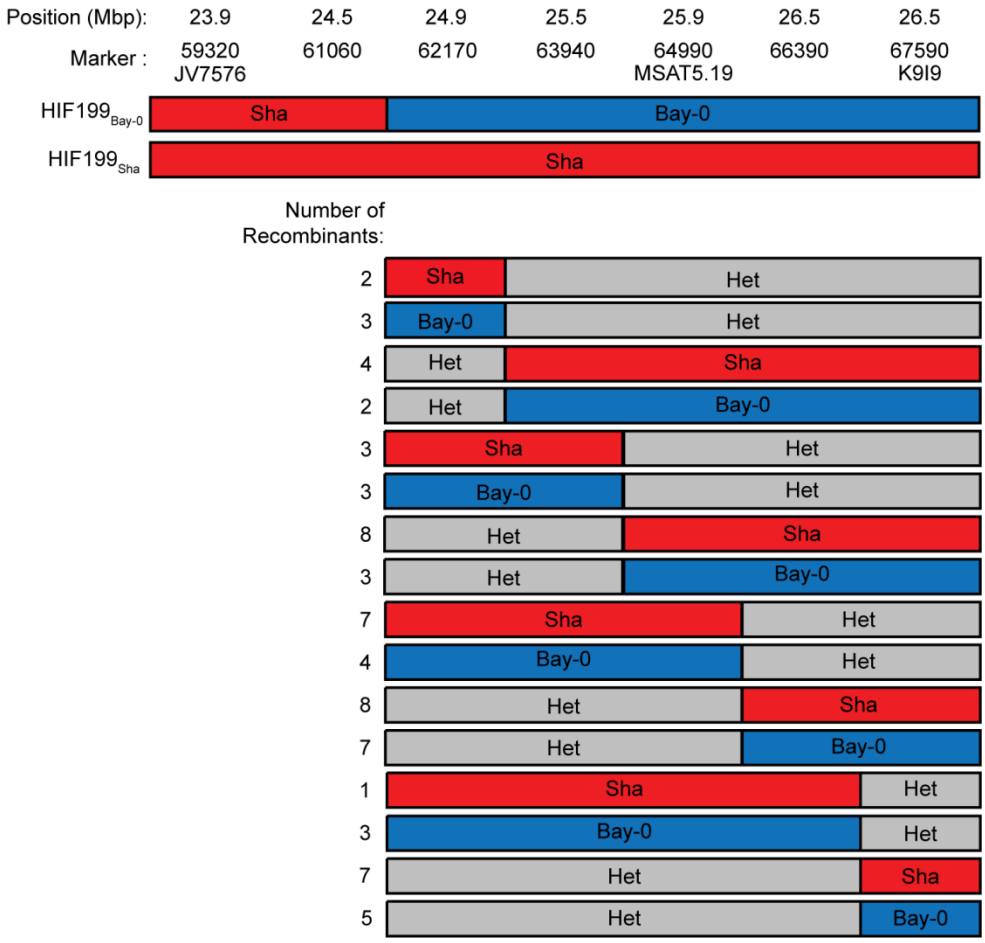

Figure 5. Recombinants for fine mapping crQTL3. RIL199 is heterozygous at markers MSAT5.19 and K9I9 while $HIF199_{Bay\text{-}0}$ and $HIF199_{Sha}$ were fixed for Bay-0 and Sha, respectively. The genomic region of interest was further defined to a 2Mbp region with additional markers (59320, 61010, 52170, 63940, 64990, 66390,and 67590). Markers flanking this region (62170 and 67590) were used to isolate 70 recombinants for fine mapping.

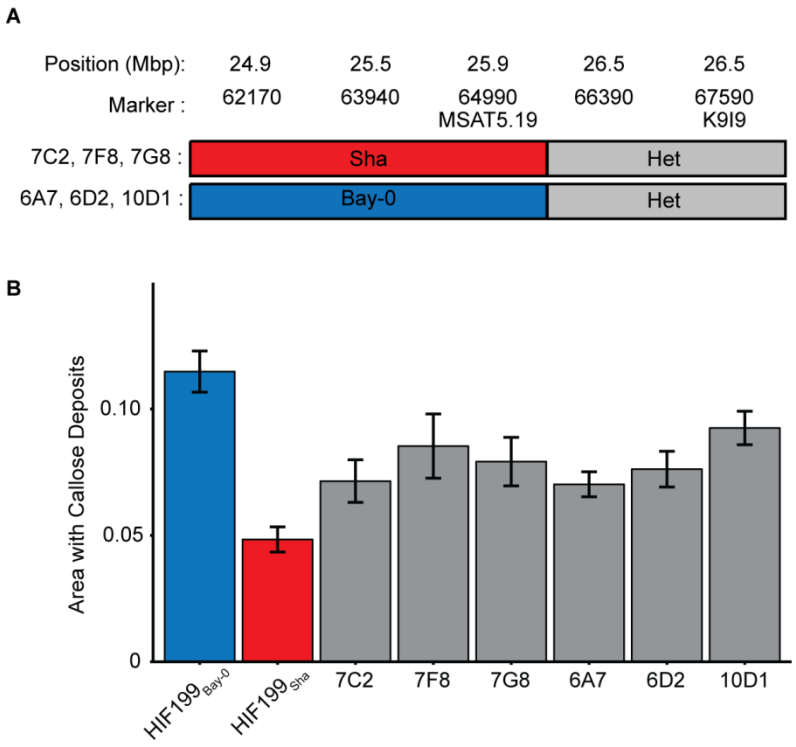

Figure 6. Elf18-induced callose deposition in select recombinants further refine the genomic region of interest to 0.6 Mbp interval. (A) Genotype of six recombinants (7C2,7F8,7G8,6A7,6D2, and 10D1) with a recombination event between markers 64990 and 66390. (B) Quantification of elf18-induced callose in the selected recombinants and the $HIF199_{Bay\text{-}0}$ and $HIF199_{Sha}$ control lines. Thirty six cotyledons were imaged per line.

4.8 Supplemental Tables

Supplemental Table I. Flg22- and elf18-induced callose responses in Bay-0 x Sha RILs. NA indicates not available.

RIL	Flg22	Elf18	RIL	Flg22	Elf18	RIL	Flg22	Elf18	RIL	Flg22	Elf18
2	0.390	0.139	104	0.437	0.557	197	0.090	0.569	314	0.667	0.374
4	0.252	0.174	106	0.610	0.606	198	0.273	0.122	315	0.416	0.443
5	0.472	0.139	111	0.347	0.175	199	0.357	0.628	316	0.502	0.519
6	0.439	0.166	113	0.596	0.363	200	0.285	0.234	318	0.226	0.065
8	0.401	0.187	114	0.297	0.170	201	0.262	0.243	321	0.277	0.146
11	0.296	0.212	115	0.310	0.267	205	0.361	0.369	326	0.468	0.183
13	0.462	0.126	116	0.379	0.241	206	0.224	0.205	328	0.223	0.357
14	0.148	0.227	117	0.308	0.192	211	0.392	0.291	329	0.147	0.211
15	0.178	0.288	119	0.277	0.131	212	0.343	0.258	330	0.237	0.311
16	0.362	0.139	120	0.244	0.226	213	0.211	0.214	331	0.539	0.135
23	0.396	0.183	121	0.333	0.144	214	0.145	0.230	332	0.532	0.235
26	0.332	0.178	122	0.325	0.331	216	0.376	0.442	334	0.566	0.248
28	0.242	0.451	123	0.481	0.262	221	0.518	0.498	335	0.469	0.141
30	0.242	0.411	124	0.574	0.168	222	0.199	0.306	341	0.559	0.434
32	0.198	0.327	125	0.396	0.252	227	0.314	0.460	342	0.404	0.161
34	0.247	0.443	126	0.393	0.146	231	0.503	0.572	343	0.376	0.121
36	0.252	0.352	132	0.177	0.134	232	0.279	0.312	348	0.430	0.154
37	0.224	0.105	133	0.324	0.381	233	0.335	0.171	349	0.375	0.274
38	0.278	0.422	135	0.528	0.243	235	0.451	0.326	350	0.463	0.450
41	0.244	0.567	136	0.390	0.207	236	0.319	0.132	351	0.738	0.372
42	0.068	0.248	139	0.343	0.120	237	0.529	0.116	355	0.478	0.276
44	0.183	0.351	140	0.373	0.183	241	0.275	0.178	356	0.420	0.446
47	0.133	0.256	142	0.336	0.181	243	0.543	0.228	359	0.383	0.297
49	0.238	0.680	143	0.166	0.117	244	0.343	0.157	362	0.439	0.218
51	0.400	0.250	144	0.295	0.157	252	0.470	0.175	363	0.170	0.206
53	0.321	0.088	149	0.362	0.189	253	0.321	NA	364	0.500	0.532
54	0.522	0.236	151	0.334	0.164	254	0.227	0.126	366	0.445	0.354
56	0.165	0.070	154	0.489	0.311	255	0.230	0.173	367	0.540	0.608
58	0.342	0.127	155	0.259	0.378	258	0.255	0.154	368	0.496	0.717
61	0.213	0.171	156	0.146	0.123	260	0.205	0.340	373	0.325	0.384
63	0.529	0.180	159	0.334	0.414	262	0.136	0.165	375	0.550	0.402
65	0.382	0.368	160	0.180	0.137	264	0.212	0.401	376	0.641	0.609
70	0.518	0.244	162	0.242	0.148	267	0.218	0.174	378	0.507	0.536
71	0.305	0.106	165	0.178	0.210	271	0.465	0.533	379	0.388	0.240
73	0.468	0.200	166	0.269	0.254	272	0.263	0.253	380	0.744	0.481
74	0.296	0.603	167	0.263	0.186	273	0.287	0.245	381	0.491	0.549
76	0.247	0.418	170	0.201	0.190	277	0.156	0.386	382	0.286	0.350
80	0.195	0.496	173	0.271	0.248	278	0.258	0.425	383	0.494	0.653
81	0.297	0.324	179	0.142	0.135	279	0.377	0.475	384	0.521	0.634
84	0.286	0.318	180	NA	0.424	280	0.364	0.420	387	0.347	0.292
85	0.171	0.459	186	0.457	0.172	281	0.187	0.222	392	0.352	0.377
86	0.560	0.416	187	0.361	0.249	285	0.197	0.281	395	0.429	0.449
89	NA	0.582	188	0.254	0.087	286	0.172	0.306	408	0.265	0.325
90	NA	0.480	189	0.294	0.248	288	0.272	0.273	410	0.412	0.335
94	0.488	0.352	190	0.230	0.326	292	0.470	0.453	413	0.163	0.345
95	NA	0.489	191	0.278	0.511	293	0.163	0.357	417	0.392	0.489
97	0.278	0.048	192	0.192	0.501	305	0.600	0.579	418	0.322	0.345
99	0.790	0.227	193	0.228	0.325	307	0.354	0.396	430	0.319	0.487
100	NA	0.263	194	0.207	0.475	309	0.268	0.228			
102	0.472	0.414	195	0.205	0.260	311	0.371	0.331			

Supplemental Table II. Cleaved Amplified Polymorphic Sequence (CAPS) markers used in this study.

Marker	Primers		Genomic Sequence		Restriction Enzyme
67590	67590-LP	CACATTCACAAATTTGCCTCA	Bay-0:	TATAAAATTTTGA	ApoI
	67590-RP	CGATTGACCAAAATCAAATCAA	Sha:	TATAAACTTTTGA	
66390	66390-LP	CTTGACGAAACAGTCGTGGA	Bay-0:	TCCATAGGCTTTG	HindIII
	66390-RP	AAAATCCCACACAACAACTGC	Sha:	TCCATAAGCTTTG	
64990	64990-LP	ACTACAGAGCCAACCCAAGG	Bay-0:	CAAAAATTCTATT	ApoI
	64990-RP	GGGAAAACGAGCATCATCAC	Sha:	CAAAAAGTCTATT	
63940	63940-LP	CCAGCTTGGCTTCAAGTACC	Bay-0:	TCTTAACTTTCTT	ApoI
	63940-RP	TGGGATCCAGTAACTGAGCA	Sha:	TCTTAAATTTCTT	
62170	62170-LP	GAGCCAGGACCAGTCTCTTC	Bay-0:	TAAATATGTATAT	SnaBI
	62170-RP	TGCTAACGAGTTCTGTCTGTTGA	Sha:	TAAATACGTATAT	
61060	61060-LP	AGGCATACCAAACGTCAACC	Bay-0:	GGGCGTCGTCTTC	BsaHI
	61060-RP	TTAGGTGCGCAAGAGGCTAT	Sha:	GGGCGTTGTCTTC	
59320	59320-LP	ATCAGCCAAAAACCGTCAAG	Bay-0:	AAATATTATTATC	SspI
	59320-RP	GAAACAGCTTTAAGACATTTTCCA	Sha:	AAATATCATTATC	

4.9 Supplemental Figures

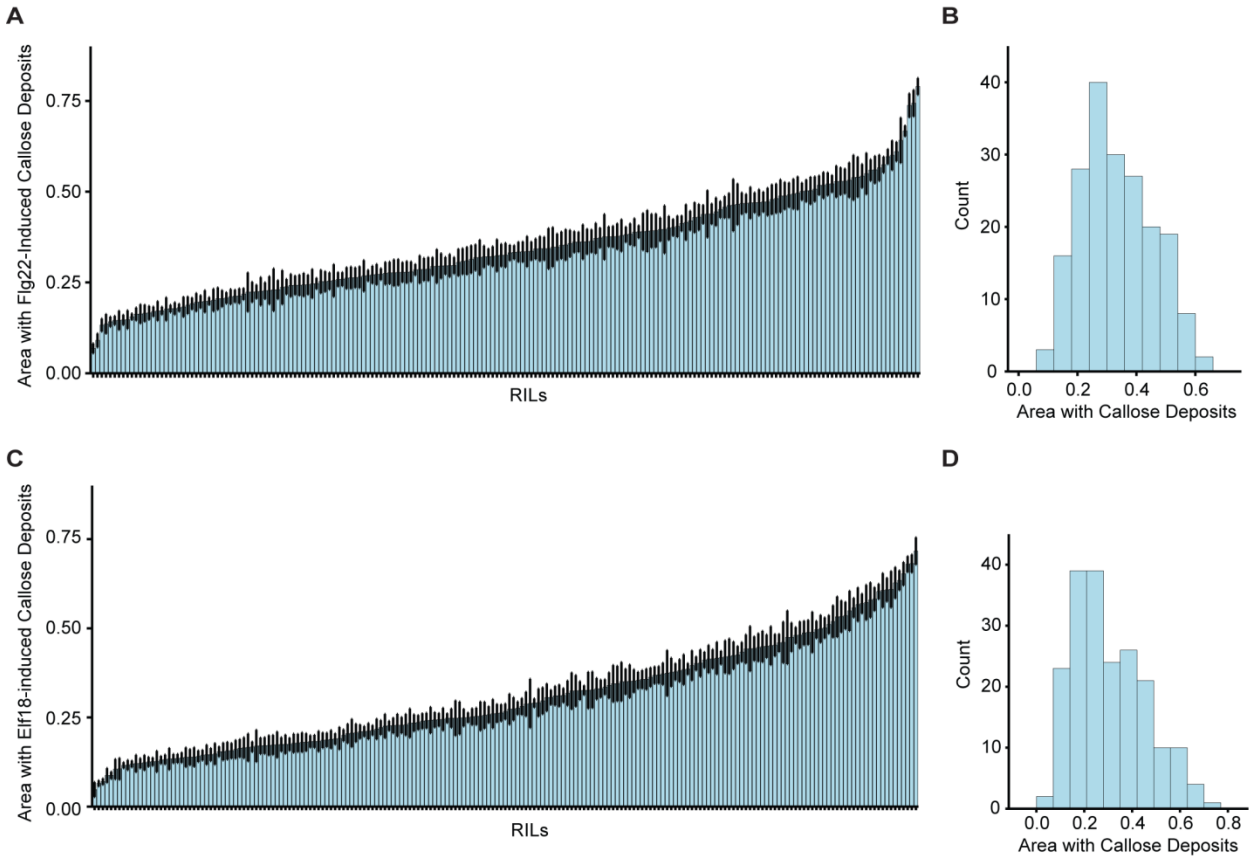

Supplemental Figure 1. MAMP-induced callose deposition in the Bay-0 x Sha RIL population. Callose deposition was quantified in 198 RILs in response to flg22 (A) or elf18 (C). Bars indicate standard error. (B,D) Histograms showing the distribution of the data in A and C.

Supplemental Figure 2. Full genome sequence of Sha indicates a 500 bp deletion in *CYP81G1*. Sequences of the *CYP81G1* gene in Bay-0 (top) and Sha (bottom) as visualized in Integrative Genomics Viewer (IGV). The red rectangle highlights a region corresponding to the 5' region of *CYP81G1* without sequencing reads in Sha.

4.10 References

Ahmad S, Gordon-Weeks R, Pickett J, Ton J (2010) Natural variation in priming of basal resistance: from evolutionary origin to agricultural exploitation. Mol Plant Pathol **11:** 817-827

Aist JR (1976) Papillae and Related Wound Plugs of Plant Cells. Annu Rev Phytopathol **14:** 145-163

Bednarek P, Pislewska-Bednarek M, Svatos A, Schneider B, Doubsky J, Mansurova M, Humphry M, Consonni C, Panstruga R, Sanchez-Vallet A, Molina A, Schulze-Lefert P (2009) A glucosinolate metabolism pathway in living plant cells mediates broad-spectrum antifungal defense. Science **323:** 101-106

Briggs AG (2010) Poly(ADP-ribosyl)ation and the plant innate immune response. PhD Thesis. University of Wisconsin-Madison

Broman KW, Wu H, Sen S, Churchill GA (2003) R/qtl: QTL mapping in experimental crosses. Bioinformatics **19:** 889-890

Chinchilla D, Zipfel C, Robatzek S, Kemmerling B, Nurnberger T, Jones JD, Felix G, Boller T (2007) A flagellin-induced complex of the receptor FLS2 and BAK1 initiates plant defence. Nature **448:** 497-500

Clay NK, Adio AM, Denoux C, Jander G, Ausubel FM (2009) Glucosinolate metabolites required for an Arabidopsis innate immune response. Science **323:** 95-101

Denby KJ, Kumar P, Kliebenstein DJ (2004) Identification of Botrytis cinerea susceptibility loci in Arabidopsis thaliana. Plant J **38:** 473-486

Dodds PN, Rathjen JP (2010) Plant immunity: towards an integrated view of plant-pathogen interactions. Nat Rev Genet **11:** 539-548

Dunning FM, Sun W, Jansen KL, Helft L, Bent AF (2007) Identification and mutational analysis of Arabidopsis FLS2 leucine-rich repeat domain residues that contribute to flagellin perception. Plant Cell **19:** 3297-3313

Ellinger D, Voigt CA (2014) Callose biosynthesis in Arabidopsis with a focus on pathogen response: what we have learned within the last decade. Ann Bot **114:** 1349-1358

Gomez-Gomez L, Boller T (2000) FLS2: an LRR receptor-like kinase involved in the perception of the bacterial elicitor flagellin in Arabidopsis. Mol Cell **5:** 1003-1011

Gómez-Gómez L, Felix G, Boller T (1999) A single locus determines sensitivity to bacterial flagellin in Arabidopsis thaliana. Plant J **18:** 277-284

Halter T, Imkampe J, Mazzotta S, Wierzba M, Postel S, Bucherl C, Kiefer C, Stahl M, Chinchilla D, Wang X, Nurnberger T, Zipfel C, Clouse S, Borst JW, Boeren S, de

Vries SC, Tax F, Kemmerling B (2014) The leucine-rich repeat receptor kinase BIR2 is a negative regulator of BAK1 in plant immunity. Curr Biol **24:** 134-143

Heese A, Hann DR, Gimenez-Ibanez S, Jones AM, He K, Li J, Schroeder JI, Peck SC, Rathjen JP (2007) The receptor-like kinase SERK3/BAK1 is a central regulator of innate immunity in plants. Proc Natl Acad Sci U S A **104:** 12217-12222

Jacobs AK, Lipka V, Burton RA, Panstruga R, Strizhov N, Schulze-Lefert P, Fincher GB (2003) An Arabidopsis Callose Synthase, GSL5, Is Required for Wound and Papillary Callose Formation. Plant Cell **15:** 2503-2513

Kadota Y, Sklenar J, Derbyshire P, Stransfeld L, Asai S, Ntoukakis V, Jones JD, Shirasu K, Menke F, Jones A, Zipfel C (2014) Direct regulation of the NADPH oxidase RBOHD by the PRR-associated kinase BIK1 during plant immunity. Mol Cell **54:** 43-55

Kliebenstein DJ (2001) Genetic Control of Natural Variation in Arabidopsis Glucosinolate Accumulation. Plant Physiol **126:** 811-825

Koornneef M, Alonso-Blanco C, Vreugdenhil D (2004) Naturally occurring genetic variation in Arabidopsis thaliana. Annu Rev Plant Biol **55:** 141-172

Li B, Meng X, Shan L, He P (2016) Transcriptional Regulation of Pattern-Triggered Immunity in Plants. Cell Host Microbe **19:** 641-650

Li L, Li M, Yu L, Zhou Z, Liang X, Liu Z, Cai G, Gao L, Zhang X, Wang Y, Chen S, Zhou JM (2014) The FLS2-associated kinase BIK1 directly phosphorylates the NADPH oxidase RbohD to control plant immunity. Cell Host Microbe **15:** 329-338

Llorente F, Alonso-Blanco C, Sanchez-Rodriguez C, Jorda L, Molina A (2005) ERECTA receptor-like kinase and heterotrimeric G protein from Arabidopsis are required for resistance to the necrotrophic fungus Plectosphaerella cucumerina. Plant J **43:** 165-180

Loudet O, Chaillou S, Camilleri C, Bouchez D, Daniel-Vedele F (2002) Bay-0 x Shahdara recombinant inbred line population: a powerful tool for the genetic dissection of complex traits in Arabidopsis. Theor Appl Genet **104:** 1173-1184

Lu D, Wu S, Gao X, Zhang Y, Shan L, He P (2010) A receptor-like cytoplasmic kinase, BIK1, associates with a flagellin receptor complex to initiate plant innate immunity. Proc Natl Acad Sci U S A **107:** 496-501

Luna E, Pastor V, Robert J, Flors V, Mauch-Mani B, Ton J (2011) Callose deposition: a multifaceted plant defense response. Mol Plant Microbe Interact **24:** 183-193

Macho AP, Zipfel C (2014) Plant PRRs and the activation of innate immune signaling. Mol Cell **54:** 263-272

Mitchell-Olds T, Schmitt J (2006) Genetic mechanisms and evolutionary significance of natural variation in Arabidopsis. Nature **441:** 947-952

Monaghan J, Matschi S, Shorinola O, Rovenich H, Matei A, Segonzac C, Malinovsky FG, Rathjen JP, MacLean D, Romeis T, Zipfel C (2014) The calcium-dependent protein kinase CPK28 buffers plant immunity and regulates BIK1 turnover. Cell Host Microbe **16:** 605-615

Nemri A, Atwell S, Tarone AM, Huang YS, Zhao K, Studholme DJ, Nordborg M, Jones JD (2010) Genome-wide survey of Arabidopsis natural variation in downy mildew resistance using combined association and linkage mapping. Proc Natl Acad Sci U S A **107:** 10302-10307

Nishimura MT, Stein M, Hou BH, Vogel JP, Edwards H, Somerville SC (2003) Loss of a callose synthase results in salicylic acid-dependent disease resistance. Science **301:** 969-972

Perchepied L, Kroj T, Tronchet M, Loudet O, Roby D (2006) Natural variation in partial resistance to Pseudomonas syringae is controlled by two major QTLs in Arabidopsis thaliana. PLoS One **1:** e123

Pfalz M, Vogel H, Kroymann J (2009) The gene controlling the indole glucosinolate modifier1 quantitative trait locus alters indole glucosinolate structures and aphid resistance in Arabidopsis. Plant Cell **21:** 985-999

Robinson JT, Thorvaldsdottir H, Winckler W, Guttman M, Lander ES, Getz G, Mesirov JP (2011) Integrative genomics viewer. Nat Biotechnol **29:** 24-26

Rowe HC, Kliebenstein DJ (2008) Complex genetics control natural variation in Arabidopsis thaliana resistance to Botrytis cinerea. Genetics **180:** 2237-2250

Schulze B, Mentzel T, Jehle AK, Mueller K, Beeler S, Boller T, Felix G, Chinchilla D (2010) Rapid heteromerization and phosphorylation of ligand-activated plant transmembrane receptors and their associated kinase BAK1. J Biol Chem **285:** 9444-9451

Stone B, Clarke A (1992) Chemistry and biology of (1, 3)-D-glucans. Victoria, Australia.: La Trobe University Press

Torres MA, Dangl JL, Jones JD (2002) Arabidopsis gp91phox homologues AtrbohD and AtrbohF are required for accumulation of reactive oxygen intermediates in the plant defense response. Proc Natl Acad Sci U S A **99:** 517-522

Tuinstra MR, Ejeta G, Goldsbrough PB (1997) Heterogeneous inbred family (HIF) analysis: a method for developing near-isogenic lines that differ at quantitative trait loci. TAG Theoretical and Applied Genetics **95:** 1005-1011

Vetter MM, Kronholm I, He F, Haweker H, Reymond M, Bergelson J, Robatzek S, de Meaux J (2012) Flagellin perception varies quantitatively in Arabidopsis thaliana and its relatives. Mol Biol Evol **29:** 1655-1667

Weigel D (2012) Natural variation in Arabidopsis: from molecular genetics to ecological genomics. Plant Physiol **158:** 2-22

Zhang J, Li W, Xiang T, Liu Z, Laluk K, Ding X, Zou Y, Gao M, Zhang X, Chen S, Mengiste T, Zhang Y, Zhou JM (2010) Receptor-like cytoplasmic kinases integrate signaling from multiple plant immune receptors and are targeted by a Pseudomonas syringae effector. Cell Host Microbe **7:** 290-301

Zhang J, Shao F, Li Y, Cui H, Chen L, Li H, Zou Y, Long C, Lan L, Chai J, Chen S, Tang X, Zhou JM (2007) A Pseudomonas syringae effector inactivates MAPKs to suppress PAMP-induced immunity in plants. Cell Host Microbe **1:** 175-185

Zipfel C, Kunze G, Chinchilla D, Caniard A, Jones JD, Boller T, Felix G (2006) Perception of the bacterial PAMP EF-Tu by the receptor EFR restricts Agrobacterium-mediated transformation. Cell **125:** 749-760

Chapter 5: Future directions

The proceeding chapters mark significant progress in our understanding of pathogenesis-related callose deposition and cell wall reinforcement. In regards to Chapter 3, unknowns certainly remain and fully understanding how 3AB inhibits MAMP-induced callose deposition is intriguing as ever. The observation that PMR4 protein abundance increases in the presence of flg22 and 3AB, despite no callose being produced, is particularly striking and deserving of further investigation. The hypothesis most consistent with our findings is that 3AB prevents the relocalization of PMR4 protein from the plasma membrane to the site of attempted pathogen ingress. This is distinct from inhibition of callose synthase activity by 2-DDG where PMR4 likely relocalizes properly but is unable to produce callose.

The most direct approach to investigate if 3AB prevents PMR4 relocalization would be to utilize a GFP-tagged line. Unfortunately, no fluorescence was observed above background levels in the *PMR4-GFP* line under control of the *PMR4* native promoter that I generated. We could overcome this issue through the use of a GFP-tagged *PMR4* overexpression line but with obvious pitfalls. Nonetheless, the previously published 35S*::PMR4-GFP* overexpression line has been obtained from Christian Voigt (Ellinger et al., 2013). As an initial experiment, we would need to confirm that 3AB still effectively inhibits callose deposition when *PMR4* is overexpressed. Depending on the precise mechanism of inhibition, it is conceivable that a higher concentration of 3AB may be required to block callose in an overexpression line.

An alternative approach is to use other proteins that localize to the papillae as a proxy for PMR4, namely PEN1 and PEN3. While I have shown that 3AB does not alter the abundance of PEN1 or PEN3, perhaps the more informative question is whether 3AB alters their relocalization from the plasma membrane to the papillae. Importantly, pharmacological inhibitors revealed that

the requirements for trafficking of PEN1 and PEN3 to the papillae are different (Underwood and Somerville, 2013). It is not entirely clear whether disruption of actin (as with PEN3) or inhibition of vesicular trafficking (as with PEN1) also impact PMR4 or if the relocalization of PMR4 is distinct from either PEN1 or PEN3. The possibility that 3AB disrupts the actin cytoskeleton is intriguing and could quickly be investigated with live cell imaging of actin in the presence or absence of 3AB (Sheahan et al., 2004).

With all of this, it is important to keep in mind that 3AB does not block wound-induced callose, also a product of the PMR4 callose synthase. The distinct requirements for pathogen-induced callose and callose deposited at wound sites have not been widely investigated. As additional mutants that disrupt pathogen-induced callose are identified, determining if they also impact wound-induced callose will be of interest. Those that alter pathogen-induced callose but not wound-induced will inform the differential regulation of these pathways and could provide insights into how 3AB is functioning as an inhibitor.

The follow-up experiments for Chapter 4 are relatively straightforward. We have additional recombinants for fine mapping in hand. Additional phenotyping of the MAMP-induced callose response in these lines should drastically reduce the size of the interval and the number of candidate genes. Having said that, it is not too soon to acquire T-DNA insertion mutants of select genes. As discussed, *CPK28* and *CYP81G1* are strong candidates and it would be worth examining if disruption of either of these genes impair MAMP-induced callose deposition.

There are of course larger questions beyond the scope of this thesis worth mentioning, both in regards to poly(ADP-ribosyl)tion and callose deposition. Although this project transitioned away from poly(ADP-ribosyl)ation, this post-translational modification has clear

roles in the plant innate immune response. Future work will likely focus on the identification of proteins that are poly(ADP-ribosyl)ated upon pathogen infection or MAMP treatment, perhaps through proteomic approaches. One of the central question of pathogenesis-related callose revolves around its precise role in the papillae. Despite the ubiquitous nature of callose in these cell wall thickenings, its importance in pathogen defense is still widely debated. This debate largely stems from the fact that *pmr4* mutants were more resistant adapted powdery mildew and the finding that *pmr4* mutants still form papillae identical to those in wild type plants (Nishimura et al., 2003). There are also open questions in terms of how salicylic acid (SA) responses are hyperactivated in the *pmr4* mutant, leading to the increased disease resistance. Does this imply a secondary role of PMR4 or callose in negatively regulating the SA pathway? Or does PMR4 have an R gene "guard" that results in the activation of defense responses upon loss of PMR4 (van der Hoorn and Kamoun, 2008)?

Much remains to be investigated about the pathway from pathogen perception to callose deposition, but utilizing a chemical genetic tool (3AB) and natural variation provided two strong approaches to identify novel aspects of this response. Future research in the coming years and decades will further unravel this important component of the plant innate immune response.

References

Ellinger D, Naumann M, Falter C, Zwikowics C, Jamrow T, Manisseri C, Somerville SC, Voigt CA (2013) Elevated early callose deposition results in complete penetration resistance to powdery mildew in Arabidopsis. Plant Physiol **161:** 1433-1444

Nishimura MT, Stein M, Hou BH, Vogel JP, Edwards H, Somerville SC (2003) Loss of a callose synthase results in salicylic acid-dependent disease resistance. Science **301:** 969-972

Sheahan MB, Staiger CJ, Rose RJ, McCurdy DW (2004) A green fluorescent protein fusion to actin-binding domain 2 of Arabidopsis fimbrin highlights new features of a dynamic actin cytoskeleton in live plant cells. Plant Physiol **136:** 3968-3978

Underwood W, Somerville SC (2013) Perception of conserved pathogen elicitors at the plasma membrane leads to relocalization of the Arabidopsis PEN3 transporter. Proc Natl Acad Sci U S A **110:** 12492-12497

van der Hoorn RA, Kamoun S (2008) From Guard to Decoy: a new model for perception of plant pathogen effectors. Plant Cell **20:** 2009-2017

Appendix A: Elf18-induced brown pigment accumulation

A brown pigment that accumulates in seedlings grown in the presence of elf18 was of interest because, like callose, its accumulation was blocked by 3AB (Adams-Phillips et al., 2010). Furthermore, a *parg1* mutant hyper-accumulates the brown pigment beyond what is observed in Col-0 wild type seedlings. Although the downstream pathways activated by flg22 and elf18 are generally considered similar, the fact that the brown pigment accumulates in response to elf18 but not flg22 was of interest.

Previous results from the Bent lab (Adams-Phillips et al., 2010) suggested that the brown pigment might be a product of the phenylpropanoid pathway. Specifically, L-a-aminooxy-b-phenylpropionic acid (AOPP), a chemical inhibitor of phenylalanine ammonia lyase (PAL) activity, reduced accumulation of the pigment, and a mutant of the chalcone synthase gene (*transparent testa 4* [*tt4*]), a key regulator in the phenylpropanoid pathway, completely lacked the pigment.

PAL is the first step of the phenylpropanoid pathway, and the Arabidopsis genome encodes four *PAL* genes (Huang et al., 2010). A previously generated *pal1pal2pal3pal4* quadruple mutant was obtained and examined for the presence of brown pigment. The *pal1pal2pal3pal4* quadruple mutant still produces brown pigment in response to elf18 (**Figure 1A**) However, given that the quadruple mutant still retains about 10% residual PAL activity (Huang et al., 2010), this result does not exclude the possibility that it is a product of the phenylpropanoid pathway. Two stains commonly used for condensed tannins, vanillin and DMACA reagent (p-dimethylaminocinnamaldehyde) were also utilized. Both readily stain the condensed tannins in the Arabidopsis seed coat, but failed to stain the elf18-induced brown pigment in the cotyledons (**Figure 1B**).

While the *tt4* mutant does lack brown pigment accumulation as reported, further experiments revealed that the particular mutant line completely fails to respond to elf18, also lacking elf18-induced callose and seedling growth inhibition (**Figure 2**). Alternative T-DNA insertion lines were obtained to determine if the inability to perceive elf18 was due to the loss of chalcone synthase or a secondary mutation in the line. Each of the T-DNA insertion lines tested responded normally to elf18 and still accumulated the brown pigment. Each of these mutants exhibited the yellow seed phenotype characteristic of transparent testa mutants confirming that they are loss of function mutations. Apparently the initial *tt4* mutant has a second mutation, perhaps in EFR itself, that renders it unable to perceive elf18. While the brown pigment may still be product of the phenylpropanoid pathway, these data cast doubt on this finding.

The identity of the brown pigment, how it is regulated, if it has a role in plant defense, and why it only accumulates in response to elf18 were all points of interest. To address these questions, I considered a forward genetics screen for loss of brown pigment accumulation in EMS mutagenized *parg1* seed. Although a given Col-0 wild type seedling may or may not produce a noticeable quantity of the brown pigment when grown in the presence of 100nM elf18, because the *parg1-2* mutant line hyper-accumulates the brown pigment, these seedlings reliably and consistently produce the brown pigment when grown in 100nM elf18 for 10 days. Therefore, while Col-0 wild type seedlings could not be used for such a screen, the *parg1* mutant is ideally suited. An EMS mutagenized population of *parg1-2* seeds was generated by previous graduate student Amy Briggs. Seeds were germinated on Murashige & Skoog (MS) plates with 1% sucrose and after five days of growth were transferred to 100 μL of liquid MS media supplemented with 100nM elf18 in 96 well plates. After ten more days, seedlings were examined under a dissecting microscope and examined for presence or absence of brown pigment

accumulation. Any seedlings lacking brown pigment were washed thoroughly to remove residual elf18 and transferred to soil. In total 12,912 seedlings were screened, and 94 seedlings were selected and transferred to soil. Unfortunately, many seedlings died soon after transfer, likely due to the stress of being subjected 10 days of elf18 treatment. Many others survived the transfer but failed to produce any seed. Ultimately, none of the remaining mutants identified consistently failed to produce elf18-induced brown pigment accumulation.

I also considered the possibility of identifying the brown pigment by analytical chemistry approaches in a collaboration with John Ralph and research scientist Fachuang Lu. For this experiment, *parg1* seedlings were grown in the presence of elf18 for 10 days alongside untreated controls. Seedlings with an abundance of brown pigment were cleared in ethanol, dried, and grown to a fine powder. The samples were analyzed by Pyrolysis-GC-Total ion Chromatogram (**Figure 3**). Fachuang reported no significant differences between the sample with brown pigment and the untreated control, and this line of research was not pursued further.

While I have shown in Chapter 3 that 3AB inhibiting callose is independent of poly(ADP-ribosyl)ation, it is not clear if this is the case for brown pigment, especially considering the hyperaccumulation of brown pigment in the *parg1* mutant. If studies were to continue on brown pigment accumulation, an important first step would be to examine the *parp1parp2parp3* mutants for a loss of brown pigment accumulation.

In the six years since the Bent lab publication, only one additional report of the brown pigment has been published, showing that it also hyperaccumulates in an *mkp1* (*map kinase phosphatase 1*) mutant in response to elf26 (Anderson et al., 2011). No identification of brown pigment or description of its role in plant immunity has been published to date.

Figures

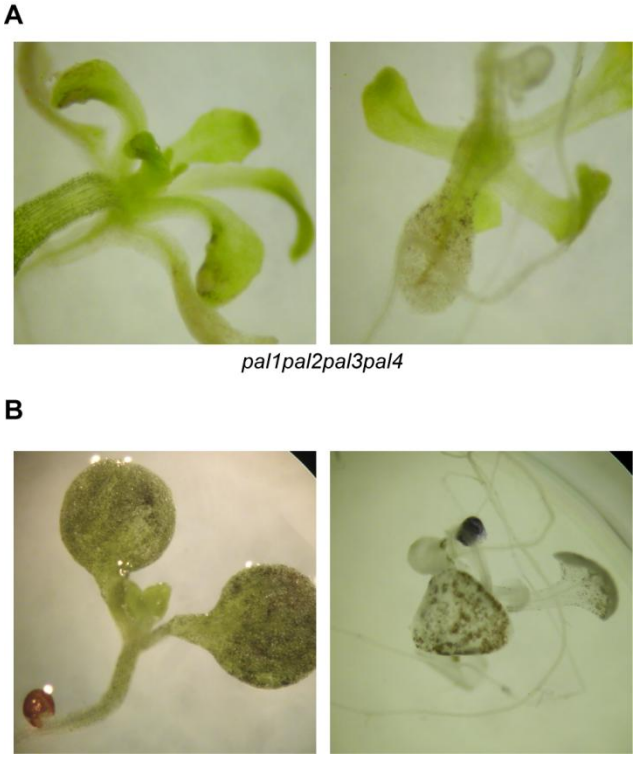

Figure 1. *pal* mutants still produce brown pigment, and it is not stained by vanillin or DMACA reagent. (A) Brown pigment accumulation in *pal1pal2pal3pal4* quadruple mutants grown in the presence of elf18 for 10 days. (B) Staining of elf18-induced brown pigment in *parg1* mutants with vanillin (left) or DMACA reagent (right). Staining of condensed tannins in the seed coat serves as a positive control.

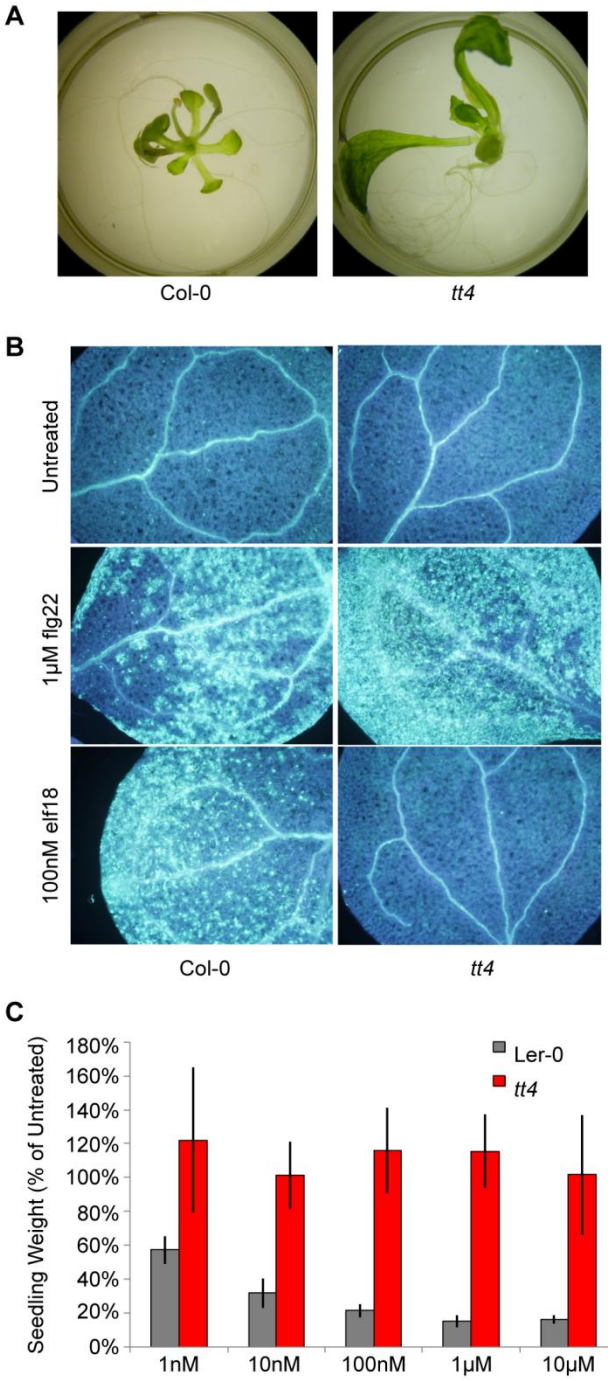

Figure 2. The chalcone synthase mutant *transparent testa 4* (*tt4-1*) is insensitive to elf18. The *tt4* mutant does not produce brown pigment (A), elf18-induced callose (B), or respond to elf18 in a seedling growth inhibition assay (C).

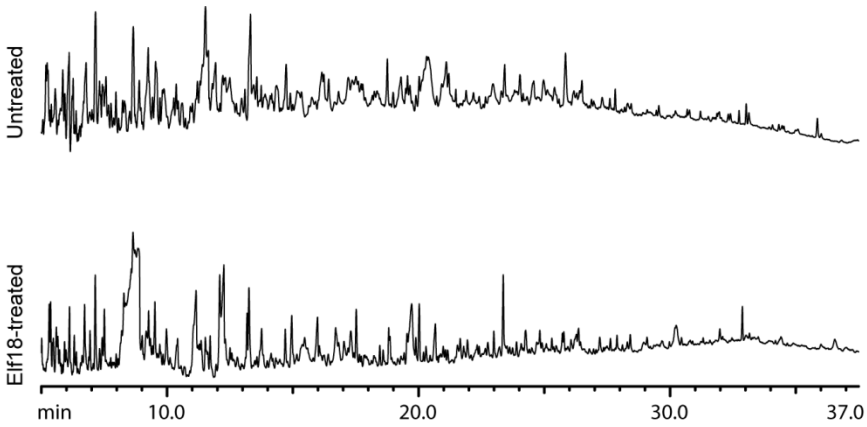

Figure 3. Pyrolysis-GC-total ion chromatogram of untreated and elf18-treated samples with brown pigment accumulation reveals no significant differences.

References

Adams-Phillips L, Briggs AG, Bent AF (2010) Disruption of poly(ADP-ribosyl)ation mechanisms alters responses of Arabidopsis to biotic stress. Plant Physiol **152:** 267-280

Anderson JC, Bartels S, Gonzalez Besteiro MA, Shahollari B, Ulm R, Peck SC (2011) Arabidopsis MAP Kinase Phosphatase 1 (AtMKP1) negatively regulates MPK6-mediated PAMP responses and resistance against bacteria. Plant J **67:** 258-268

Huang J, Gu M, Lai Z, Fan B, Shi K, Zhou YH, Yu JQ, Chen Z (2010) Functional analysis of the Arabidopsis PAL gene family in plant growth, development, and response to environmental stress. Plant Physiol **153:** 1526-1538

Appendix B: Sirtuin inhibitors block MAMP-induced callose deposition

Sirtuins are one of four classes of histone deacetylases (HDACs). The sirtuins are unique among HDACs in that they utilize NAD^+ to deacetylate lysine residues, yielding O-acetyl-ADP-ribose, nicotinamide, and the deacetylated substrate. Mammalian genomes encode seven sirtuins (*SIRT1* to *SIRT7*) but only two (*SRT1* and *SRT2*) were identified in Arabidopsis (North and Verdin, 2004). Arabidopsis *SRT1* and *SRT2* are most similar in sequence to mammalian *SIRT6* and *SIRT4*, respectively. Intriguingly, mammalian SIRT6 exhibits ADP-ribosyltransferase activity in addition to deacetylase activity while SIRT4 exhibits only ADP-ribosyltransferase activity (Liszt et al., 2005; Ahuja et al., 2007).

Sirtuins are similar to PARPs in that they both utilize NAD^+ as a substrate. Furthermore, nicotinamide is a by-product of both enzymes and acts as an inhibitor of both PARP and sirtuin activity. We sought to understand if the loss of MAMP-induced callose observed with 3AB is due to the inhibition of other NAD^+ utilizing enzymes, namely sirtuins. While 3AB inhibits mammalian PARPs and not sirtuins, this specificity has not been characterized in plants.

In order to test the role of sirtuins in the MAMP-induced callose response, chemical inhibitors known to block sirtuin activity were obtained, namely sirtinol, saleramide, and splitomicin. Sirtinol and saleramide dramatically reduced the abundance of flg22-induced callose deposition while a complete inhibition was observed for splitomicin (**Figure 1**). As with 3AB, splitomicin clearly blocked flg22-induced callose but had no impact on wound-induced callose.

In order to follow-up the promising inhibitor results, *srt1* (SALK_086287) and *srt2* (SALK_149295) mutants were acquired and crossed to obtain a *srt1srt2* double mutant. Unfortunately, no reduction in flg22-induced callose was observed in either the *srt1* and *srt2* single mutants or the *srt1srt2* double mutant (**Figure 2**). While this *srt2* T-DNA line was

previously characterized and no *SRT2* mRNA was detected by RT–PCR (Wang et al., 2010), the *srt1* mutant has not been characterized. Therefore, the possibility that this line is not a null mutant cannot be excluded. Given the conflicting results obtained with the sirtuin inhibitors and the mutants, the role of sirtuins in the MAMP-induced callose response remains unclear. Notably, both 3AB and splitomicin have the potential to alter cellular NAD^+ levels. Whether or not changes in the NAD^+ level has an impact on callose deposition is another potential avenue of future investigation (Petriacq et al., 2012; Petriacq et al., 2013).

Figures

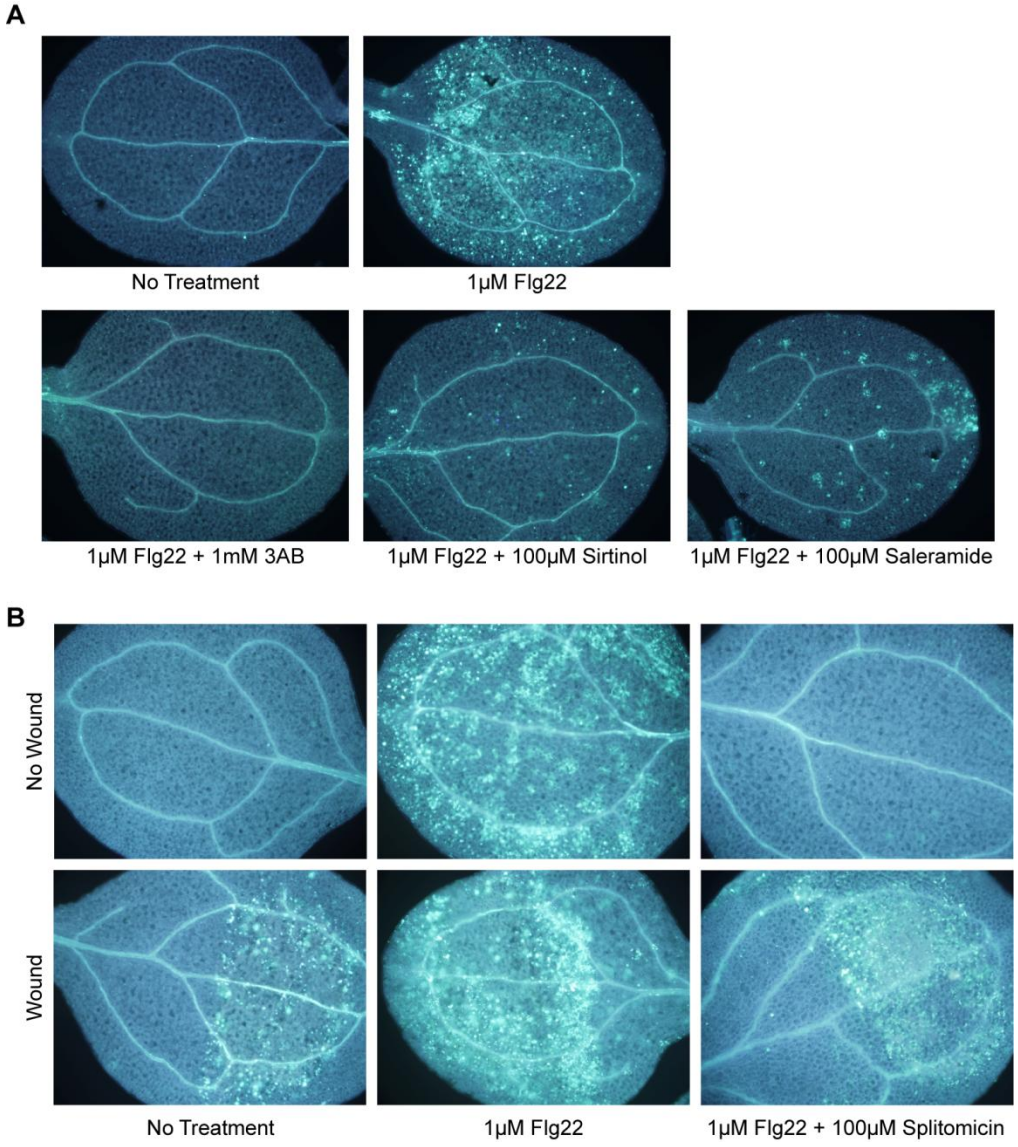

Figure 1. Sirtuin inhibitors block or reduce flg22-induced callose deposition. A, Flg22-induced callose in the presence or absence of sirtinol or saleramide. 3AB is included as a positive control for callose inhibition. B, Unwounded (top) or wounded (bottom) seedlings were treated with flg22 alone or flg22 with splitomicin.

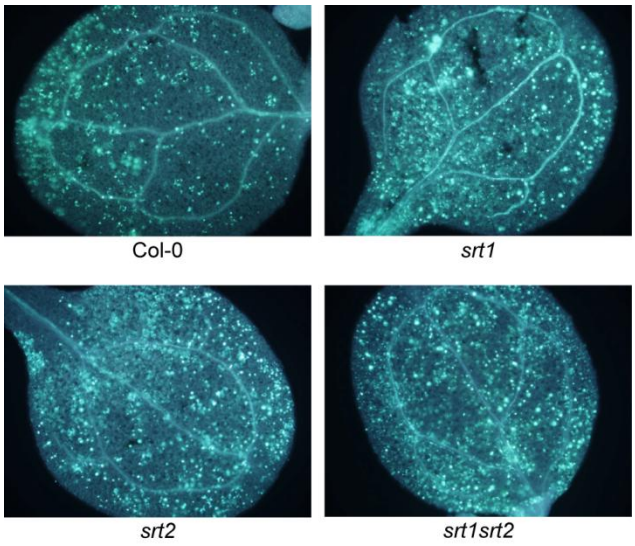

Figure 2. Sirtuin mutants do not alter flg22-induced callose deposition. Col-0 wild type, *srt1*, *srt2*, and *srt1srt2* double mutants were treated with flg22 to elicit callose deposition.

References

Ahuja N, Schwer B, Carobbio S, Waltregny D, North BJ, Castronovo V, Maechler P, Verdin E (2007) Regulation of insulin secretion by SIRT4, a mitochondrial ADP-ribosyltransferase. J Biol Chem **282:** 33583-33592

Liszt G, Ford E, Kurtev M, Guarente L (2005) Mouse Sir2 homolog SIRT6 is a nuclear ADP-ribosyltransferase. J Biol Chem **280:** 21313-21320

North BJ, Verdin E (2004) Sirtuins: Sir2-related NAD-dependent protein deacetylases. Genome Biol **5:** 224

Petriacq P, de Bont L, Hager J, Didierlaurent L, Mauve C, Guerard F, Noctor G, Pelletier S, Renou JP, Tcherkez G, Gakiere B (2012) Inducible NAD overproduction in Arabidopsis alters metabolic pools and gene expression correlated with increased salicylate content and resistance to Pst-AvrRpm1. Plant J **70:** 650-665

Petriacq P, de Bont L, Tcherkez G, Gakiere B (2013) NAD: not just a pawn on the board of plant-pathogen interactions. Plant Signal Behav **8:** e22477

Wang C, Gao F, Wu J, Dai J, Wei C, Li Y (2010) Arabidopsis putative deacetylase AtSRT2 regulates basal defense by suppressing PAD4, EDS5 and SID2 expression. Plant Cell Physiol **51:** 1291-1299